United States
Environmental Protection
Agency

National Risk Management
Research Laboratory
Ada, OK 74820

EPA/600/R-97/128b
February 1998

Estimation of Infiltration Rate in the Vadose Zone: Application of Selected Mathematical Models

Volume II

EPA/600/R-97/128b
February 1998

ESTIMATION OF INFILTRATION RATE IN VADOSE ZONE: APPLICATION OF SELECTED MATHEMATICAL MODELS

Volume II

by

Joseph R. Williams
U.S. EPA
and
Ying Ouyang
ManTech Environmental Technologies, Inc. (METI)
and
Jin-Song Chen
Varadhan Ravi
Dynamac Corporation

ALM (METI) Contract No. 68-W5-0011 DO 022
Dynamac Corp. 68-C4-0031

Project Officer **Delivery Order Project Officer**
David S. Burden **David G. Jewett**
Subsurface Protection and Remediation Division
National Risk Management Research Laboratory
Ada, Oklahoma 74820

In cooperation with:
CENTER FOR REMEDIATION TECHNOLOGY AND TOOLS
OFFICE OF RADIATION AND INDOOR AIR
OFFICE OF AIR AND RADIATION
WASHINGTON, DC 20460

NATIONAL RISK MANAGEMENT RESEARCH LABORATORY
OFFICE OF RESEARCH AND DEVELOPMENT
U.S. ENVIRONMENTAL PROTECTION AGENCY
CINCINNATI, OH 45268

NOTICE

The U.S. Environmental Protection Agency through its Office of Research and Development partially funded and collaborated in the research described here as indicated through the authors' affiliations. Additional support for this project was provided by the Office of Radiation and Indoor Air (ORIA) of the Office of Air and Radiation in collaboration with the Office of Emergency and Remedial Response (OERR) of the Office of Solid Waste and Emergency Response and the U.S. Department of Energy (EM-40). ManTech Environmental Technologies, Inc. (METI) is an in-house support contractor to NRMRL/SPRD under 68-W5-0011, Delivery Order 022 (Dr. David Jewett, Delivery Order Project Officer). Dynamac is an off-site support contractor to NRMRL/SPRD under 68-C4-0031 (Dr. David S. Burden, Project Officer). Ron Wilhelm and Robin Anderson (ORIA) provided valuable technical review and administrative support to this project. The assistance of Sierra Howry, a student in the Environmental Research Apprenticeship Program through East Central University in Ada, Oklahoma, in the completion of this project is greatly appreciated. This report has been subjected to the Agency's peer and administrative review and has been approved for publication as an EPA document.

Mention of trade names or commercial products does not constitute endorsement or recommendation for use.

All research projects making conclusions or recommendations based on environmentally related measurements and funded by the U.S. Environmental Protection Agency are required to participate in the Agency Quality Assurance Program. This project did not involve environmental related measurements and did not require a Quality Assurance Plan.

FOREWORD

The U.S. Environmental Protection Agency is charged by Congress with protecting the Nation's land, air, and water resources. Under a mandate of national environmental laws, the Agency strives to formulate and implement actions leading to a compatible balance between human activities and the ability of natural systems to support and nurture life. To meet these mandates, EPA's research program is providing data and technical support for solving environmental problems today and building a science knowledge base necessary to manage our ecological resources wisely, understand how pollutants affect our health, and prevent or reduce environmental risks in the future.

The National Risk Management Research Laboratory is the Agency's center for investigation of technological and management approaches for reducing risks from threats to human health and the environment. The focus of the laboratory's research program is on methods for the prevention and control of pollution to air, land, water, and subsurface resources; protection of water quality in public water systems; remediation of contaminated sites and ground water, and prevention and control of indoor air pollution. The goal of this research effort is to catalyze development and implementation of innovative, cost-effective environmental technologies; develop scientific and engineering information needed by EPA to support regulatory and policy decisions; and provide technical support and information transfer to ensure effective implementation of environmental regulations and strategies.

Numerous infiltration estimation methods have been developed, and have become an integral part of the assessment of contaminant transport and fate. This document selects six (6) methods having utility under varying conceptualizations. The methods are described in detail and are provided in electronic format for actual application.

Clinton W. Hall, Director
Subsurface Protection and Remediation Division
National Risk Management Research Laboratory

ABSTRACT

Movement of water into and through the vadose zone is of great importance to the assessment of contaminant fate and transport, agricultural management, and natural resource protection. The process of water movement is very dynamic, changing dramatically over time and space. Infiltration is defined as the initial process of water movement into the vadose zone through the soil surface. Knowledge of the infiltration process is prerequisite for managing soil water flux, and thus the transport of contaminants in the vadose zone.

Although a considerable amount of research has been devoted to the investigation of water infiltration in unsaturated soils, the investigations have primarily focused on scientific research aspects. An overall evaluation of infiltration models in terms of their application to various climatic characteristics, soil physical and hydraulic properties, and geological conditions has not been done. Specifically, documentation of these models has been limited and, to some extent, non existent for the purpose of demonstrating appropriate site-specific application. This document attempts to address this issue by providing a set of water infiltration models which have the flexibility of handling a wide variety of hydrogeologic, soil, and climate scenarios. More specifically, the purposes of this document are to: (1) categorize infiltration models presented based on their intended use; (2) provide a conceptualized scenario for each infiltration model that includes assumptions, limitations, boundary conditions, and application; (3) provide guidance for model selection for site-specific scenarios; (4) provide a discussion of input parameter estimation; (5) present example application scenarios for each model; and, (6) provide a demonstration of sensitivity analysis for selected input parameters.

Six example scenarios were chosen as illustrations for applications of the infiltration models with one scenario for each model. The intention of these scenarios is to provide applications guidance to users for these models to various field conditions. Each model application scenario includes the problem setup, conceptual model, input parameters, and results and discussion.

CONTENTS

NOTICE ii
ABSTRACT iv
LIST OF FIGURES vii
LIST OF TABLES ix

CHAPTER 1. INTRODUCTION 1

1.1 Phenomena of Water Infiltration in the Unsaturated Zone 1
1.2 Intended Use of this Document 3

CHAPTER 2. DESCRIPTIONS OF INFILTRATION MODELS 5

2.1 Classification of Infiltration Models Chosen in the Document 5
2.1.1 Semi-Empirical Model 5
2.1.2 Homogeneous Model 5
2.1.3 Non-Homogeneous Model 6
2.1.4 Infiltration Model for Ponding Conditions 6
2.1.5 Infiltration Model for Non-Ponding Conditions 6
2.1.6 Infiltration/Exfiltration Model 6
2.2 Infiltration Model Conceptualization 6
2.3 Selected Models 9
2.3.1 SCS Model 9
2.3.2 Philip's Two-Term Model 9
2.3.3 Green-Ampt Model for Layered Systems 10
2.3.4 Explicit Green-Ampt Model 12
2.3.5 Constant Flux Green-Ampt Model 13
2.3.6 Infiltation / Exfiltration Model 14

CHAPTER 3. METHOD FOR SELECTION OF INFILTRATION MODEL 16
3.1 Model Selection Criteria 16
3.2 Example for Selecting the Water Infiltration Model 17

CHAPTER 4. INPUT PARAMETER ESTIMATIONS 19
4.1 General Description of Parameters 19
4.2 Estimation of the F_w in SCS Model 23
4.3 Estimation of Green-Ampt Model Parameters 24
4.4 Estimation of Philip's Two-Term Model Parameters 29

CHAPTER 5. EXAMPLE APPLICATION SCENARIOS 30
5.1 Semi-Empirical Model (SCS) 30
5.2 Infiltration Model for Homogeneous Conditions (PHILIP2T) 32

5.3 Infiltration Model for Non-homogeneous Conditions (GALAYER) 34
5.4 Infiltration Model for Ponding Conditions (GAEXP) 36
5.5 Infiltration Model for Non-ponding Conditions (GACONST) 38
5.6 Infiltration and Exfiltration (INFEXF) 40

REFERENCES 42

APPENDIXES
Appendix A. User's Instructions for Mathcad Worksheets A-1

Appendix B. Mathematical Models in Mathcad B-1
1. SCS Model B1-1
2. Philip's Two-Term Model B2-1
3. Green-Ampt Model for layered systems B3-1
4. Green-Ampt Model, Explicit Model B4-1
5. Constant Flux Green-Ampt Model B5-1
6. Infiltration/Exfiltration Model B6-1

Appendix C. Sensitivity Analysis Discussion and Demonstration C-1

LIST OF FIGURES

Number Page

1. Zones of the infiltration process for the water content profile under ponded conditions (Adapted from Hillel, 1982) 2

2. Infiltration rate will generally be high in the first stages, and will decrease with time (Adapted from Hillel, 1982) 3

3. Conceptual model for simulating water infiltration using the SCS model 31

4. Surface infiltration rate as a function of daily rainfall rate 31

5. Surface runoff rate as a function of daily rainfall rate 31

6. Conceptual model for simulating water infiltration using the Philip's Two Term Model 33

7. Water infiltration as a function of time 33

8. Cumulative infiltration as a function of time 33

9. Conceptual model for simulating water infiltration into a layered soil 35

10. Comparison of water infiltration between Scenarios 1 (solid line) and 2 (dash line) 35

11. Conceptual model for simulating water infiltration using the Explicit Green-Ampt model 37

12. Water infiltration as a function of time 37

13. Cumulative infiltration as a function of time 37

14. Conceptual model for simulating water infiltration using the constant flux Green-Ampt model 39

15. Water infiltration as a function of time 39

16. Cumulative infiltration as a function of time 39

17. Conceptual model for simulating water infiltration and exfiltration 41

18. Water infiltration as a function of time 41

19. Water exfiltration as a function of time 41

LIST OF TABLES

Number Page

1. Infiltration model classification 5

2. Summary of assumptions, limitations, and mathematical boundary conditions for each model selected, where θ is the volumetric water content. In this table, features are identified as being present for the particular model (Y for YES), or not considered (N for NO). The model names are defined in next section.. 8

3. Summary of common site conditions and the selected models capabilities of simulating those conditions. *Y* indicates the model is designed for the specific site condition and *N* indicates that it is not.. 18

4. Listing of input parameters for running the infiltration models. 19

5. Curve numbers for hydrologic soil-cover complex for the average antecedent moisture condition and $I_a = 0.2F_w$. I_a is initial water abstraction (USDA-SCS, 1972). 23

6. Description of hydrologic soil groups. 24

7. Typical values of saturated volumetric water content (θ_s). 25

8. Typical values of residual volumetric water content (θ_r). 26

9. Typical values of air-entry head (h_b).. 26

10. Typical values of pore size index (λ). 27

11. Typical values for soil hydraulic property parameters (Rawls et al., 1992).. 28

12. Input parameter values for simulations with a sandy soil using the SCS model.. 30

13. Input parameter values for the simulations in a sandy soil using PHILIP2Tmodel. 32

14. Input parameter values for the simulations using GALAYER model.. 34

15. Input parameters for the simulations in a clay soil using GAEXP.. 36

16. Input parameters for the simulations with $r > K_s$ in a clay soil using GACONST.. 38

17. Input parameters for the simulations using the INFEXF model. 40

CHAPTER 1. INTRODUCTION

1.1 Phenomena of Water Infiltration in the Unsaturated Zone

Water applied to the soil surface through rainfall and irrigation events subsequently enters the soil through the process of infiltration. If the supply rate of water to the soil surface is greater than the soil's ability to allow the water to enter, excess water will either accumulate on the soil surface or become runoff. The process by which water enter the soil and thus the vadose zone through the soil-atmosphere interface is known as infiltration. Infiltrability is a term generally used in the disciplines of soil physics and hydrology to define the maximum rate at which rain or irrigation water can be absorbed by a soil under a given condition. Indirectly, infiltrability determines how much of the water will flow over the ground surface into streams or rivers, and how much will enter the soil, and thus assists in providing an estimate of water available for downward percolation through drainage, or return to the atmosphere by the process of evapotranspiration.

Understanding water movement into and through the unsaturated zone is of great importance to both policy and engineering decision-makers for the assessment of contaminant fate and transport, the management of agricultural lands, and natural resource protection. The process of water movement is very dynamic, changing dramatically over time and space. Knowledge of the infiltration process is a prerequisite for managing soil water flux, and thus the transport of contaminants in the vadose zone.

The distribution of water during the infiltration process under ponded conditions is illustrated in Figure 1. In this idealized profile for soil water distribution for a homogeneous soil, five zones are illustrated for the infiltration process.

1) Saturated zone: The pore space in the saturated zone is filled with water, or saturated. Depending on the length of time elapsed from the initial application of the water, this zone will generally extend only to a depth of a few millimeters.
2) Transition zone: This zone is characterized by a rapid decrease in water content with depth, and will extend approximately a few centimeters.
3) Transmission zone: The transmission zone is characterized by a small change in water content with depth. In general, the transmission zone is a lengthening unsaturated zone with a uniform higher water content. The hydraulic gradient in this zone is primarily driven by gravitational forces.
4) Wetting zone: In this zone, the water content sharply decreases with depth from the water content of the transmission zone to near the initial water content of the soil.
5) Wetting front: This zone is characterized by a steep hydraulic gradient and forms a sharp boundary between the wet and dry soil. The hydraulic gradient is driven primarily by matric potentials.

Beyond the wetting front, there is no visible penetration of water. Comprehensive reviews of the principles governing the infiltration process have been published by Philip (1969) and Hillel (1982).

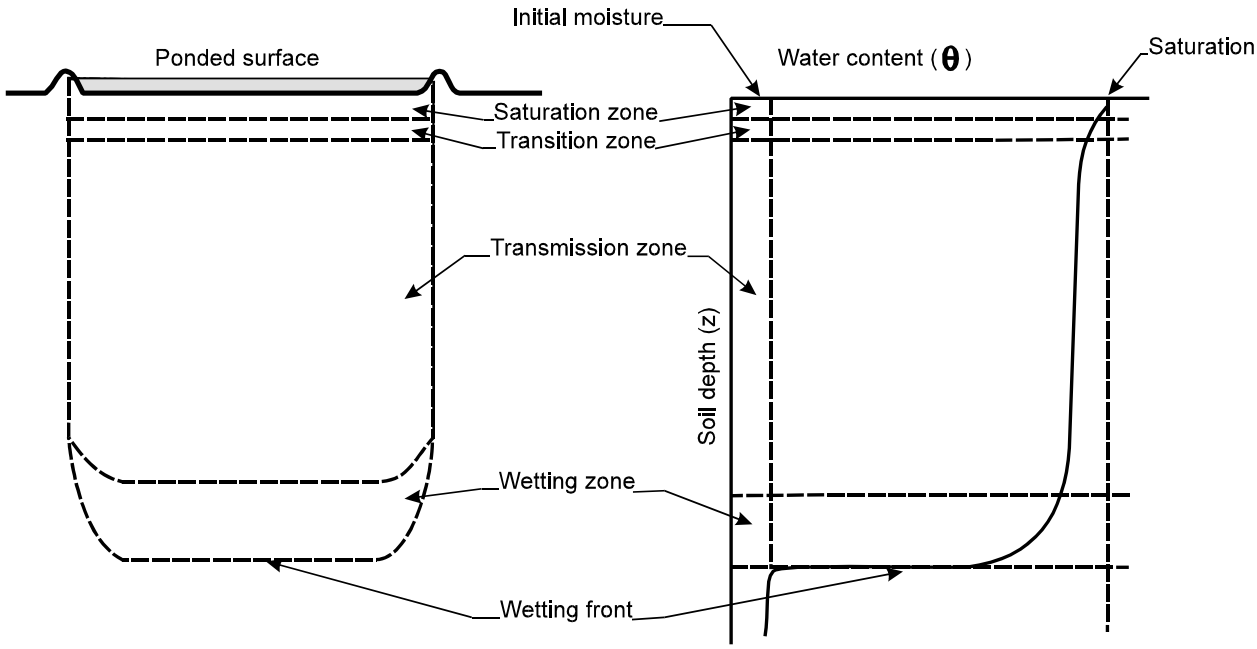

Figure 1. Zones of the infiltration process for the water content profile under ponded conditions (Adapted from Hillel, 1982).

Soil water infiltration is controlled by the rate and duration of water application, soil physical properties, slope, vegetation, and surface roughness. Generally, whenever water is ponded over the soil surface, the rate of water application exceeds the soil infiltrability. On the other hand, if water is applied slowly, the application rate may be smaller than the soil infiltrability. In other words, water can infiltrate into the soil as quickly as it is applied, and the supply rate determines the infiltration rate. This type infiltration process has been termed as *supply controlled* (Hillel, 1982). However, once the infiltration rate exceeds the soil infiltrability, it is the latter which determines the actual infiltration rate, and thus the process becomes *profile controlled*. Generally, soil water infiltration has a high rate in the beginning, decreasing rapidly, and then slowly decreasing until it approaches a constant rate. As shown in Figure 2, the infiltration rate will eventually become steady and approach the value of the saturated hydraulic conductivity (K_s).

The initial soil water content and saturated hydraulic conductivity of the soil media are the primary factors affecting the soil water infiltration process. The wetter the soil initially, the lower will be the initial infiltrability (due to a smaller suction gradient), and a constant infiltration rate will be attained more quickly. In general, the higher the saturated hydraulic conductivity of the soil, the higher the infiltrability.

Naturally formed soil profiles are rarely homogeneous with depth, rather they will contain distinct layers, or horizons with specific hydraulic and physical characteristics. The presence of these layers in the soil profile will generally retard water movement during infiltration. Clay layers impede flow due to their lower saturated hydraulic conductivity; however, when these layers are near the surface and initially very dry, the initial infiltration rate may be much higher and then drop off rapidly. Sand layers will have a tendency to also retard the movement of the

wetting front due to larger pore size and thus a higher hydraulic gradient would be required for flow into the layers.[1] The surface crust will also act as a hydraulic barrier to infiltration due to the lower hydraulic conductivity near the surface, reducing both the initial infiltrability and the eventually attained steady infiltrability.

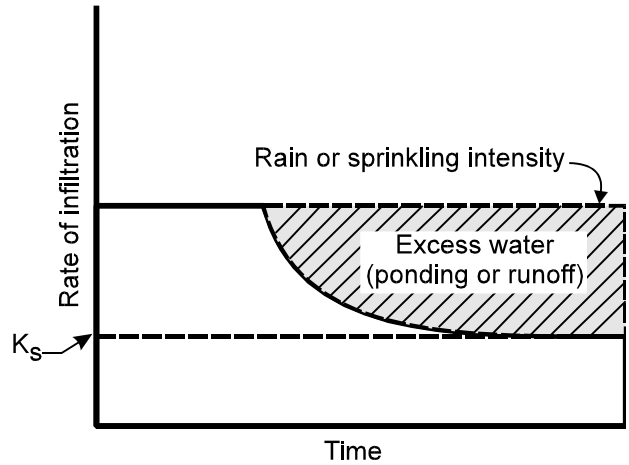

Figure 2. Infiltration rate will generally be high in the first stages, and will decrease with time (Adapted from Hillel, 1982).

As might be expected, the slope of the land can also indirectly impact the infiltration rate. Steep slopes will result in runoff, which will impact the amount of time the water will be available for infiltration. In contrast, gentle slopes will have less of an impact on the infiltration process due to decreased runoff. When compared to the bare soil surface, vegetation cover tends to increase infiltration by retarding surface flow, allowing time for water infiltration. Plant roots may also increase infiltration by increasing the hydraulic conductivity of the soil surface. Due to these effects, infiltration may vary widely under different types of vegetation.

A number of mathematical models have been developed for water infiltration in unsaturated zone (Philip, 1957; Bouwer, 1969; Fok 1970; Moore 1981; Ahuja and Ross, 1983; Parlange *et al.*, 1985; Haverkamp *et al.*, 1990; Haverkamp *et al.*, 1991). A thorough review of water infiltration models used in the fields of soil physics and hydrology has been presented in a previous volume prepared in conjunction with the current project (Ravi and Williams, 1998).

1.2 Intended Use of this Document

Soil water infiltration has been determined from experimental measurements (Parlange, *et al.*, 1985) and mathematical modeling (Philip, 1957; Bouwer, 1969; Fok 1970; Moore 1981; Ahuja and Ross, 1983; Parlange *et al.*, 1985; Haverkamp *et al.*, 1990; Haverkamp *et al.*, 19941). Although a considerable amount of research has been devoted to the investigation of water infiltration in unsaturated soils, these investigations have primarily focused on scientific research aspects. An overall evaluation of infiltration models in terms of their application to various climatic characteristics, and soil physical and geological conditions has not been done. Specifically, documentation of these type models has been limited and, to some extent, non-existent for the purpose of demonstrating appropriate site-specific application. This document attempts to address this issue by providing a set of water infiltration models which have been applied to a variety of hydrogeologic, soil, and climate scenarios. More specifically, the

---

[1]The process of water movement through layers can be investigated through an interactive software package entitled SUMATRA-1 developed by M. Th. van Genuchten (1978), USDA/ ARS, US Salinity Laboratory, Riverside, CA 92521.

purposes of this document are to: (1) categorize infiltration models presented based on their intended use; (2) provide a conceptualized scenario for each infiltration model that includes assumptions, limitations, mathematical boundary conditions, and application; (3) provide guidance for model selection for site-specific scenarios; (4) provide a discussion of input parameter estimation; (5) present example application scenarios for each model; and, (6) provide a demonstration of sensitivity analysis for selected input parameters. This document does not provide an in-depth sensitivity analysis for each model presented; however, a detailed discussion of the process is provided in Appendix C.

CHAPTER 2. DESCRIPTIONS OF INFILTRATION MODELS

2.1 Classification of Infiltration Models

Six infiltration models (Table 1) were chosen for inclusion in this document based on several considerations: (1) relatively simple approach, easy to use, and realistic in applications; (2) ability to handle various field conditions including surface ponding, non-ponding, various rainfall rates, surface runoff, and wetting and drying; and (3) application to both homogeneous or nonhomogeneous soil profiles. The categories presented are not considered to be all-inclusive, but do provide a wide range of model applications.

Infiltration models can be divided into various categories, depending on the purpose of the model, boundary conditions, and the nature of subsurface systems. In this study, six categories were identified for which the models chosen could be associated. The categories were chosen for representativeness to site-specific conditions, which is discussed in the following.

Table 1. Infiltration model classification.

Category	Model Selected	Reference
Semi-Empirical	SCS model	USDA-SCS, 1972
Homogeneous	Philip's two-term model	Philip, 1957
Nonhomogeneous	Green-Ampt model for layered systems	Flerchinger *et al.*, 1988
Ponding	Green-Ampt explicit model	Salvucci and Entekhabi, 1994
Non-ponding	Constant Flux Green-Ampt model	Swartzendruber, 1974
Wetting and Drying	Infiltration/Exfiltration model	Eagleson, 1978

2.1.1 Semi-Empirical Model: As indicated by the term *empirical*, these type infiltration models are developed entirely from field data and have little or no physical basis. The empirical approach to developing a field infiltration equation consists of first finding a mathematical function whose shape, as a function of time, matches the observed features of the infiltration rate, and then attempting a physical explanation of the process (Jury *et al.*, 1991). Most physical processes in semi-empirical models are represented by commonly accepted and simplistic conceptual methods, rather than by equations derived from fundamental physical principles. The commonly used semi-empirical infiltration models in the field of soil physics and hydrology are Kostiakov's model, Horton's model, and the SCS (Soil Conservation Service) model (USDA-SCS, 1972; Hillel, 1982).

2.1.2 Homogeneous Model: Most infiltration models have been developed for application in homogeneous porous media. These models are commonly derived from mathematical solutions based on well-defined, physically based theories of infiltration (*e.g.*, Richards equation). Since this mechanistic infiltration model is derived from the water flow equation, considerable insight is given to the physical and hydraulic processes governing infiltration. Infiltration models commonly

used for homogeneous soil profiles include the Green-Ampt infiltration model, the Philip infiltration model, the Burger infiltration model, and the Parlange infiltration model. Descriptions of these models are provided in documentation by Hillel (1982), Ghildal and Tripathi (1987), and Jury *et al.* (1991).

2.1.3 Non-Homogeneous Model: Naturally developed soil profiles are seldom uniform with depth, nor is the water content distribution uniform at the initiation of infiltration. Because of the nonuniform soil profile, field infiltration measurement data frequently show different characteristics than the models based on theoretical calculations for the uniform soil profile. For most field observations of infiltration rates, the field observations would be less than what would be predicted by models designed for homogeneous systems. In conceptualization of a non-homogeneous soil profile, it is usually more convenient to divide the profile into layers or horizons, each of which is assumed to be homogeneous (Childs and Bybordi, 1969; Hillel and Gardner, 1970). The application of the Green-Ampt equation to calculate cumulative infiltration into nonuniform soils has been studied by Bouwer (1969), Childs and Bybordi, (1969), Fok (1970), Moore (1981), and Flerchinger *et al.* (1988).

2.1.4 Infiltration Model for Ponding Conditions: When the application rate of water to the soil surface exceeds the rate of infiltration, free water (*i.e.*, surface water excess) tends to accumulate over the soil surface. This water collects in depressions, thus ponding on the soil surface. Depending on the geometric irregularities of the surface and on the overall slope of the land, some of the ponded water may become runoff, if the surface storage becomes filled. Under ponded conditions, the cumulative infiltration is a function of soil properties, initial conditions, and the ponding depth on the soil surface. Several infiltration models for ponding conditions have been developed, including those by Parlange *et al.* (1985), Haverkamp *et al.* (1990, 1994), and Salvucci and Entekhabi (1994).

2.1.5 Infiltration Model for Non-ponding Conditions: When the rate of water supply to the soil surface does not exceed the soil infiltrability, all water can percolate into the soil and no surface ponding of water occurs. This process depends on the rate of water supply, initial soil water content, and the saturated hydraulic conductivity. Infiltration models for non-ponding conditions have been developed by several researchers (Philip, 1957; Childs and Bybordi, 1969; Hillel and Gardner, 1970). Probably the most common approach is an implementation of the Green-Ampt model in an explicit approach.

2.1.6 Wetting and Drying Model: Alternate infiltration and exfiltration of water at the soil surface will result in an unsteady diffusion of water into the soil. The presence of transpiring vegetation adds another mechanism for moisture extraction distributed over a depth which is related to root structure. Infiltration models for such conditions have been developed by Eagleson (1978) and Corradini *et al.* (1994).

2.2 Infiltration Model Conceptualization

Water infiltration into unsaturated porous media for various climatic conditions, soil physical and hydraulic properties, and geological conditions is very complex, resulting in a challenge to mathematically simulate observed conditions. An understanding of the principles governing

infiltration and factors affecting infiltration processes must be attained. Since a universal mathematical model is not available to address water infiltration for all field conditions, assumptions are commonly made, and limitations are identified during the model development and application process. Assumptions used in developing water infiltration models commonly include the following:

(1) Initial soil water content profile: Most infiltration models assume a constant and uniform initial soil water content profile. However, under field conditions, the soil water content profile is seldom constant and uniformly distributed.

(2) Soil profile: There are two types of soil profiles which exist under field conditions: (a) homogeneous and (b) heterogeneous. Infiltration models developed for the homogeneous soil profile cannot be used for heterogeneous soil profile without simplifying assumptions concerning the heterogeneity.

(3) Constant and near saturated soil water content at the soil surface: This is a common assumption for most infiltration models, which will allow for the ignoring of the initially high hydraulic gradient across the soil's surface. The length of time the surface is not near saturation is very small when compared to the length of time associated with the infiltration event.

(4) Duration of infiltration process: Some infiltration models are only valid for a short term period of infiltration, which can limit their usefulness to field applications where infiltration may last for longer time periods. A short term period might be representative of a rainfall or irrigation event.

(5) Surface crust and sealing: None of the selected models can be used for the surface crusting boundary condition. This boundary condition is complex and dynamic.

(6) Flat and smooth surface: These surface boundary conditions can be easily incorporated into mathematical models, whereas an irregular surface or sloping surface can result in an added dimension to the mathematical modeling.

Boundary conditions are those conditions defined in the modeling scenario to account for observed conditions at the boundaries of the model domain. These conditions must be defined mathematically, the most common of which are given as follows:

(1) Constant or specified flux at the surface: The rate of water applied to the soil surface can be constant or time-varying. Because of its simplicity as compared to other boundary conditions, a constant flux condition has been used in most infiltration models.

(2) Surface ponding condition. The surface ponding or non-ponding conditions are dependent on the rate of water application as well as soil infiltrability. Whenever the rate of water application to the soil exceeds the soil infiltrability, the surface ponding occurs. The opposite case will result in surface non-ponding conditions.

(3) Finite column length at the lower boundary. Some infiltration models are limited to a finite column length and others may allow for an infinite column length. Infiltration models with the finite column length condition may limit their applications for deeper water infiltration.

(4) Based on Richards equation. Several infiltration models (*e.g.*, Philip's model and Eagleson's model) were developed based on Richards equation. These models commonly have well-defined physically based theories and give considerable insight into the processes governing infiltration. These would require information related to the water retention characteristics of the soil media.

A summary of assumptions, limitations, and boundary conditions for each model chosen in this document is given in Table 2. Detailed descriptions of the models are provided below.

Table 2. Summary of assumptions, limitations, and mathematical boundary conditions for each model selected, where θ is the volumetric water content. In this table, features are identified as being present for the particular model (Y for YES), or not considered (N for NO). The model names are defined in next section.

Model name	Model Features									
	Assumptions and Limitations				Boundary Conditions					
	Constant and uniform initial θ	Homogeneous soil profile	Valid for only short term infiltration	Surface crust and sealing	Constant water content at top boundary	Constant flux at the top boundary	Surface ponding condition	Finite column length	Based on Richards equation	Based on empirical equation
SCS	N	N	N	N	N	N	N	N	N	Y
Philip's two term	Y	Y	Y	N	Y	N	N	N	Y	N
Green-Ampt model for layered systems	Y	Y	N	N	Y	N	Y	Y	N	N
Green-Ampt explicit	Y	Y	N	N	Y	N	Y	Y	N	N
Constant flux Green-Ampt	Y	Y	N	N	Y	Y	N	Y	N	N
Infiltration/Exfiltration	Y	Y	N	N	Y	N	N	N	Y	N

2.3 Selected Models

2.3.1 SCS Model

Description: The empirical approach of developing a water infiltration equation consists of first identifying a mathematical function whose shape, as a function of time, matches the observed features of the infiltration rate, followed by an attempt at providing a physical explanation of the process (Jury *et al.*, 1991). For semi-empirical models, most physical processes are represented by commonly accepted, and simplistic conceptual methods rather than by equations derived from fundamental physical principles. The Soil Conservation Service (SCS)[2] model is a commonly used semi-empirical infiltration model in the field of soil physics and hydrology (USDA, 1972).

Equations: Mathematical functions for the SCS model are given as:

$$R = \begin{cases} \dfrac{(P - 0.2F_w)^2}{P + 0.8F_w} & P > 0.2F_w \\ 0, \quad otherwise: & P \leq 0.2\ F_w \end{cases} \qquad \textbf{(1)}$$

and

$$q = P - R \qquad \textbf{(2)}$$

where R is amount of runoff (*inches*), P is the daily rainfall amount (*inches*), F_w is a statistically derived parameter (also called the retention parameter) with the units of *inches*, and q is the daily infiltration amount (*inches*). Justification for the use of this model is based on a consideration that the model is simple, it requires few input parameters, and has been widely used and understood in the fields of soil physics and hydrology.

Assumptions and Limitations: A major limitation for applying the SCS model lies in that the coefficients in Equation 1 must be evaluated with field data for each specific site. Since the model is not derived from fundamental physical principles, it can only be used as a screening tool for initial approximations.

2.3.2 Philip's Two-Term Model

Description: The Philip's two-term model (PHILIP2T) is a truncated form of the Taylor power series solution presented by Philip (1957). During the initial stages of infiltration (*i.e.*, when t is very small), the first term of Equation 3 dominates. In this stage, the vertical infiltration proceeds at almost the same rate as absorption or horizontal infiltration due to the gravity

---

[2]The Mathcad worksheets provided in Appendix B are referenced in parentheses. These are also used as the filenames.

component, represented by the second term, being negligible. As infiltration continues, the second term becomes progressively more important until it dominates the infiltration process. Philips (1957) suggested the use of the two-term model in applied hydrology when *t* is not too large.

Equations: The Philip's two-term model is represented by the following equations,

$$q(t) = \frac{1}{2} S t^{-1/2} + A \qquad \textbf{(3)}$$

and

$$I(t) = S t^{1/2} + A t \qquad \textbf{(4)}$$

where *q* is infiltration rate (*cm/h*), *t* is time for infiltration (*h*), *S* is the sorptivity ($cm/h^{1/2}$) and is a function of the boundary, initial, and saturated water contents, *A* is a constant (*cm/h*) that depends on soil properties and initial and saturated water contents, and *I(t)* is the cumulative infiltration (*cm*) at any time, *t*.

Assumptions and Limitations: The three primary assumptions for this model are: (1) homogeneous soil conditions and properties; (2) antecedent (*i.e.*, conditions prior to infiltration) water content distribution is uniform and constant (*i.e.*, single-valued); and (3) water content at the surface remains constant and near saturation. There are basically four limitations for this model, which are as follows: (1) field soils are seldom homogeneous, and this model is not designed for layered systems; (2) initial moisture content is seldom uniformly distributed throughout the profile; (3) in most situations of rainfall or irrigation, the soil surface is rarely at a constant water content; and (4) the approach is not valid for large times. Regarding the third limitation identified above, if the rainfall or irrigation rate is smaller than the saturated hydraulic conductivity, the soil may never be saturated at the surface, and no ponding will occur. Under these conditions, the infiltration rate will be equal to the rainfall or irrigation rate. Even when the rate is greater than saturated hydraulic conductivity, there will be some time lag between the beginning of infiltration and the time of surface saturation and subsequent ponding. Under these circumstances the constant flux Green-Ampt model presented by Swartzendruber (1974) may be used.

2.3.3. Green-Ampt Model for Layered Systems

Description: The Green-Ampt Model has been modified to calculate water infiltration into nonuniform soils by several researchers (Bouwer, 1969; Childs and Bybordi, 1969; Fok, 1970; Moore, 1981). Flerchinger *et al.* (1988) developed a model, based on the Green-Ampt model, for calculating infiltration over time in vertically heterogeneous soils. This model is referred to as the Green-Ampt model for layered systems (GALAYER).

Equations: Mathematical formulations for this model are given below:

$$f = f^* K_n \tag{5}$$

$$f^* = \frac{F^* + 1}{F^* + z^*} \tag{6}$$

$$F^* = \frac{1}{2}[t^* - 2z^* + \sqrt{(t^* - 2z^*)^2 + 8t^*}\ ] \tag{7}$$

$$t^* = \frac{K_n\ t}{\Delta\theta(H_n + \sum_{i=1}^{n-1} z_i)} \tag{8}$$

$$z^* = \frac{K_n}{(H_n + \sum_{i=1}^{n-1} z_i)} \sum_{i=1}^{n-1} \frac{z_i}{K_i} \tag{9}$$

where f is infiltration rate (*cm/h*), f^* is dimensionless infiltration, K_n is hydraulic conductivity (*cm/h*) of the layer n containing wetting front, F^* is the dimensionless accumulated infiltration in layer n, z^* is dimensionless depth accounting for thickness and conductivity of layers behind the wetting front, t is time (*h*), $\Delta\theta$ is change in volumetric water content (cm^3/cm^3) as the wetting front passes layer n, H_n is potential head while the wetting front passes through layer n, z_i is thickness (*cm*) of layer i, and K_i is hydraulic conductivity of layer i. As can be seen, accounting for layers significantly increases the complexity of this model.

<u>Assumptions and Limitations:</u> There are basically two assumptions for this model. The first assumption is nearly saturated plug flow. An example of when this assumption may be violated is if a coarse-textured soil with a high hydraulic conductivity is underlying a fine-textured soil with a low hydraulic conductivity. In general, any time the infiltration rate becomes less than the hydraulic conductivity at the wetting front, complete wetting will not occur beyond the wetting front, and the assumption of nearly saturated flow is no longer valid. The second assumption is that the water content is uniform within each layer behind the wetting front, although it is nonuniform between layers. The limitation for this model is that this equation is valid for layered soils only if the dimensionless depth (z^*) is less than or equal to *1*. Crusted soils and surface seals are typical conditions when this criterion is not met.

2.3.4 Explicit Green-Ampt Model

Description: The Green-Ampt model is the first physically-based equation describing the infiltration of water into a soil. It has been the subject of considerable development in soil physics and hydrology owing to its simplicity and satisfactory performance for a wide variety of water infiltration problems. This model yields cumulative infiltration and infiltration rates as implicit functions of time (*i.e.*, given a value of time, *t*, *q* and *I* cannot be obtained by direct substitution). The equations have to be solved in an iterative manner to obtain these quantities. Therefore, the required functions are *q(t)* and *I(t)* instead of *t(q)* and *t(I)*. The explicit Green-Ampt model (GAEXP) for *q(t)* and *I(t)*, developed by Salvucci and Entekhabi (1994), facilitated a straightforward and accurate estimation of infiltration for any given time. This model supposedly yields less than 2% error at all times when compared to the exact values from the implicit Green-Ampt model.

Equations: Mathematical formulations for this model are as follows:

$$\frac{I}{K_s} = (1 - \frac{\sqrt{2}}{3})t + \frac{\sqrt{2}}{3}\sqrt{\chi t + t^2} + (\frac{\sqrt{2}-1}{3})\chi[\ln(t+\chi) - \ln\chi]$$

$$+ \frac{\sqrt{2}}{3}\chi[\ln(t + \frac{\chi}{2} + \sqrt{\chi t + t^2}) - \ln(\chi/2)] \qquad \textbf{(10)}$$

$$\frac{q}{K_s} = \frac{\sqrt{2}}{2}\tau^{-1/2} + \frac{2}{3} - \frac{\sqrt{2}}{6}\tau^{1/2} + \frac{1-\sqrt{2}}{3}\tau \qquad \textbf{(11)}$$

with

$$\chi = \frac{(h_s - h_f)(\theta_s - \theta_0)}{K_s} \qquad \textbf{(12)}$$

and

$$\tau = \frac{t}{t+\chi} \qquad \textbf{(13)}$$

where q is infiltration rate (*cm/h*), K_s is saturated hydraulic conductivity (*cm/h*), t is time (*h*), h_s is

ponding depth or capillary pressure head at the surface (*cm*), h_f is capillary pressure head at the wetting front (*cm*), θ_s is saturated volumetric water content (cm^3/cm^3) and θ_0 is initial volumetric water content (cm^3/cm^3).

Assumptions and Limitations: The assumptions of the model are: (1) the water content profile is of a piston-type with a well-defined wetting front; (2) antecedent (*i.e.*, prior to infiltration) water content distribution is uniform and constant; (3) water content drops abruptly to its antecedent value at the front; (4) soil-water pressure head (negative) at wetting front is h_f; (5) soil-water pressure head at the surface, h_s, is equal to the depth of the ponded water; and, (6) soil in the wetted region has constant properties. The limitations of the model are: (1) homogeneous soil conditions and properties; (2) constant, non-zero surface ponding depth; and, (3) in most situations of rainfall or irrigation, the surface is not at a constant water content.

2.3.5 Constant Flux Green-Ampt Model

Description: The constant flux Green-Ampt model (GACONST) can be used to simulate the water infiltration for non-ponding conditions, where the water flux application rate is represented by r (*cm/h*). Two cases are presented, that where the application rate is less than the saturated hydraulic conductivity $r < K_s$), and where the application rate is greater than the saturated hydraulic conductivity $r > K_s$). When $r < K_s$, the infiltration rate (q) is always equal to the surface application rate (r) and the surface is never saturated; when $r > K_s$, surface saturation first occurs at time t_o.

Equations: Mathematical formulations for this model are given below:

For r K_s and $t > 0$, we have:

$$q = r \tag{14}$$

$$I = rt \tag{15}$$

For $r > K_s$, we have the following cases:

(i) $t < t_o$

$$q = r \tag{16}$$

$$I = rt \tag{17}$$

(ii) $t > t_o$

$$q = K_s[1 - (\theta_s - \theta_0)\frac{h_f}{I}] \quad \textbf{(18)}$$

with

$$I_0 = rt_0 \quad \textbf{(19)}$$

$$K_s(t - t_0) = I - I_0 + h_f\ (\theta_s - \theta_0)\ln[\frac{I - (\theta_s - \theta_0)h_f}{I_0 - (\theta_s - \theta_0)h_f}] \quad \textbf{(20)}$$

$$t_0 = \frac{-K_s h_f\ (\theta_s - \theta_0)}{r\ (r - K_s)} \quad \textbf{(21)}$$

where q is the surface infiltration rate (*cm/h*), r is the constant water application rate at the surface (*cm/h*), t is time (*h*), K_s is saturated hydraulic conductivity (*cm/h*), θ_s is saturated volumetric water content (cm^3/cm^3), and θ_0 is initial volumetric water content (cm^3/cm^3), and h_f is capillary pressure head (< 0) at the wetting front (*cm*). In the case of $r > K_s$, before surface saturation occurs, the infiltration rate is simply equal to r.

<u>Assumptions and Limitations:</u> The assumptions and limitations are the same as those identified for the other Green-Ampt models.

2.3.6 Infiltration/Exfiltration Model

<u>Description:</u> The vertical movement of soil water between the surface and the water table can be divided into two processes according to the predominant forces involved: (1) infiltration and (2) exfiltration (evapotranspiration). An infiltration/exfiltration model (INFEXF) developed by Eagleson (1978) was selected to estimate the water infiltration during a wetting season and exfiltration during a drying season. Philip's equation, which can be used to simulate both infiltration and exfiltration, assumes the medium to be effectively semi-infinite and the internal soil water content at the beginning of each storm and inter-storm period to be uniform at the long term space-time average. The exfiltration equation is modified for presence of natural vegetation through the approximate introduction of a distributed sink representing the moisture extraction by plant roots.

Equations: Mathematical formulations for this model are given as:

$$f_i = \frac{1}{2} S_i t^{-½} + \frac{1}{2}(K_1 + K_0) \qquad \textbf{(22)}$$

for water infiltration, and

$$f_e = \frac{1}{2} S_e t^{-½} - \frac{1}{2}(K_1 + K_0) - ME_v \qquad \textbf{(23)}$$

for water exfiltration, where f_i is the infiltration rate (*cm/h*), S_i is the infiltration, sorptivity (*cm/h*$^{1/2}$), t is the time (*h*), K_1 is the hydraulic conductivity (*cm/h*)'s of soil at soil surface with water content θ, K_0 is the initial hydraulic conductivity (*cm/h*), f_e is the exfiltration rate (*cm/h*), S_e is the exfiltration sorptivity (*cm/h*$^{1/2}$), M is the vegetated fraction of land surface, and E_v is the transpiration rate (*cm/h*). During the wetting season (Infiltration), K_1 and θ_1 might represent the saturated hydraulic conductivity (K_s) and the saturated water content (θ_s) repectively for the conditions at the soil surface. During the dry season (exfiltration), K_1 might represent the hydraulic conductivity for the dry soil surface with the water content approaches to zero.

Assumptions and Limitations: Assumptions and limitations for the model are: (1) the water table depth is much greater than the larger of the penetration depth and the root depth; (2) soil water content throughout the surface boundary layer is spatially uniform at the start of each storm period and at the start of each inter-storm period at the value $s = s_o$, where s is degree of saturation and s_o is initial degree of saturation in surface boundary layer; (3) vegetation is distributed uniformly and roots extend through the entire volume of soil; and (4) homogeneous soil system.

CHAPTER 3. METHOD FOR SELECTION OF INFILTRATION MODEL

Mathematical modeling has become an important methodology in support of the planning and decision-making process. Soil infiltration models provide an analytical framework for obtaining an understanding of the mechanisms and controls of the vadose zone and ground-water flow. Results from soil water infiltration models can be used to simulate the fate and transport of contaminants by other models. For managers of water resources, infiltration models may provide an essential support for planning and screening of alternative policies, regulations, and engineering designs affecting ground-water flow and contaminant transport. A successful application of soil water infiltration models requires a combined knowledge of scientific principles, mathematical methods, and site characterization. In general, application of mathematical models involves the following processes (US EPA, 1994a): (1) model application objectives; (2) project management; (3) conceptual model development; (4) model selection; (5) model setup and input parameter estimation; (6) simulation scenarios; (7) post simulation analysis; and (8) overall effectiveness. In this chapter, the focus will be on methods for selecting appropriate soil infiltration models. A detailed discussion of model selection is reported by U.S.EPA (1994a & 1994b, 1996) and van der Heijde and Elnawawy (1992).

3.1 Model Selection Criteria

In the model application process, mathematical model selection is a critical step to ensure an optimal trade-off between project effort and result. It is the process of choosing the appropriate software, algorithm, or other analysis techniques capable of simulating the characteristics of the physical, chemical, and biological processes, as identified in the conceptual model, as well as meeting the overall objectives for the model application. In general, the major criteria in selecting a model are: (1) suitability of the model for the intended use, (2) reliability of the model, and (3) efficiency of the model application.

A major criterion in selecting a mathematical model is its suitability for the identified task. A selected mathematical model must meet the needs identified in the conceptual model. These include initial and boundary conditions (*e.g.*, surface ponding), hydrogeological properties (*e.g.*, layered soil), biological properties (*e.g.*, root water uptake), and availability of input parameters. Before a final selection is made, users should develop an understanding of the details incorporated into the mathematical model. Also, the user should be aware that each model has its strengths and weaknesses, often related to terms included in the governing equations and in the boundary conditions. It should be realized that a perfect match rarely exists between desired characteristics and the characteristics presented in the mathematical models.

Another criterion in selecting a mathematical model is model credibility. The credibility of the model, and that of the theoretical framework represented, is based on the model's proven reliability, and on its acceptance by users. Model credibility is a major concern in model use. Therefore, special attention should be given in the selection process to ensure the use of qualified simulation models which have undergone adequate review and testing.

The applicability of a model is referred to as how the model can be used for given conditions. The infiltration models chosen in this document are simple and easy to use, and yet cover a variety of field conditions, including (1) rainfall and irrigation, (2) surface runoff, (3)

multiple layers, and (4) wetting and drying conditions. Table 3 provides a guidance for the selection of a suitable infiltration model for given site conditions. It should be noted that the site conditions listed in this table are common conditions encountered in environmental remediation practices. It is impractical to list all conditions for each individual site; however, users are encouraged to read the assumptions and limitations for each model discussed in the previous section before selecting a model.

3.2 Example for Selecting the Water Infiltration Model

As an example of the selection process being implemented, the four basic steps are suggested for the following generic scenario. For this example, the infiltration rate is needed for use in a screening level application of a simplified fate and transport model. For this type model, the advective portion of the model is handled by a single estimated infiltration rate. Conceptually, the site soil profile is noticeably layered, and no surface runoff or ponding is routinely observed during rainfall events. Due to the climatic region, and the generally protected nature of the site to high evaporative demand, the wetting and drying cycle is not considered critical. No noticeable cracks or other indications of preferential flow have been noted, therefore this characteristic can be discounted.

(1) Modeling objective:	The objective of the modeling project is to estimate the soil water infiltration rate. Therefore, a soil water infiltration model is needed.
(2) Conceptual model:	The soil profile is non-homogeneous and layered. Therefore, a soil water infiltration model for layered soil is needed.
(3) Other site conditions:	No surface runoff or ponding is to be considered for the application, and preferential flow is not a concern. The wetting and drying cycle is not significant at the site.
(4) Model selection:	Based on the modeling objective and conditions listed above, Green-Ampt model for layered systems is an appropriate choice for the project.

Once an infiltration model has been selected, it is imperative that the user gather additional experience with using the model. This would include the implementation of a sensitivity analysis to establish the priority and importance of input parameters. Hopefully, the user will already be familiar with the model description, assumptions, and limitations. Input parameters for the model now become critical, and the user will need to establish the availability of quality data for the input parameters. The quality of this data must be established prior to utilization in any simulations.

Table 3. Summary of common site conditions and the selected model's capabilities of simulating those conditions. *Y* indicates the model is suitable for the specific site condition and *N* indicates that it is not.

Site Conditions	Model Name					
	SCS	Philip 2-Term	Layered Green-Ampt	Explicit Green-Ampt	Constant Flux Green-Ampt	Infiltration/ Exfiltration
Surface Ponding	N	N	Y	Y	N	N
Surface Runoff	Y	N	N	N	N	N
Rainfall & Irrigation	Y	N	N	N	Y	Y
Multiple Layers	N	N	Y	N	N	N
Wetting & Evaporation	N	N	N	N	N	Y
Homogeneous Soil Profile	Y	Y	Y	Y	Y	Y
Vegetation Cover	N	N	N	N	N	Y

CHAPTER 4. INPUT PARAMETER ESTIMATIONS

4.1 General Description of Parameters

An important step in a model project is input parameter estimation. Because of improvements in computer software and hardware, the usefulness of numerical models hinges increasingly on the availability of accurate input parameters. Approaches for obtaining input parameters in numerical modeling include field observations and measurements, experimental measurements, curve-fitting, and theoretical calculations. Table 4 provides a list of input parameters required for the use of models discussed in this document. A majority of parameter values required for these models can be found in the literature (Hillel, 1982; Carsel and Parrish, 1988; van Genuchten *et al.*, 1989; Breckenridge *et al.*, 1991; Leij *et al.*, 1996). Typical parameter values are provided in this table for common soil conditions; however, it is always a good practice to obtain site-specific values.

Table 4. Listing of input parameters for running the infiltration models.

Parameter	Symbol	Typical Value or Method	Required Model Name	Data Source
Statistically derived parameter	F_w	0.1 to 90 inches	SCS	USDA-SCS, 1972
Daily rainfall	P	0.1 to 10 inches	SCS	Weather Stations
Duration of infiltration	t	Site-Specific	All models except for SCS	
Sorptivity	S	0.1 to 1 cm/h^{½} or Calculated	Philip's two term	Philip, 1969; Jury *et al*, 1991
Empirical Constant	A	Calculated	Philip's two term	Philip, 1969; Hillel, 1982
Saturated Hydraulic Conductivity	K_s	$1x10^{-5}$ to 60 cm/h or Measured	All models except for SCS	Breckenridge *et al.*, 1991; Carsel and Parrish, 1988; Hillel, 1982; Li *et al.*, 1976
Unsaturated Hydraulic Conductivity of Layer *n*	K_n	Site-Specific or Measured	Green Ampt model for layered systems	Breckenridge *et al.*, 1991; Carsel and Parrish, 1988; Hillel, 1982; Li *et al.*, 1976
Hydraulic Conductivity of Layer *i*	K_i	Site-Specific or Measured	Green Ampt model for layered systems	Breckenridge *et al.*, 1991; Carsel and Parrish, 1988; Hillel, 1982; Li *et al.*, 1976
Thickness of Layer *i*	Z_i	Measured	Green Ampt model for layered systems	

Parameter	Symbol	Typical Value or Method	Required Model Name	Data Source
Potential Head While Wetting Front Passes Through Layer *n*	H_n	Site-Specific or Measured	Green-Ampt model for layered systems	Breckenridge *et al.*, 1991; Carsel and Parrish, 1988; Hillel, 1982; Li *et al.*, 1976
Change in Volumetric Water Content Within Layer *n*	$\Delta\theta$	Site-Specific or Measured	Green-Ampt model for layered systems	Breckenridge *et al.*, 1991; Carsel and Parrish, 1988; Hillel, 1982; Li *et al.*, 1976
Saturated Volumetric Water Content	θ_s	Site-Specific 0.3 to 0.5 cm^3/cm^3 (or Table 7)	Green-Ampt explicit & Constant flux Green-Ampt	Breckenridge *et al.*, 1991; Carsel and Parrish, 1988; Hillel, 1982; Li *et al.*, 1976
Initial Volumetric Water Content	θ_o	Site-Specific or Measured	Green-Ampt explicit & Constant flux Green-Ampt	Breckenridge *et al.*, 1991; Carsel and Parrish, 1988; Hillel, 1982; Li *et al.*, 1976
Ponding Depth	h_s	Site-Specific or Measured	Green-Ampt explicit	
Capillary Pressure at the Wetting Front	h_f	Calculated	Green-Ampt explicit	Hillel, 1982; Jury *et al.*, 1991
Constant Application Rate	r	Measured	Constant flux Green-Ampt	
Vegetated Fraction	M	Site-Specific	Infiltration/Exfilt r-ation	Eagleson, 1978
Transpiration Rate	E_v	Measured	Infiltration/Exfilt -ration	Eagleson, 1978
Infiltration Sorptivity	S_i	Eagleson's Report	Infiltration/Exfilt -ration	Eagleson, 1978
Exfiltration Sorptivity	S_e	Eagleson's Report	Infiltration/Exfilt -ration	Eagleson, 1978

A brief description of each parameter listed in Table 4 is provided as follows. These descriptions are not intended to be fully explanatory, and the reader is referred to cited references for more detail.

1. **Statistically derived parameter with some resemblance to the initial water content (F_w):** This parameter can be estimated according to USDA-SCS (1972). Detailed estimation of F_w is provided in Section 4.2. This parameter is required in the SCS model.

2. **Daily rainfall rate (*P*):** The daily rainfall rate for a specific site can be obtained from local weather station or atmospheric research institutes. This parameter is required in the SCS model.

3. **Duration of infiltration (*t*):** The duration of infiltration is site specific, and depends on rainfall rate, surface application rate, and soil infiltrability. This is also the simulation time.

4. **Sorptivity (*S*):** The sorptivity is a function of initial and saturated water contents, and can be obtained simply by determining the slope of I/t versus $t^{-1/2}$ in Equation 4. This parameter is required in Philip's two-term model.

5. **Empirical constant (*A*):** This parameter is required in Philip's two-term model. When the infiltration time is very large, the constant A is similar to hydraulic conductivity, and can be obtained simply by determining the intercept of I/t versus $t^{-1/2}$ in Equation 4.

6. **Saturated hydraulic conductivity (K_s):** This parameter measures the ability of the soil to conduct water when saturated. The value of the saturated hydraulic conductivity depends on soil types and is site-specific. This parameter can be obtained from experimental measurements and literature, and is required in Philip's two-term model, Green-Ampt model for layered systems, the Green-Ampt explicit model, and the Constant flux Green-Ampt model.

7. **Hydraulic conductivity of layer *n* (K_n):** This parameter measures the ability of the soil to conduct water in layer *n* when the soil is unsaturated. The value of the unsaturated hydraulic conductivity depends on soil types and soil water content, and is site-specific. This parameter can be obtained from experimental measurements or literature, and is required in the Green-Ampt model for layered systems.

8. **Hydraulic conductivity of layer *i* (K_i):** This parameter measures the ability of the soil to conduct water in layer *i* when the soil is unsaturated. The value of unsaturated conductivity depends on soil types and soil water content, and is site-specific. This parameter can be obtained from experimental measurements and literature, and is required in the Green-Ampt model for layered systems.

9. **Thickness of layer *i* (Z_i):** This parameter defines the thickness of layer *i* when the soil is heterogeneous. The value of each layer's thickness is site-specific, and is required in the Green-Ampt model for layered systems.

10. **Potential head while wetting front passes through layer *n* (H_n):** The potential head is the difference between the energy state of soil water and that of pure free water. The soil water potential head is a function of soil water content, and can be determined from the soil water retention curve. Users may need to know basic concepts of the soil water retention curves in order to estimate this parameter. This parameter is required in the Green-Ampt model for layered system.

11. **Change in volumetric water content within layer *i* ($\Delta\theta$):** The volumetric water content is expressed as a decimal fraction of the volume of the total soil sample. The change in volumetric water content within layer *i* is the difference between the maximum and minimum water content in the ith layer at a given time frame. This parameter is required in the Green-Ampt model for layered system.

12. **Saturated volumetric water content (θ_s):** The saturated volumetric water content is the percentage of the volume of the soil sample when all soil pore spaces are filled with water (*i.e.*, saturated). The value of the saturated volumetric water content is dependent on soil

type and is site-specific. This parameter can be obtained from experimental measurements and the literature, and is required in the Green-Ampt explicit model.

13. **Initial volumetric water content (θ_o):** This parameter defines the volumetric water content at start of the simulation. The value of the initial volumetric water content is dependent on soil type and is site-specific, and is required in the Green-Ampt explicit model.

14. **Ponding depth (h_s):** This parameter defines the thickness of water accumulated at the soil surface during water infiltration. The extent of ponding depth depends on soil types and is thus site-specific. This parameter is required in the Green-Ampt explicit model.

15. **Capillary pressure at the wetting front (h_f):** The capillary pressure is the suction of water in the pore space due to surface tension or capillary force. This parameter is a function of soil water content, and can be determined from experimental measurements (Hillel, 1982) or from the following equation $h_f = 2\gamma / r$, where γ is the surface tension of water and r is the radius of capillary. The parameter is required in the Green-Ampt explicit model, and is discussed in the section on the estimation of the Green-Ampt parameters.

16. **Constant application rate (r):** This is the rate of water application to the soil surface, and is site-specific. This parameter is required in the constant flux Green-Ampt model.

17. **Vegetated fraction (M):** This parameter defines the density of plant canopy coverage at the soil surface. This parameter is site-specific, and is required in the infiltration/exfiltration model.

18. **Transpiration rate (E_v):** This parameter defines the plant water transpiration rate. It depends on type of plant and soil water availability to roots. This parameter can be obtained from experimental measurements, and is required in the infiltration/exfiltration model.

19. **Infiltration sorptivity (S_i):** The infiltration sorptivity is a function of initial and saturated water contents. It can be obtained from Eagleson's report (1978). This parameter is required in the INFEXF model.

20. **Exfiltration sorptivity (S_e).** The exfiltration sorptivity is a function of initial and saturated water contents and surface evaporation rate. This parameter can be obtained from Eagleson (1978), and is required in the infiltration/exfiltration model.

In summary, the saturated water content at the application surface (θ_s), antecedent water content (θ_o), and respective hydraulic conductivities (K_s and K_o) are required for most infiltration models. However, the pore size index (λ) and air entry head (h_b) are also required by some of the models for the estimation of other input parameters (*e.g.*, head at the wetting front (h_f)). These values are listed in Tables 9 and 10. In addition to the tabulations indicated, the electronic database known as UNSODA (Leij *et al.*, 1996) provides information on the soil hydraulic parameters related to water retention and hydraulic conductivity. Estimates of infiltration based on tabulated parameter values should be considered only for preliminary, and order-of-magnitude type analyses. For a more reliable estimation of infiltration at a given site, it is recommended that the values of θ_s, θ_o, K_s, K_o, and the retention parameters be measured. Johnson and Ravi (1993) call for caution in the use of literature values for a specific application and discuss the resulting

uncertainty.

4.2 Estimation of F_w in SCS Model

The statistically derived parameter F_w utilized in the SCS model can be estimated based on the following equation:

$$F_w = \frac{1000}{CN_I} - 10 \qquad \textbf{(24)}$$

where CN_I is the soil moisture condition I curve number or hydrologic soil-cover complex number. CN_I is related to the soil moisture condition II curve number, CN_{II} , with the polynomial: $CN_I = -16.91 + 1.348\ CN_{II} - 0.01379(CN_{II})^2 + 0.0001177(CN_{II})^3$. F_w can be considered an estimate of the maximum potential difference between rainfall and runoff (Schwab *et al.*, 1981). The CN_{II} is based on an antecedent moisture condition (AMC) II determined by the total rainfall in the 5-day period preceding a storm (USDA-SCS, 1972). Three levels of AMC are used: (1) lower limit of moisture content, (2) average moisture content, and (3) upper limit of moisture content. Table 5 lists values for CN_{II} at the average AMC. The description of hydrologic groups used in Table 5 is provided in Table 6.

Table 5. Curve numbers CN_{II} for hydrologic soil-cover complex for the antecedent moisture condition II and $I_a = 0.2F_w$. I_a is initial water abstraction (USDA-SCS, 1972).

Land Use or Crop	Treatment or Practice	Hydrologic Condition	Hydrologic Soil Group			
			A	B	C	D
Fallow	Straight Row	---	77	86	91	94
Row Crops	Straight Row	Poor	72	81	88	91
	Straight Row	Good	67	78	85	89
	Contoured	Poor	70	79	84	88
	Contoured	Good	65	75	82	86
	Terraced	Poor	66	74	80	82
	Terraced	Good	62	71	78	81
Small Grain	Straight Row	Poor	65	76	84	88
	Straight Row	Good	63	75	83	87
	Contoured	Poor	63	74	82	85
	Contoured	Good	61	73	81	84
	Terraced	Poor	61	72	79	82
	Terraced	Good	59	70	78	81
Close-seeded Legumes or Rotation Meadow	Straight Row	Poor	66	77	85	89
	Straight Row	Good	58	72	81	85
	Contoured	Poor	64	75	83	85

	Contoured	Good	55	69	78	83
	Terraced	Poor	63	73	80	83
	Terraced	Good	51	67	76	80
Pasture or Range		Poor	68	79	86	89
		Fair	49	69	79	84
		Good	39	61	74	80
	Contoured	Poor	47	67	81	88
	Contoured	Fair	25	59	75	83
	Contoured	Good	6	35	70	79
Meadow		Good	30	58	71	78
Woods		Poor	45	66	77	83
		Fair	36	60	73	79
		Good	25	55	70	77
Farmsteads		---	59	74	82	86
Roads and Right-of-Way (Hard Surface		---	74	84	90	92

Table 6. Description of hydrologic soil groups.

Group	Description of Hydrologic Group
A	Lowest runoff potential. Includes deep sands with very little silt and clay, also deep, rapidly permeable loess.
B	Moderately low runoff potential. Mostly sandy soils less deep than Group A, and loess less deep or less aggregated than group A, but the group as a whole has above average infiltration after thorough wetting.
C	Moderately high runoff potential. Comprises shallow soils and soils containing considerable clay and colloids, though less than those of group D. The group has below-average infiltration after presaturation.
D	Highest runoff potential. Includes mostly clays of high swelling percent, but the group also includes some shallow soils with nearly impermeable subhorizons near the surface.

An example on how to determine the CN_{II} from Table 5 is given as follows. For pasture land with good hydrologic conditions, under moderately high runoff potential (Group C), the CN_{II} is 74 and CN_I is 55, and thus F_w is about 8.2 inches.

4.3 Estimation of Green-Ampt Model Parameters

The discussion presented here is relevant to the three models which utilize the Green-Ampt parameters: (1) the explicit Green-Ampt (Salvucci and Entekhabi, 1994), (2) the constant flux Green-Ampt model (Swartzendruber, 1974), and (3) the layered Green-Ampt model (Flerchinger

et al., 1988). The parameters θ_s, θ_o, K_s, and K_o are required in most models. If no measurements are available, then θ_s can be approximated based on soil texture (Table 7), and the residual or irreducible water content, θ_r, can be used in place of θ_o (Table 8), even though this would tend to overestimate infiltration. K_s and K_o correspond to the hydraulic conductivities at the respective water contents (*i.e.*, $K(\theta_s)$ and $K(\theta_o)$). K_s may be estimated based on Table 11. However, Bouwer (1966) recommended that K_s be taken as one half of K_{sat}, and K_o may be assumed to be zero. If the water content at the soil surface and the initial water content are quite different from that of the saturated and residual water contents, respectively, then K_s and K_o may be estimated from either the Brooks-Corey or the van Genuchten model for $K(\theta)$ (van Genuchten *et al.*, 1991). Typical values of θ_s, and θ_o for different textures are provided in Tables 7 and 8. Similarly, typical values of h_b and λ, respectively, for different textures are provided in Tables 9 and 10. Only the magnitude of h_b is provided in Table 9 (*i.e.*, the negative sign is omitted). Table 11 provides a summary of soil hydraulic parameters commonly used in the unsaturated zone models (Rawls *et al.*, 1992).

Table 7. Typical values of saturated volumetric water content (θ_s).

Texture	Brakensiek *et al.*, 1981	Panian, 1987	Carsel and Parrish, 1988
Sand	0.35	0.38	0.43
Loamy Sand	0.41	0.43	0.41
Sandy Loam	0.42	0.44	0.41
Loam	0.45	0.44	0.43
Silty Loam	0.48	0.49	0.45
Sandy Clay Loam	0.41	0.48	0.39
Clay Loam	0.48	0.47	0.41
Silty Clay Loam	0.47	0.48	0.43
Silty Clay	0.48	0.49	0.36
Clay	0.48	0.49	0.38

Table 8. Typical values of residual volumetric water content (θ_r).

Texture	Brakensiek *et al.*, 1981	Panian, 1987	Carsel and Parrish, 1988
Sand	0.054	0.020	0.045
Loamy Sand	0.060	0.032	0.057
Sandy Loam	0.118	0.045	0.065
Loam	0.078	0.057	0.078
Silty Loam	0.038	0.026	0.067
Sandy Clay Loam	0.188	0.093	0.100
Clay Loam	0.185	0.107	0.095
Silty Clay Loam	0.155	0.089	0.089
Silty Clay	0.182	0.102	0.070
Clay	0.226	0.178	0.068

Table 9. Typical values of air-entry head (h_b)(cm).

Texture	Brakensiek *et al.*, 1981	Panian, 1987	Carsel and Parrish, 1988
Sand	35.30	3.58	6.90
Loamy Sand	15.85	1.32	8.06
Sandy Loam	29.21	9.01	13.33
Loam	50.94	19.61	27.78
Silty Loam	69.55	31.25	50.00
Sandy Clay Loam	46.28	7.81	16.95
Clay Loam	42.28	31.25	52.63
Silty Clay Loam	57.78	30.30	100.00
Silty Clay	41.72	15.87	200.00
Clay	63.96	10.00	125.00

Table 10. Typical values of pore size index (λ).

Texture	Brakensiek *et al.*, 1981	Panian, 1987	Carsel and Parrish, 1988
Sand	0.57	0.40	1.68
Loamy Sand	0.46	0.47	1.28
Sandy Loam	0.40	0.52	0.89
Loam	0.26	0.40	0.56
Silty Loam	0.22	0.42	0.41
Sandy Clay Loam	0.37	0.44	0.48
Clay Loam	0.28	0.40	0.31
Silty Clay Loam	0.18	0.36	0.23
Silty Clay	0.21	0.38	0.09
Clay	0.21	0.41	0.09

Table 11. Typical values for soil hydraulic property parameters (Rawls *et al.*, 1992).

Texture Class	Sample Size	Total Porosity (ϕ)	Residual Water Content	Effective Porosity (ϕ_e)	Bubbling Pressure (h_b)		Pore Size Distribution (λ)		Water Retained at -33 kPa	Water Retained at -1500 kPa	Saturated Hydraulic Conductivity (K_s)
		cm³/cm³	*cm³/cm³*	*cm³/cm³*	Arithmetic *cm*	Geometric** *cm*	Arithmetic	Geometric**	*cm³/cm³*	*cm³/cm³*	*cm/hr*
Sand	762	0.437* (.374-.500)	0.020 (.001-.039)	0.417 (.354-.480)	15.98 (.24-31.72)	7.26 (1.36-38.74)	0.694 (.298-1.090)	0.592 (.334-1.051)	0.091 (.018-.164)	0.033 (.007-.059)	21.00
Loamy Sand	338	0.437 (.368-.506)	0.035 (.003-.067)	0.401 (.329-.473)	20.58 (-4.04-45.20)	8.69 (1.80-41.85)	0.553 (.234-.872)	0.474 (.271-.827)	0.125 (.060-.190)	0.055 (.019-.091)	6.11
Sandy Loam	666	0.453 (.351-.555)	0.041 (.024-.106)	0.412 (.283-.541)	30.20 (-3.61-64.01)	14.66 (3.45-62.24)	0.378 (.140-.616)	0.322 (.186-.558)	0.207 (.126-.288)	0.095 (.031-.159)	2.59
Loam	383	0.463 (.375-.551)	0.027 (.020-.074)	0.434 (.334-.534)	40.12 (-20.07-100.3)	11.15 (1.63-76.40)	0.252 (.086-.418)	0.220 (.137-.355)	0.270 (.195-.345)	0.117 (.069-.165)	1.32
Silt Loam	1206	0.501 (.420-.582)	0.015 (.028-.058)	0.486 (.394-.578)	50.87 (-7.68-109.4)	20.76 (3.58-120.4)	0.234 (.105-.363)	0.211 (.136-.326)	0.330 (.258-.402)	0.133 (.078-.188)	0.68
Sandy Clay Loam	498	0.398 (.332-.464)	0.068 (.001-.137)	0.330 (.235-.425)	59.41 (-4.62-123.4)	28.08 (5.57-141.5)	0.319 (.079-.889)	0.250 (.125-.502)	0.255 (.186-.324)	0.148 (.085-.211)	4.3
Clay Loam	366	0.464 (.409-.519)	0.075 (.024-.174)	0.390 (.279-.501)	56.43 (-11.44-124.3)	25.89 (5.80-115.7)	0.242 (.070-.414)	0.194 (.100-.377)	0.318 (.250-.386)	0.197 (.115-.279)	.23
Silty Clay Loam	689	0.471 (.418-.524)	0.040 (.038-.118)	0.432 (.347-.517)	70.33 (-3.26-143.9)	32.56 (6.68-158.7)	0.177 (.039-.315)	0.151 (.090-.253)	0.366 (.304-.428)	0.208 (.138-.278)	.15
Sandy Clay	45	0.430 (.370-.490)	0.109 (.013-.205)	0.321 (.201-.435)	79.48 (-20.15-179.1)	29.17 (4.96-171.6)	0.223 (.048-.398)	0.168 (.078-.364)	0.339 (.245-.433)	0.239 (.162-.316)	.12
Silty Clay	127	0.479 (.425-.533)	0.56 (.024-.136)	0.423 (.334-.512)	76.54 (-6.47-159.6)	34.19 (7.04-166.2)	0.150 (.040-.260)	0.127 (.074-.219)	0.387 (.332-.442)	0.250 (.193-.307)	.09
Clay	291	0.475 (.427-.523)	0.090 (.015-.195)	0.385 (.269-.501)	85.60 (-4.92-176.1)	37.30 (7.43-187.2)	0.165 (0.31-.293)	0.131 (.068-.253)	0.396 (.326-.466)	0.272 (.208-.336)	.06

*First line is the mean value, and second is one standard deviation about the mean.
**Antilog of the log mean.

The Green-Ampt model also requires two additional parameters, h_s and h_f, which correspond to the soil-water pressure at the surface and at the wetting front, respectively. While h_s is simply taken to be equal to the constant surface ponding depth, the estimation of h_f is difficult. It was believed for a long time since Green and Ampt proposed the model in 1911 that this parameter had no obvious physical significance. Bouwer (1966) was the first one to suggest that h_f can be related to measurable soil characteristics as follows:

$$h_f = \frac{1}{K_s} \int_0^{h_i} K(h)\, dh \qquad \textbf{(25)}$$

where *K(h)* is the unsaturated hydraulic conductivity expressed as a function of the soil-water pressure *h* (negative), and h_i is the initial soil-water pressure at the antecedent water content. Neuman (1976) provided a derivation of Equation 25 based on the Green-Ampt concept of piston displacement. He further stated that Equation 25 may be inappropriate for small times, since it takes some time for piston type flow to develop, and presented the following expression (Neuman, 1976) for h_f valid for small times:

$$h_f = \frac{1}{2K_s} \int_0^{h_i} \left[1 + \frac{\theta(h) - \theta_0}{\theta_s - \theta_0} \right] K(h)\, dh \qquad \textbf{(26)}$$

It is seen that if the Green-Ampt concept of an abrupt profile is invoked, then $\theta = \theta_s$, and Equation 26 immediately reduces to Equation 25. Based on a Brooks-Corey type model for *K(h)* and using Equation 25, Brakensiek and Onstad (1977) obtained the following form for h_f:

$$h_f = \frac{\eta}{\eta - 1} h_e \qquad \textbf{(27)}$$

where η is the exponent of the Brooks-Corey conductivity model and h_e is the air exit head. η is calculated as $(2 + 3\lambda)$, where λ is the exponent of the Brooks-Corey water retention model. The air exit head, h_e, may be taken as equal to one half of the air entry head, or the bubbling pressure head, h_b.

4.4 Estimation of Philip's Two-Term Model Parameters

The Philip's two-term model requires two parameters, *S* and *A*. *S* is the sorptivity of a soil defined by Equation 28 for the case of absorption or horizontal infiltration.

$$S = I/\sqrt{t} \qquad \textbf{(28)}$$

Sorptivity embodies in a single parameter the influence of capillarity on the transient infiltration process that occurs when a soil is introduced to a step change in water content at the surface from θ_o to θ_s. It should be noted that *S* depends strongly upon θ_o and θ_s, and has meaning only in relation to an initial state of the soil and an imposed boundary condition (Philip, 1969). Therefore, *typical S values for different soil textures cannot be tabulated*.

The primary difficulty in the application of the Philip's two-term model lies in the use of *A* over the whole time range. It is seen from Equation 3 that as *t* approaches infinity, the infiltration rate decreases monotonically to final infiltration rate, which is equal to K_s. This does not imply that *A* must be equal to K_s. Philip (1969) showed that other reasonable values for *A* are, $K_s/2$, $2K_s/3$, and $0.38K_s$. Further, Philip (1974) showed that *A* can also be equal to $0.363K_s$, and that this value for *A*, among all the others, resulted in the best agreement with the *exact q(t)* calculations for a real soil. Due to these reasons, Philip (1969) recommended that this model be only used for times that are not very large.

CHAPTER 5. EXAMPLE APPLICATION SCENARIOS

Six example application scenarios were chosen, and are illustrated in the following discussion. An application scenario is presented for each model. The intention of these scenarios is to provide guidance for users to apply infiltration models for various field conditions.

5.1 Semi-Empirical Model (SCS)

Statement of the Problem: This scenario was chosen to simulate water infiltration through a loamy sand soil for conditions with rainfall and surface runoff. A hypothetical site has been contaminated with hazardous waste materials and an estimate of the contaminant transport through the vadose zone is desired. Since the soil water infiltrating flux is an important factor controlling contaminant migration in the vadose zone, it must be first estimated before performing the contaminant transport modeling.

Conceptual model: Figure 3 is a schematic diagram of the hypothetical site showing the conceptual model for this scenario. The sandy material is bounded above by the soil surface and below by the ground-water table. Factors that affect the rate of water infiltration into the soil include initial soil moisture content, rainfall rate and duration, and surface runoff.

In this scenario, the purpose is to calculate the daily infiltration amount into the soil profile vertically during a process of rainfall and surface runoff. Since little is known concerning the mathematical boundary conditions for the site and little soil physical data available, the semi-empirical model known as the SCS model is chosen for the simulations.

Input Parameters: Input parameters for running the simulations are obtained from several sources. Attempts are made to obtain realistic values for the input parameters. Table 12 lists the input parameter values used for this scenario. In this model, only two input parameters are required (refer to Equations 1 and 2). For detailed estimation of F_w under different soil conditions, readers are encouraged to read the USDA report cited in the table. The daily rainfall amount can be obtained from a local weather station or climatic research institutes.

Table 12. Input parameter values for simulations with a sandy soil using the SCS model.

Parameter	Symbol	Value	Units	Reference
Statistically Derived	F_w	8.2	inches	USDA-SCS, 1972
Daily Rainfall Amount	P	0.1 to 10.0	inches	Assumed

Simulation Results: Figure 4 shows the daily infiltration amount as a function of the daily rainfall amount while Figure 5 shows the surface runoff as a function of the daily rainfall amount. Each point on the curves of Figures 4 and 5 could represent one rainfall event. In Figure 5, the runoff does not occur in the event where the daily rainfall amount is smaller than 1.64 inches ($0.2F_w$ =1.64 inches). Before runoff occurs, the daily infiltration amount equals the daily rainfall amount. After that, the daily infiltration amount increases as the daily rainfall amount increases but the rate of the increase of the daily infiltration decreases (Fig. 4). Note that the SCS model is applicable to the situation in which the *daily* amounts of rainfall, runoff and infiltration are of interest.

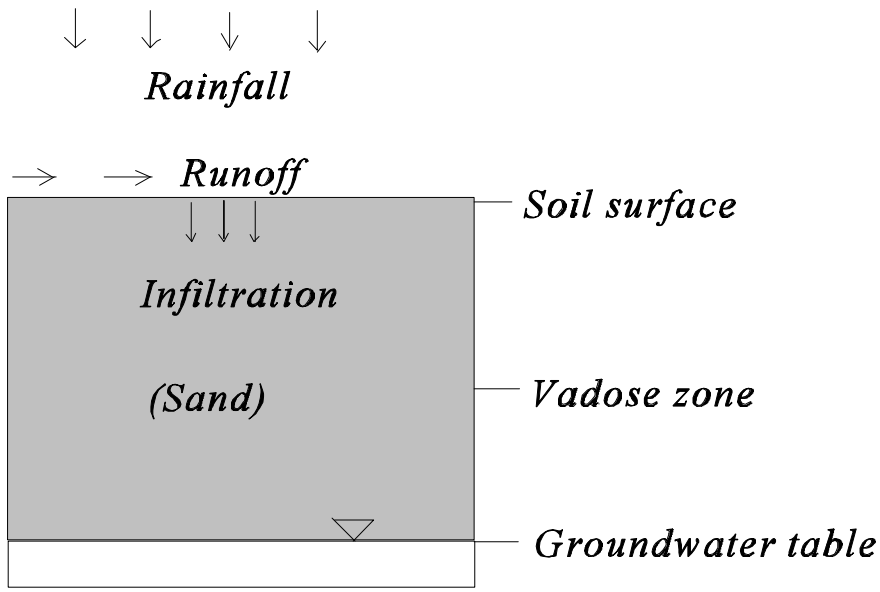

Figure 3. Conceptual model for simulating water infiltration using the SCS model.

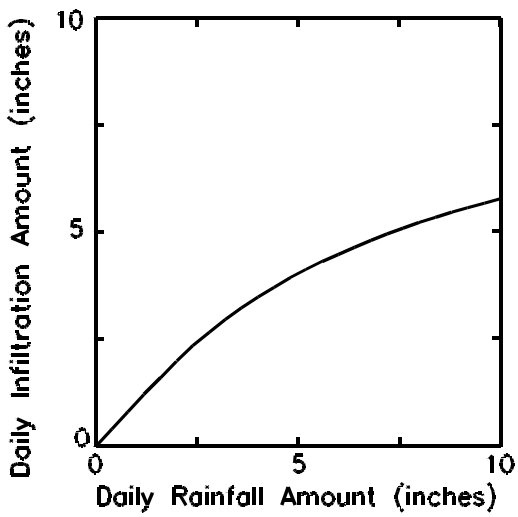

Figure 4. Daily infiltration amount as a function of daily rainfall amount.

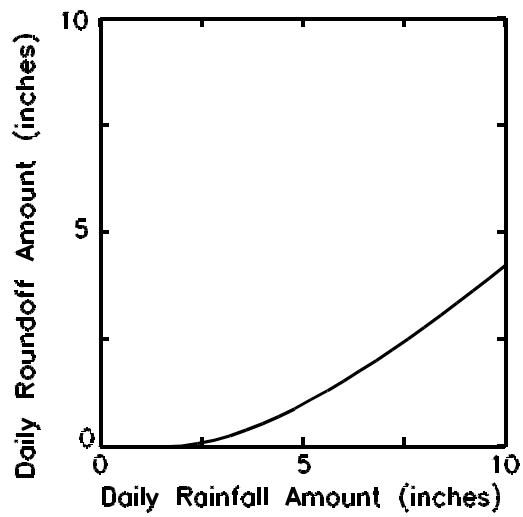

Figure 5. Daily runoff amount as a function of daily rainfall amount.

5.2 Infiltration Model for Homogeneous Conditions (PHILIP2T)

Statement of the Problem: This scenario was chosen to simulate the vertical infiltration of water into a sandy soil with a homogeneous soil profile. A hypothetical site has been contaminated with hazardous waste materials. In order to estimate the transport of the contaminants in the vadose zone, the infiltration rate (water flux) must be known before performing transport modeling. Initial soil water constant at the site is approximately uniformly distributed and constant. Soil water content at the inflow end (at the surface) is held constant and near saturation. Other soil physical properties such as saturated water content and saturated hydraulic conductivity values are available.

Conceptual model: Figure 6 is a schematic diagram of the hypothetical site showing the conceptual model for this scenario. This site is bounded above by the soil surface and below by the ground-water table. The water depth is much greater than the water penetration depth. The free water is available in excess at the surface and a constant water content at the surface is maintained through the infiltration period. In this scenario, the Philip's two-term model was selected for the simulations.

Input Parameters: Input parameters for running the simulations are obtained from several sources. Attempts are made to obtain realistic values for the input parameters. Table 13 lists the input parameter values used in the simulations. The sorptivity (*S*) and the constant (*A*) can be obtained simply by determining the slope and intercept of I/t versus $t^{-1/2}$ in Equation 4, respectively.

Table 13. Input parameter values for the simulations in a sandy soil using PHILIP2T model.

Parameter	Symbol	Value	Units	Reference
Duration of Infiltration	t	1 to 24	h	Assumed
Sorptivity	S	1	$cm/h^{1/2}$	Philip, 1969
Constant	A	7.6 (=0.363 k_s)	cm/h	Jury *et al.*, 1991
Saturated Hydraulic Conductivity	K_s	21	cm/h	Carsel and Parrish, 1988

Simulation Results: Figure 7 shows a typical soil infiltration pattern, with an infiltration rate relatively high at the onset of the infiltration, then decreasing, and eventually approaching a constant rate at $t > 20\ h$. Figure 8 illustrates a linear relationship between the cumulative infiltration and time. By knowing the soil water infiltration rate, the movement of contaminants in the soil could be evaluated using other transport models.

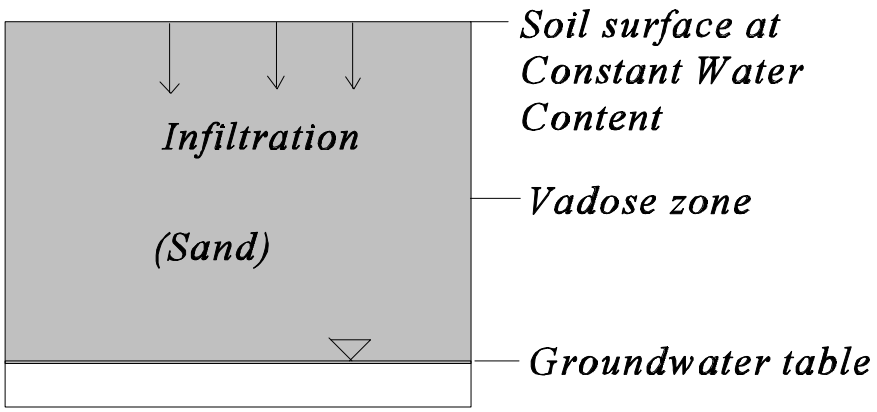

Figure 6. Conceptual model for simulating water infiltration using Philip's Two-Term Model.

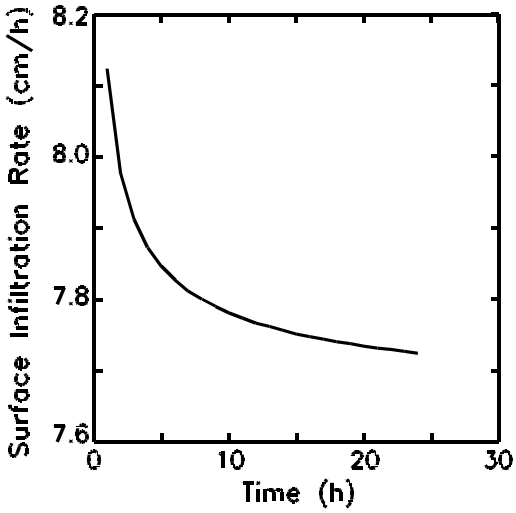

Figure 7. Surface water infiltration rate as a function of time.

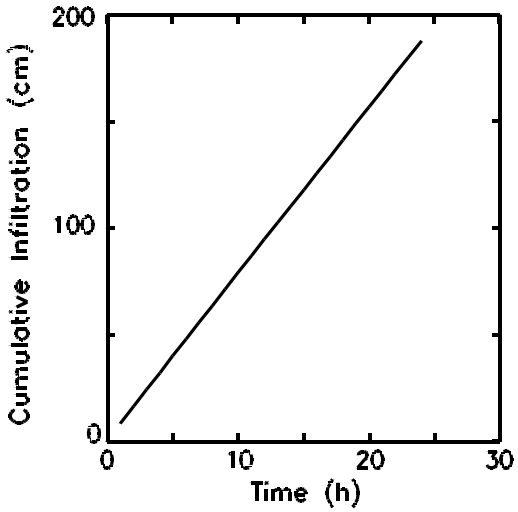

Figure 8. Cumulative infiltration as a function of time.

5.3. Infiltration Model for Nonhomogeneous Conditions (GALAYER)

Statement of the Problem: Since the soil profiles are differentiated into layers, the water distribution during infiltration is not uniform. Two scenarios were selected to calculate water infiltration into layered soils. In Scenario 1, the soil consists of two layers with a sand layer underlain by a loam. In Scenario 2, the soil consists of three layers with a sand layer underlain by a loam, and the loam underlain by a clay layer. Under such conditions, the infiltration rate is initially controlled by the sand layer, and with time the infiltration rate will become controlled by the lower fine-textured layer with the low hydraulic conductivity. Simulation results from these scenarios would provide information concerning water infiltrating into nonhomogeneous soil profiles.

Conceptual model: Figures 9a and 9b are the schematic diagrams of the layered soils showing the conceptual model for the Scenario 1 and the Scenario 2, respectively. In Scenario 1, the soil profile consists of sand and loam. The thickness of the sand layer is *10 cm.* The loam layer extends from the bottom of the first layer to the bottom of the soil profile. Scenario 1 is to estimate water infiltration into the sand layer and continuing through the loam layer. Scenario 2 is to estimate water infiltration into three layers (with sand, loam and clay in sequence). The thickness of the upper layers (sand and loam) is *10 cm.* The lowest layers (loam or clay) extend to the rest of the soil profile. In these scenarios, the GALAYER (Flerchinger et al., 1988) model for layered soils was selected for the simulations. The comparison of the two scenarios for water infiltration was also provided.

Input Parameters: Input parameters for running the simulations are obtained from several sources. Attempts are made to obtain realistic values for the input parameters. Table 14 listed the input parameter values used in the simulations.

Table 14. Input parameter values for the simulations using the GALAYER (Flerchinger et al., 1988) model.

Parameter	Symbol	Value	Units	Reference
Duration of Infiltration	t	1 to 24	h	Assumed
Saturated Hydraulic Conductivity (Layer 1)	K_1	1	cm/h	Hillel, 1982
Saturated Hydraulic Conductivity (Layer 2)	K_2	0.5	cm/h	Hillel, 1982
Saturated Hydraulic Conductivity (Layer 3)	K_3	0.1	cm/h	Hillel, 1982
Change in Volumetric Water Content in Layer 2 for Scenario 1.	$\Delta\theta_2$	0.2	cm^3/cm^3	Assumed
Change in Volumetric Water Content in Layer 3 for Scenario 2.	$\Delta\theta_3$	0.1	cm^3/cm^3	Assumed
Suction Head of Layer 2 for Scenario 1.	H_2	3000	cm	Hillel, 1982
Suction Head of Layer 3 for Scenario 2.	H_3	7000	cm	Hillel, 1982

Simulation Results: Water infiltration into the layered soil as a function of time is shown in Figure 10. The infiltration rate was relatively high at the onset of the infiltration, then decreased, and eventually approached a constant rate. Comparison of the two scenarios revealed that water infiltration is faster in the soil with two layers (Scenario 1) than in the soil with three layers (Scenario 2).

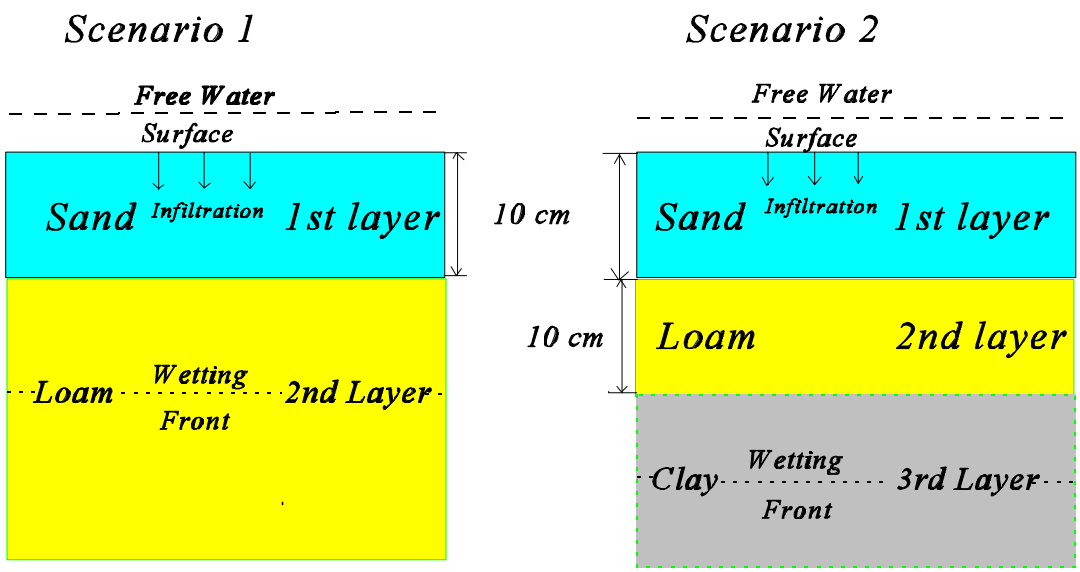

Figure 9. Conceptual model for simulating water infiltration into a layered soil.

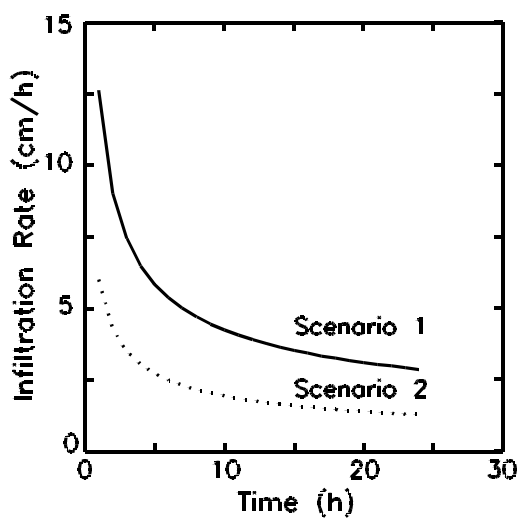

Figure 10. Comparison of water infiltration between Scenario 1 (solid line) and Scenario 2 (dotted line).

5.4 Infiltration Model for Ponding Conditions (GAEXP)

Statement of the Problem: This scenario was chosen to simulate water infiltration into a sandy soil under surface ponding conditions. A water depth of 1 cm was applied at the soil surface. The initial soil water content of *0.05* cm^3/cm^3 is uniformly distributed in the soil profile. Under such continuous ponding conditions, the infiltration rate (equal to the infiltrability) can be expected to settle down to a steady-induced rate which is practically equal to the saturated conductivity.

Conceptual model: Figure 11 is a schematic diagram of a sandy soil profile showing the conceptual model for this scenario. This soil profile is bounded above by the soil surface which is under the water ponding condition and below by a groundwater table. In this scenario, the Explicit Green-Ampt model was selected for the simulations.

Input Parameters: Input parameters for running the simulations are obtained from several sources. Attempts are made to obtain realistic values for the input parameters. Table 15 lists the input parameter values used in the simulations.

Table 15. Input parameters for the simulations in a clay soil using GAEXP Model.

Parameter	Symbol	Value	Units	Reference
Saturated Hydraulic Conductivity	K_s	21	cm/h	Carsel and Parrish, 1988
Ponding Depth	h_s	1	cm	Assumed
Saturated Volumetric Water Content	θ_s	0.43	cm^3/cm^3	Hillel, 1982
Initial Volumetric Water Content	θ_o	0.05	cm^3/cm^3	Assumed

Simulation Results: Figures 12 and 13 show the surface infiltration and cumulative infiltration as a function of time, respectively. A typical soil infiltration pattern, with an infiltration rate relatively high at the onset of the infiltration, then decreasing, and eventually approaching a constant rate was obtained for this sandy soil (Figure 12).

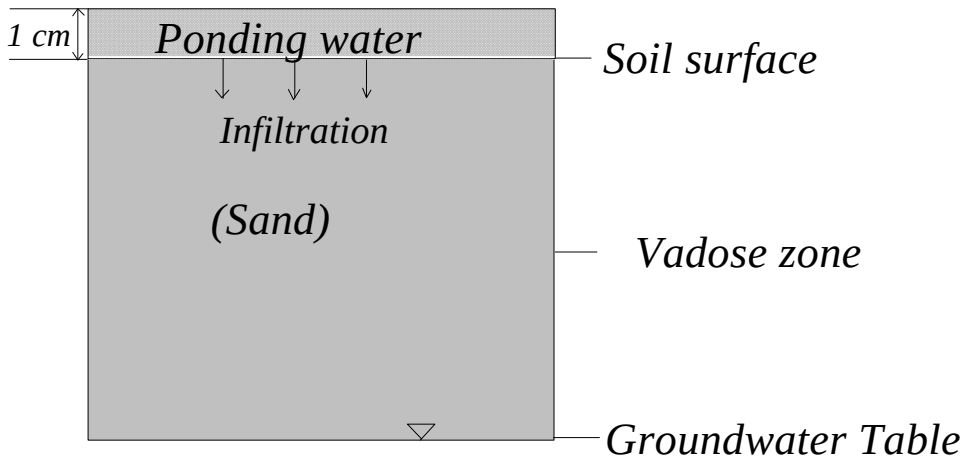

Figure 11. Conceptual model for simulating water infiltration using the Explicit Green-Ampt model.

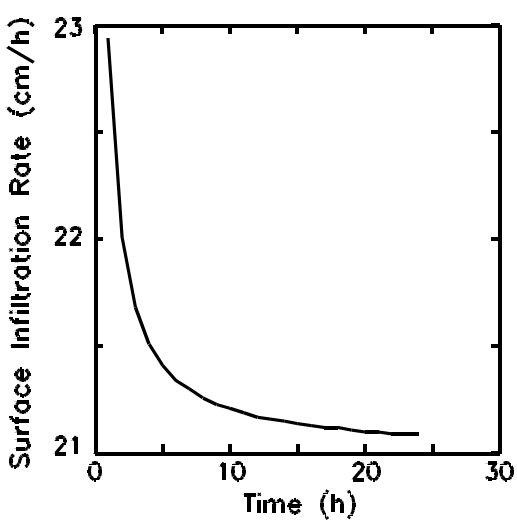

Figure 12. Water infiltration as a function of time.

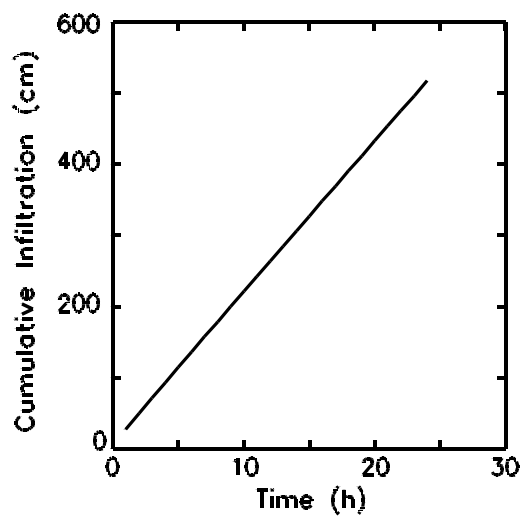

Figure 13. Cumulative infiltration as a function of time.

5.5 Infiltration Model for Non-ponding Conditions (GACONST)

Statement of the Problem: This scenario was chosen to simulate water infiltration into a sandy loam soil under non-ponding conditions. The initial soil water content of *0.05 cm³/cm³* is uniformly distributed in the soil profile. Under this non-ponding condition, water from rainfall or surface irrigation either enters the soil or flows over the surface as runoff.

Conceptual model: Figure 14 is a schematic diagram of a sandy loam soil profile showing the conceptual model for this scenario. This soil profile is bounded above by the soil surface which is under the non-ponding conditions and below by the groundwater table. No ponding occurs after the soil is saturated and the excess water is discharged as surface run-off. Several infiltration models for non-ponding conditions have been developed (Philip, 1957; Swartzendruber, 1974). In this scenario, the Constant Flux Green-Ampt Model was chosen for the simulations.

Input Parameters: Input parameters for running the simulations are obtained from Carsel and Parrish (1988). Attempts are made to obtain realistic values for the input parameters. Table 16 listed the input parameter values used in the simulations.

Table 16. Input parameters for the simulations with $r > K_s$ in a sandy loam soil using the GACONST model.

Parameter	Symbol	Value	Units	Reference
Saturated Hydraulic Conductivity	K_s	2.59	cm/h	Carsel and Parrish, 1988
Constant Application Rate	r	3.5	cm/h	Assumed
Saturated Volumetric Water Content	θ_s	0.41	cm^3/cm^3	Carsel and Parrish, 1988
Initial Volumetric Water Content	θ_o	0.05	cm^3/cm^3	Assumed
Air Exit Head	h_e	-13.33	cm	Carsel and Parrish, 1988
Pore Size Index	λ	0.89	-	Carsel and Parrish, 1988

Simulation Results: Figure 15 shows a constant-flux infiltration pattern when $r>K_s$. Before the surface saturation first occurs at time t_0 (5 hours), infiltration rate is constant and equals to r, after that, infiltration rate decreases with time. Figure 16 illustrates a linear relationship between the cumulative infiltration and time.

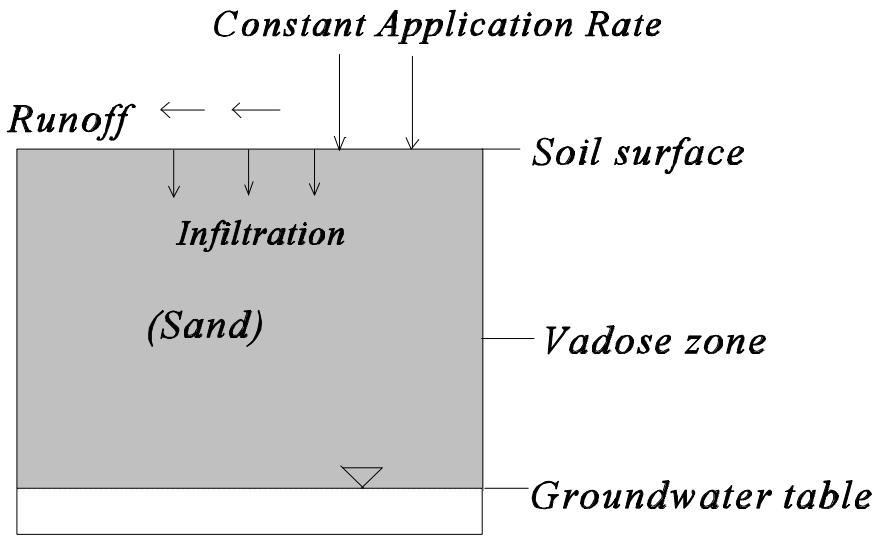

Figure 14. Conceptual model for simulating water infiltration using the constant flux Green-Ampt model.

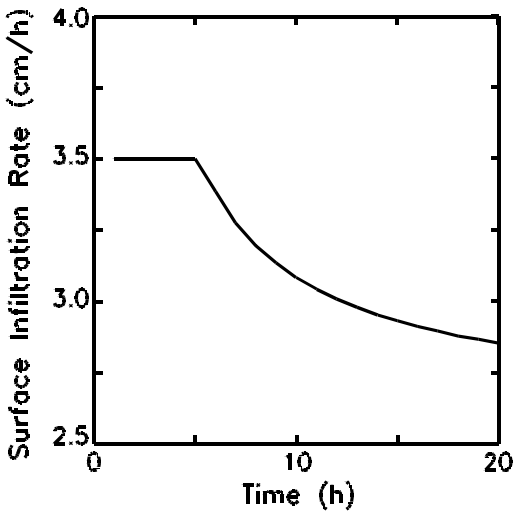

Figure 15. Water infiltration as a function of time.

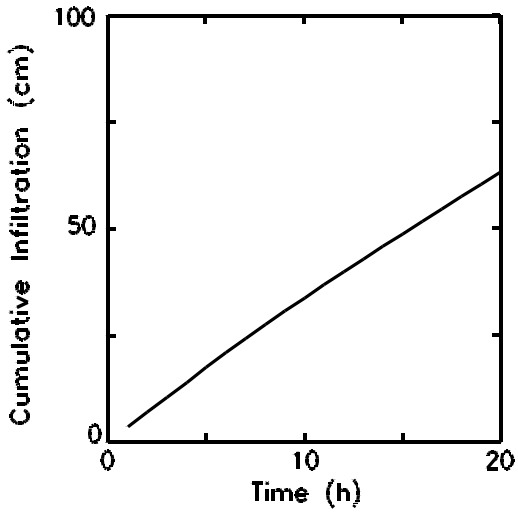

Figure 16. Cumulative infiltration as a function of time.

5.6 Infiltration and Exfiltration Model (INFEXF)

Statement of the Problem: The vertical movement of soil water in subsurface environments can be divided into two major processes: (1) infiltration and (2) exfiltration. An example was selected to calculate water infiltration and exfiltration in a homogeneous soil profile during wetting and drying seasons. The exfiltration process includes the capillary rise mechanism, evaporation, and water uptake by plant roots (transpiration).

Conceptual Model: Figure 17 is a schematic diagram of a sandy loam soil profile showing the conceptual model for this scenario. This soil profile is semi-infinite. The groundwater table is much greater than the water penetration depth. The surface rainfall, evaporation, and transpiration are included in the model. In this scenario, the INFEXF (Eagleson, 1978) model was chosen for the simulations. Two cases are presented separately. The first case is for infiltration. Infiltration is simulated during the storm period. The initial water content (θ_0) before the storm is 0.07 cm^3/cm^3. This case only considers the condition that rainfall intensity is greater than the infiltration capacity. In the second case, a uniform initial water content (θ_0) of 0.20 cm^3/cm^3 is assumed through redistribution after the storm. Also potential evaporation is assumed to be greater than the exfiltration capacity. The dry condition at the soil surface causes capillary rise and evaporation of water out of the soil surface. This case is simulated by the exfiltration equation 23.

Input Parameters: Input parameters for running the simulations are obtained from Eagleson (1978) and Carsel and Parrish (1988). Attempts are made to obtain realistic values for the input parameters. Table 17 lists the input parameter values used in the simulations. For estimations of other parameters in Equations 22 and 23, readers are referred to the report by Eagleson (1978).

Table 17. Input parameters for the simulations using the INFEXF model.

Parameter	Symbol	Value	Units	Reference
Saturated Hydraulic Conductivity	K_s	2.59	cm/h	Carsel and Parrish, 1988
Vegetated Fraction	M	0.2		Eagleson, 1978
Transpiration Rate	E_v	0.1	cm/h	Eagleson, 1978
Saturated Volumetric Water Content	θ_s	0.41	cm^3/cm^3	Carsel and Parrish, 1988
Initial Volumetric Water Content	θ_o	0.05	cm^3/cm^3	Assumed
Pore Distribution Index	λ	.89	-	Eagleson, 1978
Initial Volumetric Water Content During Interstorm Period	θ_o	0.20	cm^3/cm^3	Assumed

Simulation Results: Figure 18 shows a typical soil infiltration pattern, with an infiltration rate relatively high at the onset of the infiltration, then decreasing, and eventually approaching a constant rate. Figure 19 illustrates that exfiltration (actual evaporation) decreases with time. Negative value of exfiltration indicates that exfiltration has ceased (at the time of 11 hours in this case) but transpiration is still going on.

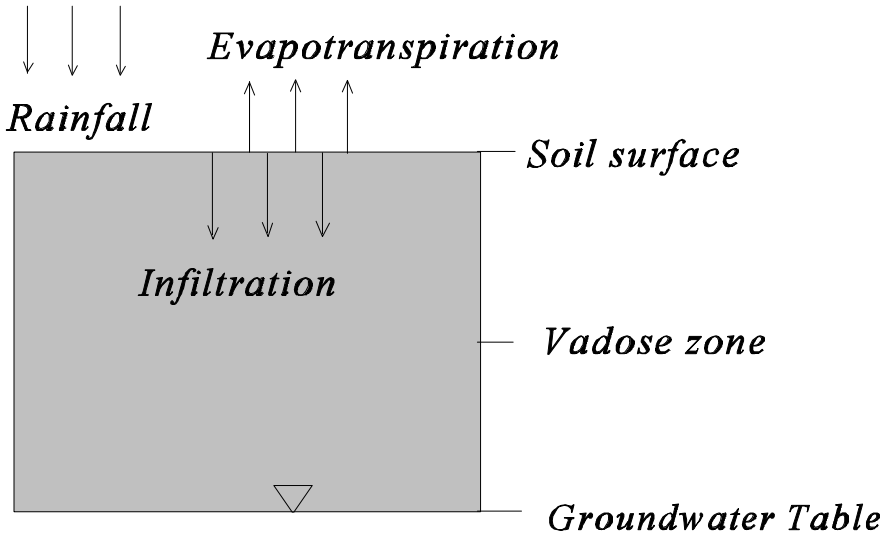

Figure 17. Conceptual model for simulating water infiltration and exfiltration.

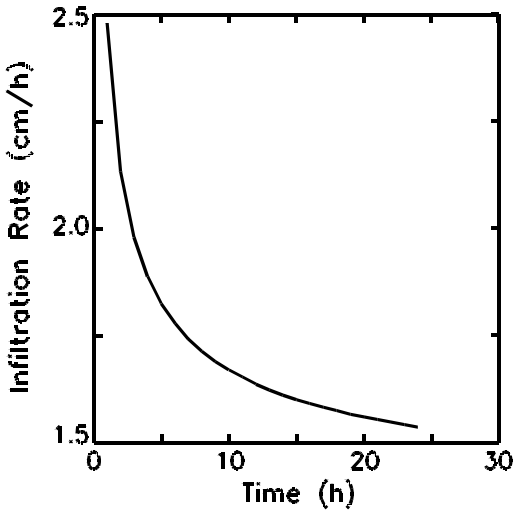

Figure 18. Water infiltration as a function of time.

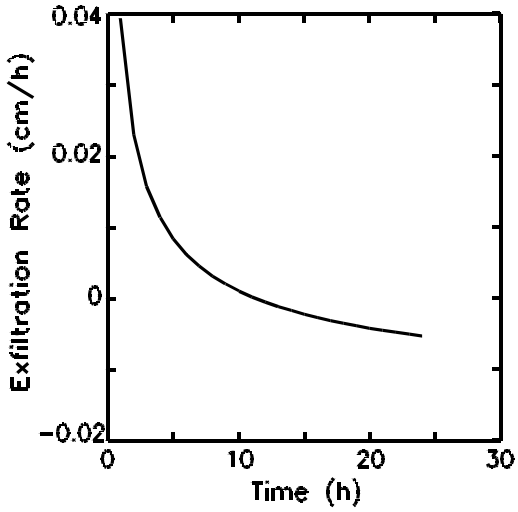

Figure 19. Water exfiltration as a function of time.

REFERENCES

Ahuja, L.R. and J.D. Ross. 1983. A new Green-Ampt type model for infiltration through a surface seal permitting transient parameters below the seal. In: Advance infiltration (Proc. Nat. Conf. On Advances in Infiltration), ASAE. 147-162.

Bouwer, H. 1966. Rapid field measurement of air entry value and hydraulic conductivity of soil as significant parameters in flow system analysis. Water Resour. Res., 2:729-738.

Bouwer, H. 1969. Infiltration of water into nonuniform soil. J. Irrigation and Drainage Division of ASCE 95:451-462.

Brakensiek, D. L., R. L. Engelman, and W. J. Rawls. Variation within texture classes of soil water parameters, Transaction of the ASAE 24:335-339, 1981.

Brakensiek, D.L., and C.A. Onstad, Parameter estimation of the Green and Ampt infiltration equation. Water Resour. Res., 13:1009-1012, 1977.

Breckenridge, R.P., J.R. Williams, and J.F. Keck. 1991. Characterizing soil for hazardous waste site assessments. EPA Ground-Water Issue Paper. EPA/540/4-91/003.

Carsel, R.F., and R.S. Parrish. 1988. Developing joint probability distributions of soil water retention characteristics. Water Resour. Res., 24:755-769.

Childs, E.C., and M. Bybordi. 1969. The vertical movement of water in stratified porous materials. I. Infiltration. Water Resour. Res., 5:446-459.

Corradini, C., F. Melone, and R.E. Smith. 1994. Modeling infiltration during complex rainfall sequences. Water Resour. Res., 30:2777-2784.

Eagleson, P. 1978. Climate, soil, and vegetation. 3. A simplified model of soil moisture movement in the liquid phase. Water Resour. Res., 14:722-730.

Flerchinger, G.N., F.J. Waltts, and G.L. Bloomsburg. 1988. Explicit solution to Green-Ampt equation for nonuniform soils. J. Irrig. and Drain. Div., ASCE, 114:561-565.

Fok, Y. -S. 1970. One-dimensional infiltration into layered soils. J. Irrig. and Drain. Div., ASCE, 90:121-129.

Ghildal, B.P., and R.P. Tripathi. 1987. Soil Physics. John Wiley & Sons. New York.

Haverkamp, R, J.Y. Parlange, J.L. Starr, Schmitz, and C. Fuentes. 1990. Infiltration under ponded conditions: 3. A predictive equation based on physical parameters. Soil Sci., 149:292-300.

Haverkamp, R., P.J. Ross, and J.Y. Parlange. 1994. Three-dimensional analysis of infiltration from the disc infiltrometer, 2. Physically based infiltration equation. Water Resour. Res. 30:2931-2935.

Hillel, D. 1982. Introduction to Soil Physics. Academic Press. New York.

Hillel, D., and W.R. Gardner. 1970. Measurement of unsaturated conductivity diffusivity by infiltration

through an impeding layer. Soil Sci., 109:149.

Johnson, J. A., and V. Ravi. 1993. Uncertainty in the use of literature soil hydraulic parameter data in ground-water modeling of the vadose zone, Robert S. Kerr Environmental Research Laboratory, Ada, Oklahoma (unpublished).

Jury, W.A., W.R. Gardner, and W.H. Gardner. 1991. Soil Physics. John Wiley & Sons. New York.

Leij, F.J., W.J. Alves, Martinus Th. van Genuchten, and J.R. Williams. 1996. The UNSODA unsaturated soil hydraulic database, User's Manual Version 1.0. National Risk Management Research Laboratory, Office of Research and Development, U.S. EPA, Cincinnati, Ohio 45268. EPA/600/R-96/095.

Li, E. A., V.O. Shanholtz, and E. W. Carson. 1976. Estimating saturated hydraulic conductivity and capillary potential at the wetting front. Department of Agricultural Engineers, Virginia Polytechnic Institute and State University, Blacksburg.

Moore, I.D. 1981. Infiltration equation modified for subsurf`ce effects. J. Irrigation and Drainage Division, ASCE(107:71-86.

Neuman, S.P. 1976. Wetting front pressure head in the infiltration model of Green and Ampt. Water Resour. Res., 12:564-566.

Pajian, T. F. 1987. Unsaturated flow properties data catalog, Volume II, Publication #45061, Water Resources Canter, Desert Research Institute, DOE/NV/10384-20.

Parlange, J. Y., R. Haverkamp, and J. Touma. 1985. Infiltration under ponded conditions. 1. Optimal analytical solution and comparison with experimental observations. Soil Sci., 139: 305-311.

Philip, J.R. 1957. The theory of infiltration* 4. Sorptivity and algebraic infiltration equations. Soil Sci., 84:257-264.

Philip, J.R. 1969. Theory of infiltration. Advances in Hydroscience. 5:215-296. Academic Press, New York, NY.

Philip, J.R. 1974. Recent progress in the solution of nonlinear diffusion equations. Soil Sci,, 117: 257-264,

Ravi, V and J.R Williams. 1998. Estimation of infiltration rate in the vadose zone: Compilation of simple mathematical models. Volume I. U.S. Environmental Protection Agency, Subsurface Protection and Remediation Division, National Risk Management Research Laboratory, Ada, Oklahoma, 74820. EPA/600/R-97/128a.

Rawls, W.J., L. R. Ahuja, and D. L. Brakensiek. 0992. Estimatinf soil hydraulic properties from soils data. In: van Genuchten, M. Th, F. J. Leij, and L. J. Lund (ed.). Indirect Methods for Estimating the Hydraulic Properties of Unsaturated Soils. Proceedings of the international workshop on indirect methods for estimating the hydraulic properties of unsaturated soils. Riverside, California, October 11-13, 1989. University of California, Riverside, CA 92521, USA.

Salvucci, G.D., and D. Entekhabi. 1994. Explicit expressions for Green-Ampt (Delta function diffusivity) infiltration rate and cumulative storage. Water Resour. Res., 30:2661-2663.

Schwab, G. O., R. F. Frevert, T. W. Edminster, and K. K. Barnes. 1981. Soil and Water Conservation

Engineering. 3rd Edition. John Wiley and Sons, New York.

Swartzendruber, D. 1974. Infiltration of constant-flux rainfall into soil as analyzed by the approach of Green and Ampt. Soil Sci., 117: 272-281.

van der Heijde, P.K.M., and O.A. Elnawawy. 1992. Quality assurance and quality control in the development and application of ground-water models. Robert S. Kerr Environmental Research Laboratory, U.S. Environmental Protection Agency, Ada, OK 74820. EPA/600/R-93/011.

van Genuchten, M. Th., F.J. Leij, and L.J. Lund. 1989. Indirect methods for estimating the hydraulic properties of unsaturated soils. Proceedings of the international workshop on indirect methods for estimating the hydraulic properties of unsaturated soils. Riverside, California, October 11-13, 1989. University of California, Riverside, CA 92521, USA.

van Genuchten, M. Th., F.J. Leij, and S. R. Yates. 1991. The RETC code for quantifying the Hydraulic Functions of unsaturated soils. Robert S. Kerr Environmental Research Laboratory, U.S. Environmental Protection agency, Ada, OK 74820. EPA/600/2-91/065.

USDA-SCS. 1972. National Engineering Handbook, Hydrology Section 4. USDA, Washington,DC.

US EPA, 1994a. Assessment framework for ground-water model applications. OSWER Directive #9029.00. EPA/500/B-94/003.

US EPA, 1994b. A technical guide to ground-water model selection at sites contaminated with radioactive substances. EPA/402/R-94/012.

US EPA, 1996. Documenting ground-water modeling at sites contaminated with radioactive substances. EPA/540/R-96/003, PB96-963302, January 1996.

APPENDICES

APPENDIX A

User's Instructions for MathCad Worksheets

Appendix A

User Instructions for Mathcad Worksheets

Infiltration models presented in this report have been incorporated into MathCad Plus 6.0® worksheets to facilitate their ease of use.[3] These worksheets are provided in both hardcopy and electronic formats, and are also available through the U.S.EPA/NRMRL/SPRD's Center for Subsurface Modeling Support (CSMoS). They have been developed on systems running Windows 3.x and Windows 95. The electronic formats from CSMoS can be obtained via diskette exchange or through the Center's website at *http://www.epa.gov/ada/kerrlab.html*. Each model is presented with a brief description, definition of variables, equations, results, discussion, and an example sensitivity analysis.

Before using these worksheets, make a backup copy of the files for retrieval of the initially distributed worksheets including equations and variable quantities. For greater accessibility to the worksheets, copy them to a subdirectory of the hard disk, preferably under a Mathcad associated directory. For example, if the main Mathcad subdirectory has the name *winmcad*, create a subdirectory under this directory with the name *infiltra* by entering the following from a DOS prompt.

```
C:\>cd winmcad
C:\winmcad>md infiltra
C:\winmcad>cd infiltra
C:\winmcad\infiltra>copy a:*.mcd
```
(Assuming that the distribution diskette is in drive A:.)

MathCad can now be executed from Windows, and the files of interest loaded from the *winmcad\infiltra* directory. There are a total of six (6) files distributed including: SCS.mcd, philip2t.mcd, galayer.mcd, gaexp.mcd, gaconst.mcd, stochmac.mcd, and infexf.mcd. Values for the various parameters can be easily changed, and the resulting output can quickly be observed to evaluate any changes resulting in the output. By utilizing the tiling features within Windows, the same worksheet can be loaded several times to allow side-by-side evaluation of results. As a word of caution, these files are not protected in any way from changes that can be made by the user. Therefore, any changes made and saved back to the same file name will result in the original information being lost.

[3]MathCad Plus 6.0 is a registered trademark of Mathsoft, Inc., of Cambridge, Massachusetts. Mention and use of this package, or any other commercial product does not constitute endorsement or recommendation for use.

Appendix B

MathCad Worksheets for Infiltration Models

Note that all references cited in the individual worksheets are listed in the references section of this document.

Appendix B

MathCad Worksheets for Infiltration Models

Note that all references cited in the individual worksheets are listed in the references section of this document.

B1. SCS Model

A. Description

The empirical approach to develop water infiltration equation consists of first finding a mathematical function whose shape as a function of time matches the observed features of the infiltration rate and then attempting a physical explanation of the process (Jury *et al*., 1991). In semi-empirical models, most physical processes are represented by commonly accepted and simplistic conceptual methods rather than by equations derived from fundamentally physical principles. The commonly used semi-empirical infiltration model in the fields of soil physics and hydrology is Soil Conservation Service (SCS) model. A scenario was chosen to simulate water infiltration into a soil for conditions with rainfall and surface run off by using the SCS model. Input parameters and simulation results are discussed below.

B. Definition of Variables

$P := 0.0, 0.4 .. 10.0$ **Daily rainfall amount (inches)**

$F_w := 8.2$ **Statistically derived parameter (Water retention parameter), (inches)**

C. Equations

$$R(P) := \begin{cases} \dfrac{(P - 0.2 \cdot F_w)^2}{P + 0.8 \cdot F_w} & \text{if } P > 0.2 \cdot (F_w) \\ 0 & \text{otherwise} \end{cases}$$

Daily surface runoff (inches) **(1)**

$$q(P) := P - R(P)$$

Daily infiltration amount (inches) **(2)**

D. Results

P	R(P)	q(P)
0	0	0
0.4	0	0.4
0.8	0	0.8
1.2	0	1.2
1.6	0	1.6
2	0.015	1.985
2.4	0.064	2.336
2.8	0.144	2.656
3.2	0.249	2.951
3.6	0.378	3.222
4	0.527	3.473
4.4	0.695	3.705

4.8	0.879	3.921
5.2	1.078	4.122
5.6	1.29	4.31
6	1.514	4.486
6.4	1.748	4.652
6.8	1.993	4.807
7.2	2.247	4.953
7.6	2.509	5.091
8	2.778	5.222
8.4	3.055	5.345
8.8	3.338	5.462
9.2	3.626	5.574
9.6	3.921	5.679
10	4.22	5.78

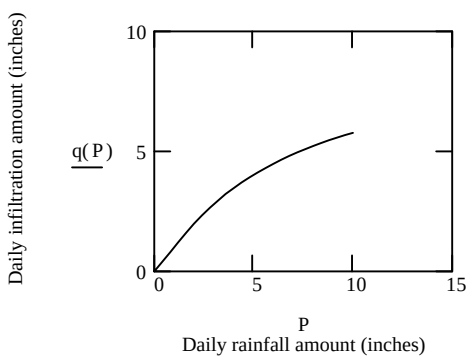

Figure B1-1. Daily infiltration amount as a function of daily rainfall amount.

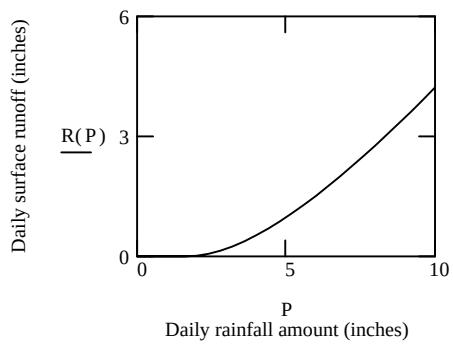

Figure B1-2. Daily runoff amount as a function of daily rainfall amount.

E. Discussion

Figure B1-1 shows the daily infiltration amount as a function of the daily rainfall amount while Figure B1-2 shows the surface runoff as a function of the daily rainfall amount. Each point on the curves of Figs. B1-1 and B1-2 could represent one rainfall event. In figure B1-2, the runoff does not occur in the event where the daily rainfall amount is smaller than 1.64 inches ($0.2F_w$ =1.64 inches). Before runoff occurs, the infiltration amount equals the rainfall amount. After that, the daily infiltration amount increases as the daily rainfall amount increases but the rate of the increase of the daily infiltration decreases (Fig. B1-1). Note that the SCS model is applicable to the situation in which the *daily* amounts of rainfall, runoff and infiltration are of interest.

B2. Philip's Two-Term Model (PHILIP2T)

A. Description

The Philip's two-term model (PHILIP2T) is a truncated form of the power series solution of Philip (1957). During the initial stages of infiltration, *i.e.*, when *t* is very small, the first term of Equation 1 below dominates. In this stage the vertical infiltration proceeds at almost the same rate as absorption or horizontal infiltration, because the gravity component, represented by the second terms of Equation 1, is negligible. As infiltration continues, the second term becomes progressively more important until it dominates the infiltration process. Philips (1957) suggested the use of the two-term model in applied hydrology when *t* is not too large. A scenario was chosen to simulate the water infiltration into a sandy soil by using the PHILIP2T model. Input parameters and simulation results were given below.

B. Definition of Variables

$t := 1..24$	**Duration of infiltration (h)**
$S := 1.0$	**The sorptivity of a soil defined by $S = I/(t)^{1/2}$ $(cm/h^{1/2})$ for the horizontal infiltration and is a function of the boundary and initial water contents Θ_0 and saturated water content Θ_s (Philip, 1969)**
$K_s := 21$	**Saturated hydraulic conductivity (cm/h)**
$A := 0.363 \cdot K_s$	**A constant in Equation 3 (cm/h)**

C. Equations

$$q(t) := \frac{1}{2} \cdot S \cdot t^{-\frac{1}{2}} + A \qquad \textbf{Infiltration rate} \qquad (1)$$

$$I(t) := S \cdot t^{\frac{1}{2}} + A \cdot t \qquad \textbf{Cumulative infiltration} \qquad (2)$$

D. Results

t	q(t)	I(t)
1	8.123	8.623
2	7.977	16.66
3	7.912	24.601
4	7.873	32.492
5	7.847	40.351
6	7.827	48.187
7	7.812	56.007
8	7.8	63.812
9	7.79	71.607
10	7.781	79.392
11	7.774	87.17
12	7.767	94.94
13	7.762	102.705

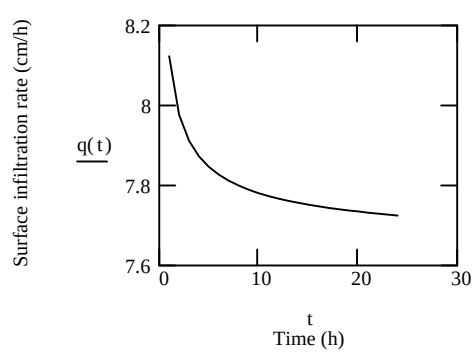

Figure B2-1. Surface infiltration as a function of time.

14	7.757	110.464
15	7.752	118.218
16	7.748	125.968
17	7.744	133.714
18	7.741	141.457
19	7.738	149.196
20	7.735	156.932
21	7.732	164.666
22	7.73	172.396
23	7.727	180.125
24	7.725	187.851

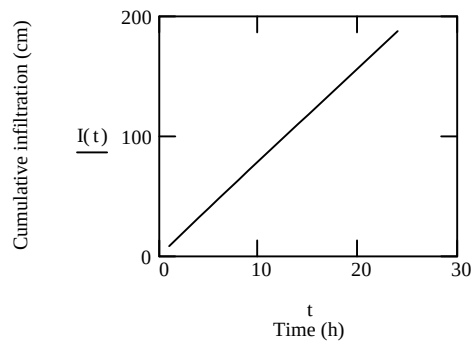

Figure B2-2. Cumulative Infiltration as a function of time.

E. Discussion

Figure B2-1 shows a typical soil infiltration pattern, with an infiltration rate relatively high at the onset of the infiltration, then decreasing, and eventually approaching a constant rate. The infiltration rate decreased by about 4% within the first 5 hours, then the infiltration rate decreased by 1.4% from from 5 to 20 hours, and finally decreased to 0.1% from 20 to 24 hours. Figure B2-2 illustrates that the cumulative infiltration increased with time. This occurred because more water accumulated in the soil as the time increase.

F. Sensitivity and Relative Sensitivity of Infiltration Rate to the Sorptivity of Soil

A sensitivity analysis is an estimation for how important an input parameter is to affecting the simulation results. Mathematically the sensitivity coefficient, S_s, is defined as:

$$S_s = df/dx \qquad (3)$$

where f represents the output of interest and x represents the input parameter (McCuen, 1973). The value of S_s calculated from this equation has units associated with it. This make it difficult to compare sensitivities for different input parameters. This problem can be overcome by using the relative sensitivity, S_r, given by

$$S_r = S\,(x/f) \qquad (4)$$

The relative sensitivity S_r gives the percentage change in response for each one percent change in the input parameter. If the absolute value of S_r is greater than *1*, the absolute value of the relative change in model output will be greater than the absolute value of the relative change in input parameter. If the absolute value of S_r is less than *1*, the absolute value of the relative change in model output will be less than the absolute value of the relative change in input (Nofziger *et al.*, 1994).

This section shows the sensitivity, S_s, and the relative sensitivity, S_r, of the surface infiltration rate, q, to the sorptivity of a soil, S. The expressions were obtained by applying Equations 3 and 4 to Equation 1 .

F.1. Input Data

$t := 5$ $\qquad$ $S := 0, 0.1 .. 2$

F.2. Sensitivity

$$S_s(S) := \frac{1}{2} \cdot t^{-\frac{1}{2}} \tag{5}$$

F.3. Relative Sensitivity

$$S_r(S) := \frac{S \cdot t^{-\frac{1}{2}}}{\left[S \cdot \left(t^{-\frac{1}{2}} \right) + 2 \cdot A \right]} \tag{6}$$

F.4. Results

S	$S_s(S)$	$S_r(S)$
0	0.224	0
0.1	0.224	$2.925 \cdot 10^{-3}$
0.2	0.224	$5.832 \cdot 10^{-3}$
0.3	0.224	$8.723 \cdot 10^{-3}$
0.4	0.224	0.012
0.5	0.224	0.014
0.6	0.224	0.017
0.7	0.224	0.02
0.8	0.224	0.023
0.9	0.224	0.026
1	0.224	0.028
1.1	0.224	0.031
1.2	0.224	0.034
1.3	0.224	0.037
1.4	0.224	0.039
1.5	0.224	0.042
1.6	0.224	0.045
1.7	0.224	0.047
1.8	0.224	0.05
1.9	0.224	0.053
2	0.224	0.055

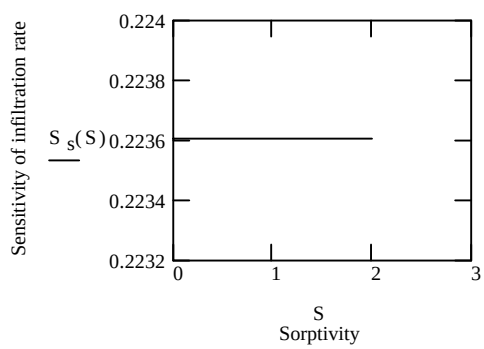

Figure B2-3. Sensitivity of infiltration rate for different values of sorptivity of the soil at *t = 5 h*.

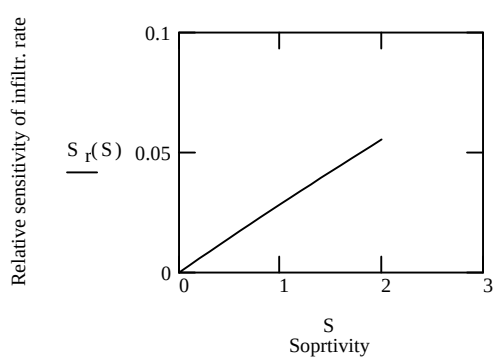

Figure B2-4. Relative sensitivity of infiltration rate for different values of sorptivity of the soil at *t = 5 h*.

F.5. Discussion

Figure B2-3 shows a sensitivity of the infiltration rate for different values of sorptivity of a soil, which has a constant value of *0.224* for all sorptivities of the soil at $t = 5\ h$. This implies that a 10-fold increase in sorptivity will have a 2.24-fold increase in infiltration rate. Figure B2-4 shows the relative sensitivity of infiltration rate for different values of sorptivity of the soil. The relative sensitivity increased as the sorptivity of the soil increased.

B3. Green-Ampt Model for Layered Systems (GALAYER)

A. Description

The Green-Ampt Model has been modified to calculate water infiltration into nonuniform soils by several researchers (Bouwer, 1969; Fok, 1970; Moore, 1981; Ahuja and Ross, 1983). In this section, the Green-Ampt model for layering systems (GALAYER) developed by Flerchinger *et al.* (1989) was selected to calculate water infiltration over time in vertically heterogeneous soils. Two simulation scenarios were selected in the application. The first scenario was to estimate water infiltration into a soil with two layers (sand and loam), while the second scenario was to estimate the water infiltration into a soil with three layers (with sand, loam, and clay in sequence). Comparison of the two scenarios for water infiltration was also provided.

B. Definition of Variables

$K_1 := 1$	**Hydraulic conductivity (cm/h) for layer 1 (Top layer)**
$K_2 := 0.5$	**Hydraulic conductivity (cm/h) for layer 2 (Middle layer)**
$K_3 := 0.1$	**Hydraulic conductivity (cm/h) for layer 3 (Bottom layer)**
$t := 1 .. 24$	**Time for infiltration (h)**
$\Delta\theta_{n1} := 0.2$	**Change in volumetric water content as wetting front passes in last layer for Scenario 1 (cm^3/cm^3)**
$K_{n1} := K_2$	**Hydraulic conductivity for last layer in Scenario 1 (cm/h)**
$H_{n1} := 3000$	**Potential head (cm) as the wetting front passes last layer for Scenario 1.**
$n := 2$	**Number of soil layers**
$Z_1 := 10$	**Depth of layer 1 (cm)**
$Z_2 := 10$	**Depth of layer 2 (cm)**
$\Delta\theta_{n2} := 0.1$	**Change in volumetric water content as wetting front passes in last layer for Scenario 2 (cm^3/cm^3)**
$K_{n2} := K_3$	**Hydraulic conductivity for last layer in Scenario 2 (cm/h)**
$H_{n2} := 7000$	**Potential head (cm) as the wetting front passes last layer for Scenario 2.**
$Z_3 := 10$	**Depth of layer 3 (cm) for scenario 2 with n=3**

C. Equations and Results

a. Scenario 1

$n := 2$

$n1 := n$

$$td(t) := \frac{K_{n1} \cdot t}{\Delta\theta_{n1} \cdot \left[H_{n1} + \sum_{i=1}^{n-1} Z_i \right]}$$

Dimensionless time since wetting front penetration. **(1)**

$$zd := \frac{K_{n1}}{\left[H_{n1} + \sum_{i=1}^{n-1} Z_i \right]} \cdot \sum_{i=1}^{n-1} \frac{Z_i}{K_i}$$

Dimensionless depth accounting for the thickness and conductivity of layers behind wetting front. **(2)**

$$Fd(t) := \frac{1}{2} \cdot \left[td(t) - 2 \cdot zd + \sqrt{(td(t) - 2 \cdot zd)^2 + 8 \cdot td(t)} \right]$$

Dimensionless accumulated infiltration. **(3)**

$$fd(t) := \frac{Fd(t) + 1}{Fd(t) + zd}$$

Dimensionless infiltration rate. **(4)**

$$f1(t) := fd(t) \cdot K_{n1}$$

Infiltration rate. **(5)**

t	f1(t)
1	12.618
2	9.036
3	7.448
4	6.501
5	5.855
6	5.378
7	5.007
8	4.708
9	4.461
10	4.251
11	4.071
12	3.914
13	3.775
14	3.652
15	3.541
16	3.441
17	3.349
18	3.266
19	3.189
20	3.118
21	3.052
22	2.99
23	2.933

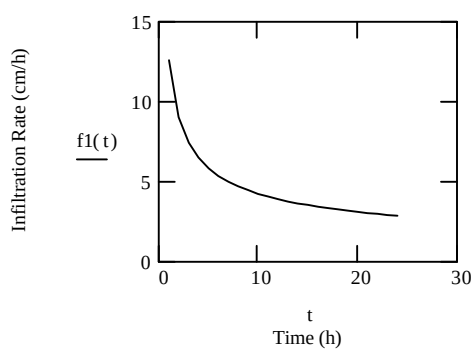

Figure B3-1. Water infiltration as a function of time through the layered soil profile in Scenario 1.

b. Scenario 2 2.879

$n := 3$

$n2 := n$

$$td(t) := \frac{K_{n2} \cdot t}{\Delta\theta_{n2} \cdot \left[H_{n2} + \sum_{i=1}^{n-1} Z_i \right]}$$

Dimensionless time since wetting front penetration. **(6)**

$$zd := \frac{K_{n2}}{\left[H_{n2} + \sum_{i=1}^{n-1} Z_i \right]} \cdot \sum_{i=1}^{n-1} \frac{Z_i}{K_i}$$

Dimensionless depth accounting for the thickness and conductivity of layers behind wetting front. **(7)**

$$Fd(t) := \frac{1}{2} \cdot \left[td(t) - 2 \cdot zd + \sqrt{(td(t) - 2 \cdot zd)^2 + 8 \cdot td(t)} \right]$$

Dimensionless accumulated infiltration. **(8)**

$$fd(t) := \frac{Fd(t) + 1}{Fd(t) + zd}$$

Dimensionless infiltration rate. **(9)**

$$f2(t) := fd(t) \cdot K_{n2}$$

Infiltration rate. **(10)**

t	f2(t)
1	5.996
2	4.262
3	3.494
4	3.036
5	2.724
6	2.493
7	2.314
8	2.169
9	2.049
10	1.948
11	1.861
12	1.785
13	1.718
14	1.658
15	1.604
16	1.556
17	1.512
18	1.471
19	1.434
20	1.4
21	1.368
22	1.338
23	1.31
24	1.284

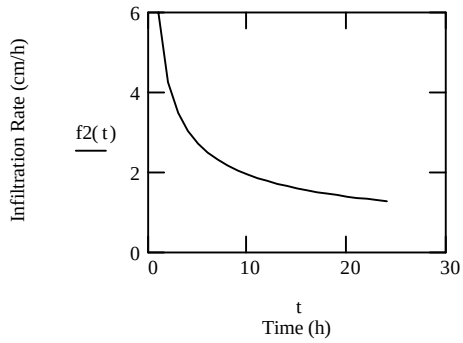

Figure B3-2. Water infiltration as a function of time through the layered soil profile in Scenario 2.

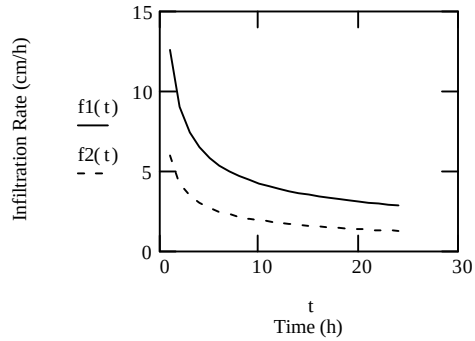

Figure B3-3. Comparison of water infiltration between Scenarios 1[solid line] and 2 [dash line].

E. Discussion

Water Infiltration into a two-layer soil (Scenario 1) and a three-layer soil (Scenario 2) as a function of time is given in Figures B3-1 and B3-2, respectively. These figures show that the infiltration rate is relatively high at the onset of the infiltration, then decreasing, and eventually approaching a constant rate at *t > 20 h*. Comparison of the two scenarios revealed that water infiltration is faster in the two-layer soil than in the three-layer soil.

F. Sensitivity of Infiltration Rate to $\Delta\Theta$

This section shows the sensitivity coefficient (S_s) and the relative sensitivity (S_r) of the surface infiltration rate to the change in volumetric water content. The expressions were obtained by applying Equations 3 and 4 in Section B2 (PHILIP2T model) to Equation 5 in this section. The input parameters were the same as in Scenario 2 except for $\Delta\Theta$ and t as shown below.

F.1. Input Data

$n := 3$

$n2 := n$

$\Delta\theta_n := 0.1, 0.11 .. 0.2$ $\qquad$ $t := 5$

F.2. Sensitivity Calculation Equations

$$td(\Delta\theta_n) := \frac{K_{n2} \cdot t}{\Delta\theta_n \cdot \left[H_{n2} + \left[\sum_{i=1}^{n-1} Z_i \right] \right]}$$

Dimensionless time since wetting front penetration. **(11)**

$$zd(\Delta\theta_n) := \frac{K_{n2}}{\left[H_{n2} + \sum_{i=1}^{n-1} Z_i \right]} \cdot \sum_{i=1}^{n-1} \frac{Z_i}{K_i}$$

Dimensionless depth accounting for the thickness and conductivity of layers behind wetting front. **(12)**

$$Fd(\Delta\theta_n) := \frac{1}{2} \cdot \left[td(\Delta\theta_n) - 2 \cdot zd(\Delta\theta_n) + \sqrt{\left(td(\Delta\theta_n) - 2 \cdot zd(\Delta\theta_n)\right)^2 + 8 \cdot td(\Delta\theta_n)} \right] \quad \textbf{(13)}$$

$$fd(\Delta\theta_n) := \frac{Fd(\Delta\theta_n) + 1}{Fd(\Delta\theta_n) + zd(\Delta\theta_n)} \quad \textbf{(14)}$$

$$f(\Delta\theta_n) := fd(\Delta\theta_n) \cdot K_{n2} \quad \textbf{(15)}$$

$$S_s(\Delta\theta_n) := \frac{d}{d\Delta\theta_n}\left(f(\Delta\theta_n)\right)$$ **Sensitivity** **(16)**

F.3. Results

$\Delta\theta_n$	$S_s(\Delta\theta_n)$
0.1	13.24
0.11	12.624
0.12	12.086
0.13	11.612
0.14	11.189
0.15	10.81
0.16	10.466
0.17	10.154
0.18	9.867
0.19	9.604
0.2	9.361

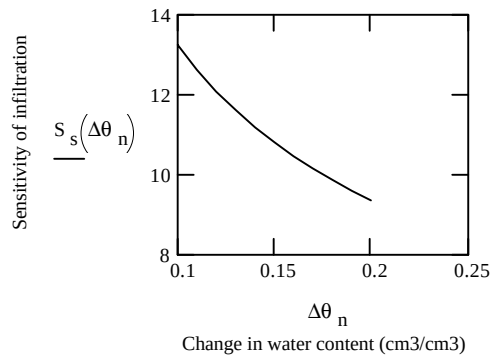

Figure B3-4. Sensitivity of infiltration rate for different values of the change in volumetric water content at the wetting front at *t = 5 h*.

F.4. Discussion

Figure B3-4 shows a sensitivity of the infiltration rate for different values of $\Delta\theta_n$. The sensitivity decreased as $\Delta\theta_n$ increased. A ten-fold increase in $\Delta\theta_n$ resulted in 30% decrease in sensitivity for conditions used in this application.

B4. Green-Ampt Explicit Model (GAEXP)

A. Description

The Green-Ampt model is the first physically-based equation describing the infiltration of water into a soil. It has been the subject of considerable developments in soil physics and hydrology owing to its simplicity and satisfactory performance for a great variety of water infiltration problems. This model yields cumulative infiltration and infiltration rate as implicit functions of time, *i.e.*, given a value of time, *t*, *q* and *I* cannot be obtained by direct substitution. The equations have to be solved in an iterative manner to obtain these quantities. Therefore, the required functions are *q(t)* and *I(t)* instead of *t(q)* and *t(I)*. The Green Ampt explicit model (GAEXP) for *q(t)* and *I(t)*, developed by Salvucci and Entekhabi (1994), facilitated a straight forward and accurate estimation of infiltration for any given time. This model supposedly yield less than 2% error at all times when compared to the exact values from the implicit Green-Ampt model. A scenario was chosen to simulate the water infiltration into a sandy soil under ponding conditions by using the GAEXP model. A ponding depth of 1 cm was applied at the soil surface. Input parameters and simulation results were given below.

B. Definition of Variables

$h_e := -6.9$	**Air exit head and is equal to one half of the bubbling pressure head (cm)**
$\lambda := 1.68$	**The exponent of the Brooks-Corey water retention model**
$\theta_s := 0.43$	**Saturated volumetric water content (cm^3/cm^3)**
$\theta_0 := 0.05$	**Initial volumetric water content (cm^3/cm^3)**
$K_s := 21$	**Saturated hydraulic conductivity (cm/h)**
$h_s := 1$	**Ponding depth or capillary pressure head at the surface (cm)**
$t := 1..24$	**Duration of infiltration (h)**

Values given above were obtained from Carsel and Parrish (1988) for a sandy soil.

C. Equations

$$\eta := (2 + 3\cdot\lambda) \tag{1}$$

$$h_f := \frac{\eta}{(\eta - 1)}\cdot h_e$$ **Capillary pressure head at the wetting front** **(2)**

$$\chi := \frac{(h_s - h_f)\cdot(\theta_s - \theta_0)}{K_s} \tag{3}$$

$$\tau(t) := \frac{t}{(t + \chi)} \tag{4}$$

$$q(t) := \left[\left(\frac{\sqrt{2}}{2}\right)\cdot\tau(t)^{\left(-\frac{1}{2}\right)} + \left(\frac{2}{3}\right) - \left(\frac{\sqrt{2}}{6}\right)\cdot\tau(t)^{\frac{1}{2}} + \left(\frac{1-\sqrt{2}}{3}\right)\cdot\tau(t)\right]\cdot K_s$$ **Infiltration rate** **(5)**

$$I(t) := \left[\left(1-\frac{\sqrt{2}}{3}\right)\cdot t+\frac{\sqrt{2}}{3}\cdot\sqrt{\chi\cdot t+t^2}+\left(\frac{\sqrt{2}-1}{3}\right)\cdot\chi\cdot(\ln(t+\chi)-\ln(\chi))+\frac{\sqrt{2}}{3}\cdot\chi\cdot\left(\ln\left(t+\frac{\chi}{2}+\sqrt{\chi\cdot t+t^2}\right)-\ln\left(\frac{\chi}{2}\right)\right)\right]\cdot K_s \quad \textbf{(6)}$$

Cumulative infiltration

D. Results

t	q(t)	I(t)
1	22.94	28.01
2	22.01	50.38
3	21.68	72.2
4	21.51	93.79
5	21.41	$1.15\cdot10^2$
6	21.34	$1.37\cdot10^2$
7	21.3	$1.58\cdot10^2$
8	21.26	$1.79\cdot10^2$
9	21.23	$2\cdot10^2$
10	21.21	$2.22\cdot10^2$
11	21.19	$2.43\cdot10^2$
12	21.17	$2.64\cdot10^2$
13	21.16	$2.85\cdot10^2$
14	21.15	$3.06\cdot10^2$
15	21.14	$3.28\cdot10^2$
16	21.13	$3.49\cdot10^2$
17	21.12	$3.7\cdot10^2$
18	21.12	$3.91\cdot10^2$
19	21.11	$4.12\cdot10^2$
20	21.1	$4.33\cdot10^2$
21	21.1	$4.54\cdot10^2$
22	21.09	$4.75\cdot10^2$
23	21.09	$4.96\cdot10^2$
24	21.09	$5.18\cdot10^2$

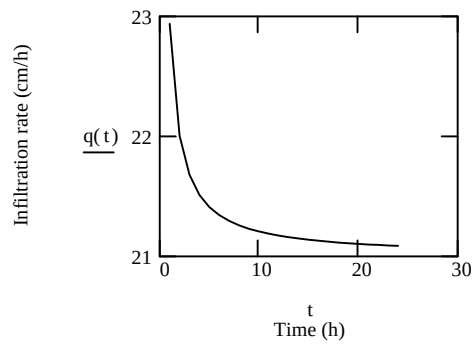

Figure B4-1. Soil infiltration as a function of time.

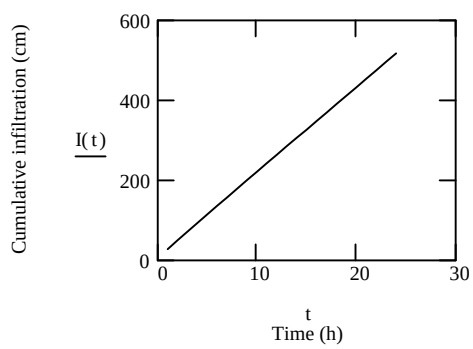

Figure B4-2. Cumulative Infiltration as a function of time.

E. Discussion

Figures B4-1 and B4-2 show the soil water infiltration rate and cumulative infiltration as a function of time, respectively. A rapid decrease in water infiltration rate was observed within the first 5 hours. From 5 to 24 hours, the water infiltration rate decreased gradually and finally approached a constant rate at t > 20 hours.

F. Sensitivity Analysis of Infiltration Rate to Saturated hydraulic Conductivity

This section shows the sensitivity coefficient (S_s) and the relative sensitivity (S_r) of the surface infiltration rate, q, to the saturated hydraulic conductivity (K_s) at the time of 5 hours. The expressions were obtained by applying Equations 3 and 4 in Section B2 (PHILIP2T model) to Equation 5 in this section.

F.1. Input Data

$$K_s := 20.5, 20.6 .. 21.5 \qquad t := 5$$

F.2. Sensitivity Calculation Equations

$$\chi(K_s) := \frac{(h_s - h_f)\cdot(\theta_s - \theta_0)}{K_s} \tag{7}$$

$$\tau(K_s) := \frac{t}{(t + \chi(K_s))} \tag{8}$$

$$q(K_s) := \left[\left(\frac{\sqrt{2}}{2}\right)\cdot\tau(K_s)^{\left(-\frac{1}{2}\right)} + \left(\frac{2}{3}\right) - \left(\frac{\sqrt{2}}{6}\right)\cdot\tau(K_s)^{\frac{1}{2}} + \left(\frac{1-\sqrt{2}}{3}\right)\cdot\tau(K_s)\right]\cdot K_s \tag{9}$$

$$S_s(K_s) := \frac{d}{dK_s} q(K_s) \qquad \textbf{Sensitivity} \tag{10}$$

$$S_r(K_s) := \left(\frac{d}{dK_s} q(K_s)\right)\cdot\left(\frac{K_s}{q(K_s)}\right) \qquad \textbf{Relative Sensitivity} \tag{11}$$

F.3.Results

K_s	$q(K_s)$	$S_s(K_s)$	$S_r(K_s)$
20.5	20.91	1.0003354	0.98
20.6	21.01	1.0003322	0.98
20.7	21.11	1.0003291	0.98
20.8	21.21	1.000326	0.98
20.9	21.31	1.000323	0.98
21	21.41	1.00032	0.98
21.1	21.51	1.000317	0.98
21.2	21.61	1.0003141	0.98
21.3	21.71	1.0003113	0.98
21.4	21.81	1.0003084	0.98
21.5	21.91	1.0003057	0.98

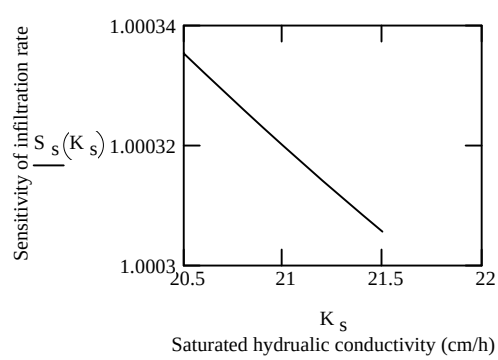

Figure B4-3. Sensitivity of infiltration rate for different values of saturated hydraulic conductivity at t = 5 hours.

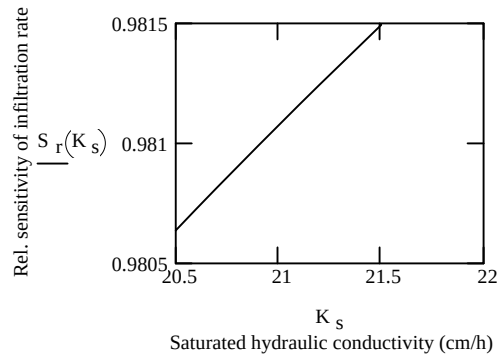

Figure B4-4. Relative sensitivity of infiltration rate for different values of saturated hydraulic conductivity at t = 5 hours.

F.4. Discussion

Figure B4-3 shows a sensitivity of the infiltration rate for different values of saturated hydraulic conductivity. The sensitivity decreased as the saturated hydraulic conductivity increased. Figure B4-4 shows the relative sensitivity of the infiltration rate for different values of saturated hydraulic conductivity. The relative sensitivity increased as the saturated hydraulic conductivity increased.

B5. Constant Flux Green-Ampt Model (GACONST)

A. Description

Let the water flux application rate at the surface be *r (cm/h)*. Here two cases need to be considered, first where $r > K_s$, and second where $r < K_s$. When $r > K_s$, surface water saturation first occurs at time t_0; when $r < K_s$, the infiltration rate *(q)* is always equal to the surface application rate *(r)* and the surface is never saturated. A scenario was chosen to simulate the water infiltration into a sandy soil under non-ponding conditions (a negligible thin layer of water ponds on the soil surface) by using the Green-Ampt model with constant application rate (GACONST). Input parameters and simulation results were given below.

B. Definition of Variables

$t := 1, 2 .. 20$	**Duration of infiltration (h)**
$r := 3.5$	**Constant water application rate at the surface (cm/h)**
$K_s := 2.59$	**Saturated hydraulic conductivity (cm/h)**
$\theta_s := 0.41$	**Saturated volumetric water content (cm^3/cm^3)**
$\theta_0 := 0.05$	**Initial volumetric water content (cm^3/cm^3)**
$\lambda := 0.89$	**The exponent of the Brooks-Corey water retention model**
$h_e := -13.33$	**Air exit head and is equal to one half of the bubbling pressure head (cm)**
$I_0 := 0.01$	**Initial guess for cumulative infiltration (cm)**

C. Equations

$$\eta := (2 + 3 \cdot \lambda) \tag{1}$$

$$h_f := \frac{\eta}{(\eta - 1)} \cdot h_e \tag{2}$$

$$t_0 := \begin{cases} \dfrac{-K_s \cdot h_f \cdot (\theta_s - \theta_0)}{r \cdot (r - K_s)} & \text{if } r > K_s \\ \infty & \text{otherwise} \end{cases} \qquad t_0 = 4.966 \tag{3}$$

$$Q_t(r, K_s, t, t_0) := \begin{cases} r & \text{if } (r \le K_s) \cdot (t > 0) \\ r & \text{if } (r > K_s) \cdot (t \le t_0) \end{cases} \tag{4}$$

$$I_1(r, K_s, t, t_0) := \begin{cases} r \cdot t & \text{if } (r \le K_s) \cdot (t > 0) \\ r \cdot t & \text{if } (r > K_s) \cdot (t \le t_0) \end{cases} \tag{5}$$

$$I_0 := \begin{cases} r \cdot t_0 & \text{if } r > K_s \\ \infty & \text{otherwise} \end{cases} \tag{6}$$

$$f_1(K_s, t, t_0, I, I_0) := \left[I - I_0 + h_f \cdot (\theta_s - \theta_0) \cdot \ln\left[\frac{I - (\theta_s - \theta_0) \cdot h_f}{I_0 - (\theta_s - \theta_0) \cdot h_f} \right] \right] - K_s \cdot (t - t_0) \tag{7}$$

$$f(t, I) := \left(\mathrm{root}\left(f_1(K_s, t, t_0, I, I_0), I\right)\right) \tag{8}$$

$$f(t, I) := \begin{cases} \left(\mathrm{root}\left(f_1(K_s, t, t_0, I, I_0), I\right)\right) & \text{if } (r > K_s) \cdot (t \geq t_0) \\ I_1(r, K_s, t, t_0) & \text{otherwise} \end{cases} \tag{9}$$

$$I_t := \begin{cases} \left(f(t, I_t)\right) & \text{if } (r > K_s) \cdot (t \geq t_0) \\ I_1(r, K_s, t, t_0) & \text{otherwise} \end{cases} \tag{10}$$

$$q_t := \begin{cases} K_s \cdot \left[1 - (\theta_s - \theta_0) \cdot \frac{h_f}{f(t, I_t)} \right] & \text{if } (r > K_s) \cdot (t \geq t_0) \\ Q_t(r, K_s, t, t_0) & \text{otherwise} \end{cases} \tag{11}$$

D. Results

t	q_t	I_t
1	3.5	3.5
2	3.5	7
3	3.5	10.5
4	3.5	14
5	3.494	17.5
6	3.346	20.915
7	3.243	24.207
8	3.167	27.41
9	3.108	30.546
10	3.06	33.629
11	3.021	36.67
12	2.989	39.674
13	2.961	42.649
14	2.937	45.597
15	2.916	48.524
16	2.898	51.43
17	2.881	54.319
18	2.867	57.193
19	2.853	60.053
20	2.841	62.9

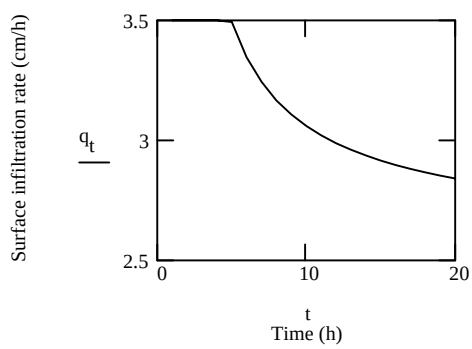

Figure B5-1. Surface infiltration rate as a function of time.

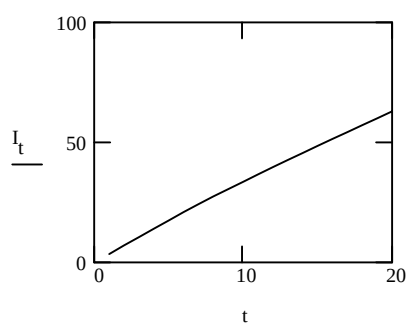

Figure B5-2. Cumulative Infiltration as function of time.

$r := 2.5$

$$t_0 := \begin{cases} \dfrac{-K_s \cdot h_f \cdot (\theta_s - \theta_0)}{r \cdot (r - K_s)} & \text{if } r > K_s \\ \infty & \text{otherwise} \end{cases} \qquad t_0 = 1 \cdot 10^{307} \tag{12}$$

$$Q_t(r, K_s, t, t_0) := \begin{cases} r & \text{if } (r \le K_s) \cdot (t > 0) \\ r & \text{if } (r > K_s) \cdot (t \le t_0) \end{cases} \tag{13}$$

$$I_1(r, K_s, t, t_0) := \begin{cases} r \cdot t & \text{if } (r \le K_s) \cdot (t > 0) \\ r \cdot t & \text{if } (r > K_s) \cdot (t \le t_0) \end{cases} \tag{14}$$

$$I_0 := \begin{cases} r \cdot t_0 & \text{if } (r > K_s) \\ \infty & \text{otherwise} \end{cases} \tag{15}$$

$$f_1(K_s, t, t_0, I, I_0) := \left[I - I_0 + h_f \cdot (\theta_s - \theta_0) \cdot \ln\left[\frac{I - (\theta_s - \theta_0) \cdot h_f}{I_0 - (\theta_s - \theta_0) \cdot h_f} \right] \right] - K_s \cdot (t - t_0) \tag{16}$$

$$f(t, I) := \begin{cases} \left(\mathrm{root}\left(f_1(K_s, t, t_0, I, I_0), I\right)\right) & \text{if } (r > K_s) \cdot (t \ge t_0) \\ I_1(r, K_s, t, t_0) & \text{otherwise} \end{cases} \tag{17}$$

$$I_t := \begin{cases} \left(f(t, I_t)\right) & \text{if } (r > K_s) \cdot (t \ge t_0) \\ I_1(r, K_s, t, t_0) & \text{otherwise} \end{cases} \tag{18}$$

$$q_t := \begin{cases} K_s \cdot \left[1 - (\theta_s - \theta_0) \cdot \dfrac{h_f}{f(t, I_t)} \right] & \text{if } (r > K_s) \cdot (t \ge t_0) \\ Q_t(r, K_s, t, t_0) & \text{otherwise} \end{cases} \tag{19}$$

t	q_t	I_t
1	2.5	2.5
2	2.5	5
3	2.5	7.5
4	2.5	10
5	2.5	12.5
6	2.5	15
7	2.5	17.5
8	2.5	20
9	2.5	22.5
10	2.5	25
11	2.5	27.5
12	2.5	30
13	2.5	32.5
14	2.5	35
15	2.5	37.5
16	2.5	40
17	2.5	42.5
18	2.5	45
19	2.5	47.5
20	2.5	50

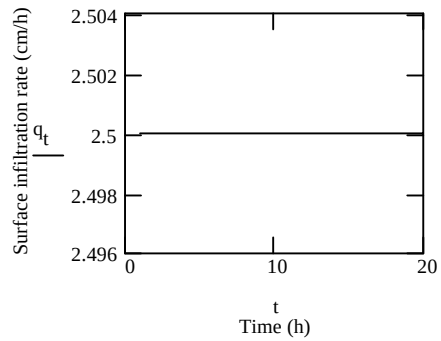

Figure B5-3. Surface infiltration rate as a function of time.

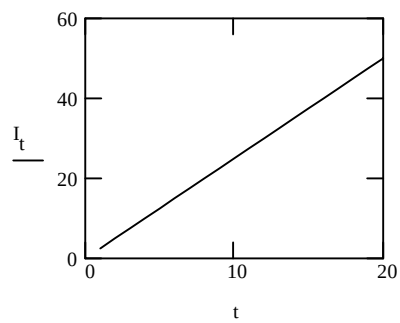

Figure B5-4. Cumulative Infiltration as function of time.

E. Discussion

Figure B5-1 shows a constant-flux infiltration pattern when $r>K_s$. Before the surface saturation first occurs at time t_0 (5 hours), infiltration rate is constant (=r) , after that, infiltration rate decreases with time. Figure B5-3 illustrates a soil infiltration with a constant rate equal to r. Figures B5-2 and B5-4 deplict a nearly linear relationship between the cumulative infiltration and time during the infiltration period.

B6. Infiltration/Exfiltration Model (INFEXF)

A. Description

The vertical movement of soil water between the surface and the water table can be divided into two processes according to the predominant forces involved: (1) infiltration and (2) exfiltration (evaportranspiration). An infiltration/exfiltration model (INFEXF) developed by Eagleson (1978) was selected to estimate the water infiltration during wetting season and exfiltration during drying season. Infiltration and exfiltration are described by Philip's equation, which assumes the medium to be effectively semi-infinite and the internal soil water content at the beginning of each storm and interstorm period is assumed to be uniform at its long term space-time average. The exfiltration equation is modified for presence of natural vegetation through the approximate introduction of a distributed sink representing the moisture extraction by plant roots. Two cases were presented in this application. The first case is the water infiltration into a sandy loam during storms. A boundary condition with saturated water content on the soil surface is assumed. In this case, rainfall intensity is assumed to be greater than the infiltration capacity. The second case is the exfiltration during drying surface (interstorm) periods with a dry soil surface and under the assumption that potential evaporation is greater than the exfiltration capacity.

B. Definition of Variables

$\theta_s := 0.41$	**Saturated volumetric water content at the soil surface (cm^3/cm^3)**
$\theta_0 := 0.07$	**Initial volumetric water content (cm^3/cm^3)**
$K_s := 2.59$	**Saturated hydrualic conductivity (cm/h)**
$\lambda := 0.89$	**Pore size distribution index**
$c := \frac{2 + 3\cdot\lambda}{\lambda}$	**Soil index based on the pore distribution index**

C. Equations and Results

a. Infiltration during Rainy Seasons

$t := 1 .. 24$	**Time (h)**
$\theta_1 := 0.41$	**Soil water content at surface (cm^3/cm^3)**
$S(\theta) := \frac{\theta}{\theta_s}$	**Degree of saturation**
$K(\theta) := K_s\cdot(S(\theta))^c$	**Hydraulic conductivity (cm/h)**
$\Psi 1 := -13.33$	**Near saturated soil water suction (cm)**

$$\Psi(\theta) := \Psi 1 \cdot S(\theta)^{\frac{-1}{\lambda}}$$ **Soil water suction (cm)** **(1)**

$$D(\theta) := K(\theta) \cdot \frac{d}{d\theta}(\Psi(\theta))$$ **Soil water diffusivity (cm²/h)** **(2)**

$$Di := \frac{5}{3} \cdot (\theta_1 - \theta_0)^{-\frac{5}{3}} \cdot \int_{\theta_0}^{\theta_1} (\theta - \theta_0)^{\frac{2}{3}} \cdot D(\theta)\, d\theta$$ **Diffusivity over range θ_1-θ_0, (cm/h$^{1/2}$)** **(3)**

$$Di = 38.218$$

$$S_i := 2 \cdot (\theta_1 - \theta_0) \cdot \left(\frac{Di}{\pi}\right)^{\frac{1}{2}}$$ **Sorptivity (cm/h$^{1/2}$)** **(4)**

$$fi_t := \frac{1}{2} \cdot S_i \cdot t^{\frac{-1}{2}} + \frac{1}{2} \cdot (K(\theta_1) + K(\theta_0))$$ **Infiltration rate (cm/h)** **(5)**

$$K(\theta_1) = 2.59 \qquad K(\theta_0) = 2.427 \cdot 10^{-4}$$

t	fi_t
1	2.481
2	2.134
3	1.98
4	1.888
5	1.825
6	1.779
7	1.743
8	1.714
9	1.69
10	1.67
11	1.653
12	1.637
13	1.624
14	1.612
15	1.601
16	1.592
17	1.583
18	1.575
19	1.567
20	1.56
21	1.554
22	1.548
23	1.542
24	1.537

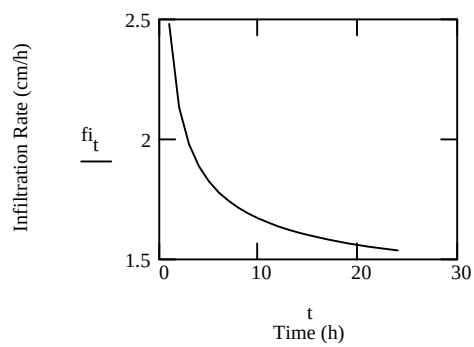

Figure B6-1. Water infiltration as a function of time during rainy season.

b. Exfiltration During Drying Season

$t := 1 .. 24$ **Time (h)**

$\theta_1 := 0.0001$ **Soil water content at dry surface (cm^3/cm^3)**

$\theta_0 := 0.15$ **Initial soil water content (cm^3/cm^3)**

$\Psi 1 := -13.33$ **Near saturated soil water suction (cm)**

$Ev := 0.05$ **Transpiration rate (cm/h)**

$M := 0.2$ **Vegetated fraction of land surface**

$$\Psi(\theta) := \Psi 1 \cdot S(\theta)^{\frac{-1}{\lambda}}$$ **Soil water suction (cm)** **(6)**

$$D(\theta) := K(\theta) \cdot \frac{d}{d\theta}(\Psi(\theta))$$ **Soil water diffusivity (cm^2/h)** **(7)**

$$De := (1.85) \cdot \left(\theta_0 - \theta_1\right)^{-(1.85)} \cdot \int_{\theta_1}^{\theta_0} \left(\theta_0 - \theta\right)^{0.85} \cdot D(\theta)\, d\theta$$ **Desorption diffusivity (cm^2/h)** **(8)**

$De = 0.439$

$$Se := 2 \cdot \left(\theta_0 - \theta_1\right) \cdot \left(\frac{De}{\pi}\right)^{\frac{1}{2}}$$ **Exfiltration sorptivity ($cm/h^{1/2}$)** **(9)**

$Se = 0.112$

$$fe_t := \frac{1}{2} \cdot Se \cdot t^{\frac{-1}{2}} - \frac{1}{2} \cdot \left(K\left(\theta_1\right) + K\left(\theta_0\right)\right) - M \cdot Ev$$ **Exfiltration rate (cm/h)** **(10)**

t	fe_t
1	0.039
2	0.023
3	0.016
4	0.011
5	$8.427 \cdot 10^{-3}$
6	$6.245 \cdot 10^{-3}$
7	$4.549 \cdot 10^{-3}$
8	$3.182 \cdot 10^{-3}$
9	$2.049 \cdot 10^{-3}$
10	$1.091 \cdot 10^{-3}$
11	
12	

12	$2.669 \cdot 10^{-4}$
13	$-4.52 \cdot 10^{-4}$
14	$-1.086 \cdot 10^{-3}$
15	$-1.651 \cdot 10^{-3}$
16	$-2.159 \cdot 10^{-3}$
17	$-2.618 \cdot 10^{-3}$
18	$-3.036 \cdot 10^{-3}$
19	$-3.419 \cdot 10^{-3}$
20	$-3.771 \cdot 10^{-3}$
21	$-4.096 \cdot 10^{-3}$
22	$-4.398 \cdot 10^{-3}$
23	$-4.679 \cdot 10^{-3}$
24	$-4.942 \cdot 10^{-3}$
	$-5.188 \cdot 10^{-3}$

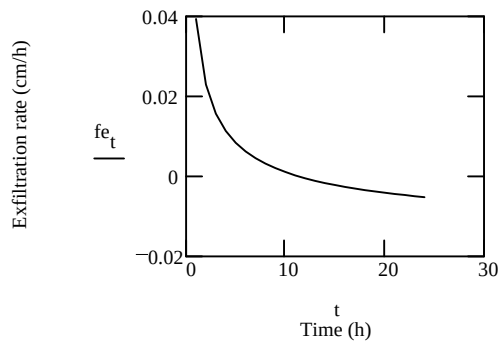

Figure B6-2. Water exfiltration as a function of time during drying season.

D. Discussion

Water Infiltration into and exfiltration out of soil surface as a function of time is shown in Figures B6-1 and B6-2, respectively. Figure B6-1 shows a typical soil infiltration pattern, with an infiltration rate relatively high at the onset of the infiltration, then decreasing, and eventually approaching a constant rate. Figure B6-2 (Case 2) illustrates that exfiltration (actual evaporation) decreases with time. Nagative value of exfiltration indicates that exfiltration has ceased (at the time of 11 hours in this case) but transpiration is still going on.

APPENDIX C

Sensitivity Analysis Discussion and Demonstration

Sensitivity Analysis Discussion and Demonstration

1. Introduction

Sensitivity analysis should be considered an essential step to all mathematical-based model applications. To the users of these models, the sensitivity analysis can provide a basis for greater understanding of the processes identified in a site conceptualization. This appendix is provided to model users as (1) an explanation of the purpose of the sensitivity analysis, (2) a working definition of sensitivity coefficients, (3) an explanation of approaches to the sensitivity analysis, (4) an explanation of the role of sensitivity in an parameter uncertainty analysis, and (5) a set of tools, or procedures for conducting a sensitivity analysis. As an example, a sensitivity analysis is given for the Philip's two-term model using a published dataset from an infiltration experiment. Uncertainty estimation of model outputs due to uncertain input parameters is also analyzed using another set of reported field experimental data. Implications of the case studies of sensitivity analysis using these two sets of experimental data for Philip's two-term model are also discussed.

2. Purpose of Sensitivity Analysis

The purpose of conducting a sensitivity analysis is two-fold. That is, first to evaluate model's response to changes in input parameters, and secondly, to quantify the likely uncertainty of the calibrated model resulting from uncertainties associated with the input parameters, stresses, and boundary conditions (Anderson and Woessner, 1992; Zheng and Bennett, 1995). The sensitivity analysis can be used to estimate model parameters, design experiments, and analyze ground-water management problems (Skaggs and Barry, 1996). In field sampling, sensitivity analysis can assist with the identification of parameters requiring more accurate measurements. This will be driven by the need to reduce overall uncertainty in the model results, as well as to identify parameters requiring less precision and thereby saving time, money and effort in the data collection process. In the model development process, sensitivity analysis can be utilized to determine the need for specific parameters in the final model. This would be dependent on the significance of the parameter to the model output (Hamby, 1994).

3. Sensitivity Coefficients

Sensitivity (S) is a measure of the impact of change in one input parameter on an output result. The sensitivity ($S_{i,j}$) of the jth model dependent variable (y_j) to the ith model input parameter (x_i) is the partial derivative of the dependent variable with respect to the input parameter, and is expressed as

$$S_{i,j} = \frac{\partial y_i}{\partial x_j} \qquad \text{(C1)}$$

where i is the index for i^{th} model dependent variable (*i.e.*, model output), j is the index for j^{th}

model input parameter. For a model with *n* output variables and *m* input parameters, the number of sensitivity coefficients that could be generated is given by *nm*. The units for $S_{i,j}$ are the units of y_i over the units of x_i. For convenience of comparing the sensitivity coefficients of varying parameters and dependent variables, as well as comparing different models, a normalized form of the sensitivity coefficient defined in Equation C1 is utilized. The normalized form is given by Equation C2.

$$S_{i,j}^{r} = \frac{\partial y_i}{\partial x_j} \frac{x_j}{y_i} \tag{C2}$$

The normalized sensitivity, $S_{i,j}^{r}$, is referred to as the relative sensitivity of dependent variable y_i with respect to independent input parameter x_j. The normalized sensitivity coefficient $S_{i,j}^{r}$ is dimensionless.

4. Approaches to Computing Sensitivity Coefficients

Three approaches for computing sensitivity coefficients are commonly recognized and used. They are the direct, the perturbation, and the adjoint methods (Skaggs and Barry, 1996). The *direct method* computes the sensitivity coefficients analytically through the solving of the coefficients' governing equations. These equations are obtained by differentiating the governing equation and associated boundary and initial conditions with respect to model input parameters of interest. Sensitivity coefficients are calculated from the sensitivity equations using a base set of model parameters. The *perturbation method*, also known as the divided difference method, computes a numerical approximation to the sensitivity coefficients for the model input parameters. The perturbation method is the simplest of the sensitivity methods and is widely used. The adjoint method also makes use of sensitivity equations, but rather than solving them directly, the sensitivities are obtained by solving the adjoint problem. In the adjoint method, the functionals (e.g., concentration in solute transport problem), that dependent on state variables (e.g., velocity and head) and model parameters, are formulated, and the sensitivity of functionals are computed without evaluating the sensitivities of the state variables. As a result, it can lead to computational savings. The details of this method can be seen in Skaggs and Barry (1996).

Complex models, for which analytical sensitivity equations are not easily derived, generally result in the need for using the perturbation method. The sensitivity coefficients are calculated using the approximation forms (*i.e.*, the difference equations) of Equations C1 and C2. The difference forms for these equations are given by

$$S_{i,j} = \frac{\partial y_i}{\partial x_j} \approx \frac{\Delta y_i}{\Delta x_j} \tag{C3}$$

and

$$S_{i,j}^{r} = \frac{\partial y_i}{\partial x_j}\frac{x_j}{y_i} \approx \frac{\Delta y_i}{\Delta x_j}\frac{x_j}{y_i} \qquad \text{(C4)}$$

where Δy_i is the change of y_i due to an infinitesimal change (Δx_j) in x_j.

In addition to these three methods of calculating sensitivity coefficients, other approaches are also used based on differing needs and objectives. Furthermore, the reader must be aware that slightly different definitions of "sensitivity coefficients" could be defined in literature. In this regard, Hamby (1994, 1995) has provided a detailed review and evaluation of more than ten sensitivity methods.

5. Role of Sensitivity in Uncertainty Analysis

To examine the deviation of model output (Δf) due to the deviation (x-x_o) of input parameters, the Taylor's formula can be used

$$\Delta f = f(x) - f(x_o) = \frac{(x - x_o)}{1!} f_x(x_o) + \frac{(x - x_o)\sup 2}{2!} f_{xx}(x_o) + \ldots + \frac{(x - x_o)^n}{n!} f_{(n)}(x_o) + R_n(x_o) \qquad \text{(C5)}$$

where $f(x_o)$ is the function value in the neighborhood of a point $x=x_o$; $f_x(x_o)$, $f_{xx}(x_o)$, $f_{(n)}(x_o)$, are the first, second, and nth derivatives of $f(x)$ with respect to x at $x=x_o$, and $R_n(x_o)$ is the remainder. Here $f_x(x_o)$ is the sensitivity coefficient as defined in Equation C1 and evaluated at $x=x_o$. When high-order terms are ignored, Δf is approximated by the first term, $(x-x_o)\cdot f_x$, in Equation C5. In other words, the deviation of the model output (Δf) can be approximated by the product of deviation of input parameter (x-x_o) and sensitivity ($f_x=S_{i,j}$)

Equation C5 is useful for the analysis of a single set of input parameters (*i.e.*, only one realization). The common way to quantify uncertainty is to treat the input parameters as random variables. For examining model uncertainty (in terms of variance or covariance) due to uncertain input parameters, the First-Order Second-Moment (FOSM) technique can be used. It provides a method of calculating the mean, variance, and covariance of model outputs from means, variances, covariance and sensitivity coefficients for the model inputs. The following equations are used to determine these quantities (Dettinger and Wilson, 1981).

$$\underline{y} = \underline{f}(\underline{x}) \qquad \text{(C6)}$$

where the variables are defined as follows:

$$\underline{m_y} = \underline{f(m_x)} + \frac{1}{2}\underline{\frac{\partial^2 f}{\partial x^2}}\underline{var(x)} \qquad \text{(C7)}$$

$$\underline{cov(y)} = \underline{S_{i,j}}\ \underline{cov(x)}[\underline{S_{i,j}}]^T \qquad \text{(C8)}$$

n is the number of model outputs,
k is the number of model input parameters,
$\underline{y}$ is a (*n x 1*) vector of model outputs,
$\underline{f(x)}$ is the (*n x 1*) vector of model outputs with inputs of $\underline{x}$, $\underline{x}$ is a (*k x 1*) vector of model parameters,
$\underline{m_y}$ is a (*n x 1*) vector of mean model outputs,
$\underline{f(m_x)}$ is a (*n x 1*) vector of model outputs where the model is evaluated at $\underline{m_x}$,
$\underline{m_x}$ is a (*k x 1*) vector of mean parameter values,
$\underline{\partial^2 f/\partial x^2}$ is a (*n x k*) matrix of 2nd partial derivatives of $\underline{f(m_x)}$,
$\underline{cov(x)}$ is a (*k x k*) covariance matrix of the input parameters,
$\underline{cov(y)}$ is a (*n x n*) covariance matrix of model outputs,
$\underline{var(x)}$ is a (*k x 1*) vector of variances of parameters, and
$\underline{S_{i,j}}$ is a (*n x k*) matrix of sensitivity coefficients of model outputs to input parameters. The First-Order Second-Moment analysis is most appropriate when the model is not too nonlinear with respect to its input parameters, and the coefficients of variation for the parameters are small. When the model is highly nonlinear, or the model is so complex that sensitivity coefficients are not easily obtained, a Monte Carlo method could be used. The methodology of conducting uncertainty analysis using the Monte Carlo method for transport models can be seen in Nofziger *et al.*, (1993). Using Equations C6 through C8, uncertainty of model outputs, $\underline{cov(y)}$, can be obtained when uncertainty of input parameters, $\underline{cov(x)}$, and sensitivity coefficients of model outputs to input parameters, $\underline{S_{i,j}}$, are known.

6. Procedures for Sensitivity Analysis

An optimal set of input parameters for the problem of interest should be identified before the sensitivity analysis is conducted. This set of input parameters is referred to as the *base set*. The basic procedures for the sensitivity analysis are outlined as follows:

1. Gathering of input parameters: When site-specific input parameters are not available, the base set of parameters could be obtained either from indirect estimation using other data at the site (*e.g.*, to estimate conductivity using soil texture data) or from the

"best justified" mean values of published data which are "appropriate" for the site conditions. When experimental data are available, calibration of the model to obtain an optimal set of input parameters (*i.e.*, base set) should be performed first before sensitivity analysis.

2. After an optimal set of parameters has been identified, sensitivity analysis is performed to quantify the sensitivity of the model results with respect to model parameters. It is typically performed by changing one parameter at a time while keeping the rest constant. By changing the parameter over a range (*e.g.*, above and below a certain percent or standard deviation of the base set value), the responses of model output to input parameters can be examined. The results are usually presented by a) presenting the model outputs for several values of input parameters; b) plotting (absolute or relative) sensitivity coefficients versus input parameters; and c) providing the ranking descriptors, such as high, medium, and low.

If the sensitivity results show that the model results are highly sensitive to a particular parameter, the uncertainty associated with that parameter will significantly affect the ability of the model to make meaningful interpretations and predictions. This is specifically true when that parameter exhibits great spatial variability in the field, and/or great uncertainty due to experimental measurement/estimation of parameters. On the other hand, if the model results are not sensitive to a given parameter, the uncertainty in that parameter will have little impact on the model's interpretative or predictive capabilities and that parameter might be eliminated.

7. Case Studies

In this section, two sets of infiltration experimental data are used for performing sensitivity analysis with the Philip's two-term infiltration model. The model outputs are cumulative infiltration (I) and infiltration rate (q). The model input parameters are sorptivity (s) and a constant, A, that depends on the soil properties, saturated water content and initial water content.

<u>Data Set 1</u>: The experimental data for infiltration into the Grenoble sand of Barry *et al.*, (1995) is used for illustration of model calibration and performing sensitivity analysis. The infiltration experiment was conducted on a vertical, ponding column (*93.5 cm* in length and *6 cm* in diameter) filled with air-dried, graded Grenoble sand. The reported cumulative infiltration (I) is shown in Figure C1a. From cumulative infiltration data, infiltration rates are calculated from the infiltration data (Figure C1a) and presented in Figure C1b. The experimental conditions and hydraulic properties of the Grennoble sand is given in Table C1.

Table C1. Experimental conditions and hydraulic properties for the Grenoble sand infiltration experiment (Barry *et al.*, 1995).

Quantity	Value
Porosity	0.37
Initial soil pressure head within the soil profile	89 cm
Head at the soil surface	23 cm
Initial moisture content	0.082 cm^3/cm^3
Saturated moisture content	0.31 cm^3/cm^3
Saturated hydraulic conductivity	15.4 cm/h
Estimated sorptivity	9.54 $cm/h^{1/2}$

To calibrate Philip's two-term model, either the cumulative infiltration data, infiltration rate or both can be used. Model parameter estimation can be accomplished through either regression techniques or graphical methods. Table C2 presents six methods (Cases 1, 2, 3, 4, 5, and 6) which illustrate the combinations of the estimation methods and the datasets used in the calibration. In Case 1, the estimated value ($9.54\ cm/h^{1/2}$) of sorptivity by Barry *et al.*, (1995) is used and calibration is only conducted for estimating A. For Cases 2, 3, and 4, calibration is carried out to estimate s and A using a regression method. In Case 5 and Case 6, a graphical method is used to estimate s and A. The estimates of s and A are given in Table C2. The standard error is also given in Table C2. Calculated infiltration and infiltration rate using these six sets of estimated parameters are depicted in Figures C2a and C2b respectively. These figures indicate that experimental infiltration data are reasonably described using the values of estimates obtained from Case 4 and Case 5. Figures C2a and C2b also depict that variation of the estimates of input parameters can result in significant differences in model prediction.

Table C2. Calibration of Philip's two-term model parameters using the experimental infiltration data of Barry *et al.*, (1995).

Case	*s*, (cm/h$^{1/2}$)	A, (cm/h^2)
Case 1: Reported sorptivity of *9.54 cm/h$^{1/2}$* (Barry *et al.*, 1995) is used. Calibration is performed on *A* only using cumulative infiltration data.	[9.54]	10.62±0.08†
Case 2: Calibration is performed on both *s* and A using cumulative infiltration data.	8.92±0.19†	11.78±0.36†
Case 3: Calibration is performed on both *s* and *A* using infiltration rate data.	12.65±1.19†	7.35±2.13†
Case 4: Calibration is performed on both *s* and *A* using both cumulative infiltration and infiltration rate data.	11.17±0.99†	8.13±1.74†
Case 5: Graphical estimation of *s* and *A* from the plot of *I(t)/t* versus $t^{-½}$.	11.0±0.46†	9.00±0.15†
Case 6: Graphical estimation of *s* from the plot of *q(t)* versus $t^{-½}$.	8.0±0.41†	--

†.. Estimated value ±Standard error

Figures C2a and C2b also indicate that using the estimates of *s* and *A* of Case 4 and Case 5 provides better fits of both the observed cumulative infiltration and infiltration rate data than using those estimates from Case 1, 2, 3, and 6. From this evaluation, the estimates of either Case 4 or Case 5 can be chosen as the optimal set. However, the estimates of *s* and *A* obtained from Case 4 is arbitrarily selected as an optimal set (*i.e.*, the base set).

To compute sensitivity and relative sensitivity, the direct method is selected for this example due to its simplicity. The sensitivity and relative sensitivities equations are given in Table C3. Table C3 gives the analytically derived sensitivities for infiltration rate, *q(t)*, and cumulative infiltration, *I(t)*, with respect to sorptivity (*s*) and the constant term (*A*). Note that the sensitivities of *I(t)* with respect to *s* (or *A*) and *q(t)* with respect to *s* (or *A*) are independent with *s* (or *A*). In other words, the sensitivities are constant at given particular time over the whole range of *s* (or *A*). However, sensitivities vary with time for Philip's two-term model.

Table C3. Sensitivity and relative sensitivity of infiltration rate, *q(t)*, and cumulation infiltration, *I(t)* with respect to sorptivity, *s* and soil-dependent constant, *A*, of Philip's two-term model.

Model Output	Input Parameter	Sensitivity $S_{i,j}$	Relative Sensitivity $S_{i,j}^{r}$	Second Derivatives of Output with respect to input Parameter
$q(t) = \frac{1}{2}st^{-\frac{1}{2}} + A$	s	$\frac{1}{2}t^{-\frac{1}{2}}$	$\frac{s}{s + 2A\sqrt{t}}$	0
	A	1	$\frac{2A\sqrt{t}}{st + 2A\sqrt{t}}$	0
$I(t) = st^{\frac{1}{2}} + At$	s	$t^{\frac{1}{2}}$	$\frac{s\sqrt{t}}{s\sqrt{t} + At}$	0
	A	t	$\frac{At}{s\sqrt{t} + At}$	0

Using the identified base set of estimates, sensitivity analysis is conducted and presented in the following four areas.

1. Examining the time changes of infiltration by changing one parameter while keeping the rest of parameters fixed (Figures C3a and C3b);
2. Examining sensitivity changes of infiltration with respect to *s* or *A* over a range of input parameter at different time periods, *t*. The range of input parameter is presented in terms of relative ratios of that parameter to the base value (Figures C4a and C4b);
3. Examining time changes of sensitivities of infiltration with respect to *s* or *A* over time using 60%, 100%, and 140% of base values of input parameters (Figures C4c and C4d); and
4. Examining the changes of relative sensitivities over a range of one particular parameter at different time periods (Figures C5a and C5b).

The results indicate:

1. sensitivities of infiltration with respect to *s* (or *A*) are constant over a range of 60% to 140 % of *s* (or *A*) at any given time (Figures C4a and C4b);
2. sensitivities of infiltration with respect to *s* (or *A*) vary with time but they are independent of *s* (or *A*) (Figures C4c and C4d);
3. Relative sensitivities of infiltration with respect to sorptivity, *s*, are greater than those with respect to constant *A* (Figures C5a and C5b).

4. Similar results (not shown) are obtained for sensitivities of infiltration rate with respect to *s* and A.

The results of sensitivities shown in Figures C4a, C4b, C5a, and C5b, indicate that *s* is the most sensitive parameter in Philip's two-term model for the range of input parameters examined. Similar results are also observed for infiltration rates (not shown).

To examine the impact of deviation of the estimates of input parameters, *s* and *A* from the values of the base set on the deviation of infiltration, Taylor's formula (Equation C5) is applied to Philip's two-term infiltration model. Taking up to second-order terms, deviation (difference) of infiltration (ΔI) is expressed as

$$\Delta I = I(s,A) - I(s_o,A_o) = \frac{(s-s_o)}{1!} I_s(s_o,A_o) + \frac{(s-s_o)^2}{2!} I_{ss}(s_o) + (s-s_o)(A-A_o) I_{sA}(s_o,A_o) + \frac{(A-A_o)}{1!} I_A(s_o,A_o) + \frac{(A-A_o)^2}{2!} I_{AA}(s_o,A_o) + R_3(s_o,A_o) \quad \text{(C9)}$$

where

- $I_s(s_o,A_o)$, $I_{ss}(s_o,A_o)$ are the first, and second derivatives of $I(s,A)$ with respect to s at $s=s_o$ and $A=A_o$ respectively;
- $I_A(s_o,A_o)$, $I_{AA}(s_o,A_o)$ are the first, and second derivatives of $I(s,A)$ with respect to A at $s=s_o$ and $A=A_o$ respectively;
- $I_{sA}(s_o,A_o)$ is the partial derivative of $I(s,A)$ with respect to s and A; and
- $R_3(s_o,A_o)$ is the remainder for the terms in the order of 3 and up.

Here, $I_s(s_o,A_o)$ and $I_A(s_o,A_o)$ are the sensitivity coefficients of $I(t)$ with respect to s, and A respectively. It is worth noting that analytical values of I_{ss}, I_{AA} and I_{sA} and higher-order derivatives are zeros (Table C3). Accordingly, the deviation (ΔI) of $I(s,A)$ from $I(s_o,A_o)$, $(I(s,A)-I(s_o,A_o))$ is given by

$$\Delta I = I(s,A) - I(s_o,A_o) = I_s(s_o,A_o)(s-s_o) + I_A(s_o,A_o)(A-A_o) \quad \text{(C10)}$$

Equation C10 states that deviation of $I(s,A)$ from $I(s_o,A_o)$ can be estimated from the sum of the products of sensitivity and deviation of a parameter value from its base value.

Assuming s_o and A_o are the optimal values (Case 4 in Table C2) for *s* and *A* in Philip's two-term model, there is interest in how the sensitivities of *I* with respect to *s* and *A* will impact the prediction of infiltration. Taking Case 5 (*e.g.*, using the graphical method to estimate *s* and *A* from infiltration data) as an example, deviation (difference) of predicted infiltration, due to estimated *s* and *A*, from using the optimal data set is shown in Figure C6. The differences between predicted infiltration are approximately equal to the sum of the products of sensitivity

and the difference between estimated and optimal values. Figure C6 indicates that: (a) contribution of deviation of infiltration due to deviation of the constant *A* term (*i.e.*, the second term on the right-hand-side of Equation C10, $I_A \cdot (A-A_o)$) is greater than contribution of deviation of infiltration due to deviation of sorptivity (*i.e.*, the first term on the right-hand-side of equation, $I_s \cdot (s-s_o)$) and (b) the difference of predicted infiltration (maximum value is around *0.1 cm*) is negligible compared to the magnitudes of infiltration during the first *0.4 hours* (Figures C6 and Figure C2a). It is worth noting that the difference of predicted infiltration is dependent on sensitivities as well as the deviation of input parameters from base set values.

8. Uncertainty Analysis using Sensitivity Results

After obtaining sensitivity coefficients of input parameters, uncertainty of model outputs due to uncertainty of input parameters can be quantified using Equation C8. Here uncertainty is expressed in terms of variance (or covariance) which is the expected value of the square of the difference between a random variable and its mean (*e.g.*, Variance of sorptivity is $E((s-\bar{s})^2)$. Here $\bar{s}$ is the mean of sorptivity.). To demonstrate quantifying uncertainty of predicted infiltration due to uncertainty of input parameters (*s* and *A*), another set of reported experimental data is used.

<u>Data Set #2</u>: A set of field measurement data for sorptivity (*s*) and conductivity at the surface (K_o) in a field study using disk permeameters had been reported by Lien (1989). Field measurements of infiltration were conducted at four locations in a field of about *35 hectares*. The dominant soils in the field are Casa Grande - Trix fine loamy soils. The Cassel ring and the disc permeameters at a *2 cm* positive head, and the *10 cm* and the *5 cm* tension disc permeameters were used. For this case study, values of K_o were used to estimate constant *A* ($A=0.363\ K_o$) (Philip, 1974). The reported values and their statistics of sorptivity (*s*) and the calculated values of *A* are given in Table C4. Note that this data set includes uncertainty due to spatial variability as well as differences among the measurement methods.

Table C4. Statistics of parameters used in FOSM uncertainty analysis for Casa Grande/Trix fine-loamy soils .

	Sorptivity, *s*	Constant, *A*
Mean	4.03	2.38
Coefficient of Variance	0.93	1.16
log† Mean	1.08	0.44
log† Coefficient of Variance	0.73	2.11
Correlation Matrix		
	log (s)	log (A)
log (s)	1.00	
log (A)	0.69	1.00

† Natural logarithm; The sample size is 16.

The infiltration phenomena is examined during the first hour infiltration period. The means of sorptivity and the constant *A* (Table C4), second derivatives (all zeros for the two-term model, Table C3), and variances are used to calculate the means of infiltration ($\bar{I}$) and infiltration rates ($\bar{q}$) (Equation C7). The sensitivity coefficients and covariances for *s* and *A* (Table C4) are used to calculate covariances (*cov(I)* and *cov(q)*) of infiltration (*I*) and infiltration rates (*q*) using Equation C8. The means of infiltration, 97.5% confidence values are given in Figures C7a and C7b. Here, 97.5% confidence values for infiltration are obtained as ($\bar{I} \pm \alpha \cdot \sigma_I$) and ($\bar{q} \pm \alpha \cdot \sigma_q$) respectively. Here α's are confidence coefficient (±1.96) at 97.5% confidence percentiles. σ_i and σ_q are standard deviations (square root of variance) for infiltration (*I*) and infiltration rate (*q*) respectively. Since sorptivity, the constant *A*, the predicted infiltration and infiltration rates follow log-normal distributions, calculation is performed using the log-transformed values for *s*, *A*, *I* and *q*. The First-Order Second-Moment (FOSM) technique used is simple and straight forward. For comparison, the Monte Carlo technique is also used to quantify uncertainty of infiltration. The results are shown in Figures C7a and C7b. It indicates that great variability of infiltration exists due to the uncertainty of parameter measurement and their spatial variabilities in the field. Figures C7a and C7b also show that both FOSM and Monte Carlo approaches give very close results for uncertainty estimation.

Table C5. Statistics of parameters used in FOSM uncertainty analysis for Grenoble sand.

	Sorptivity, *s*	Constant, *A*
Mean	10.2	9.38
Coefficient of Variance	0.169	0.167
Correlation Matrix		
	s	A
s	1.00	
A	-0.69	1.00

Remark: The sample size is 6.

To examine the impact of uncertainty of estimates using different methods on predicted infiltration, the same procedures are repeated for Grenoble sand except normal distributions are used for the input parameters, *s* and *A*, and output parameters, *I* and *q*. The estimates of *s* and *A* obtained from different parameterization methods (Cases 1, 2, 3, 4, 5 and 6 in Table C2) are found to be better described by the normal distribution. The statistics of these estimates are given in Table C5. As a result, predicted values of *I* and *q* form normal distributions. Uncertainty results for Grenoble sand are shown in Figures C8a and C8b. It indicates that

a) The predicted infiltration and infiltration rates satisfactorily described the observed data using estimates of *s* and *A*. Although differences exist due to different parameter methods, prediction of infiltration using any set of estimates in Table C2 are reasonably good and the predicted values are fallen within the 95% confidence intervals (Figures C2a, C2b, C8a, and C8b).
b) Uncertainty of predicted infiltration using data set #2 is much greater than using data set #1 since data set #2 possess greater uncertainty in measured values of *s* and *A*.

Furthermore, sensitivity results are also used to examine predicted uncertainty of infiltration due to uncertainty of estimates of input parameters. Contribution of uncertainty of predicted infiltration is quantified by using Equation C8. Expanding Equation C8 for infiltration (*I*), we can describe uncertainty of *I* as follows

$$\mathrm{var(I)} = I_s^2\,\mathrm{var(s)} + I_A^2\,\mathrm{var(A)} + I_{sA}\,\mathrm{cov(s,A)} \qquad \text{(C11)}$$

where *var(s)* and *var(A)* are variances of *s* and *A* respectively, and *cov(s,A)* are covariances of *s* and *A*. The term, *var(I)*, in the left-hand side of Equation C11 represents uncertainty of predicted infiltration due to uncertainty of *s* and *A*. The term $I_s^2 \cdot var(s)$ represents the contribution resulting

from s. The term $I_A^2 \cdot var(A)$ represents the amount of contribution resulted from A. The term $I_{sA} \cdot cov(s,A)$ represents the amount of contribution resulted from both s and A. The case study is given for the Casa Grande - Trix fine-loamy soils using data set #2. The results are shown in Figure C9a. It indicates that contribution of uncertainty of predicted infiltration due to sorptivity is much greater than that due to the constant A. The similar results are also found for infiltration rate particularly in the earlier infiltration time period ($t < 0.4h$, Figure C9b). In this case, infiltration is more sensitive to s than to A and variability of s is greater than variability of A. As the result, the model parameter s is more important than the constant A.

9. Implications

In Philip's two term model, the first term (Equation C3) represents the contribution of the influence of the matric suction, and the second term. represents the contribution of the influence of gravity (Philip, 1969). The analysis has illustrated that

a) Infiltration rate dramatically decreases with time and gradually reaches a constant value. In other words, matric suction (sorptivity) will mostly contribute to infiltration at the early stage. On the other hand, gravity (the constant A) increasingly contributes more to infiltration at later stage. This phenomena is clearly observed from the results of the sensitivity/uncertainty analysis.
b) For Grenoble sand, uncertainty of infiltration due to uncertainty of sorptivity is about two thirds or greater of overall total uncertainty of predicted infiltration during the first hour of infiltration (Figure C9). Therefore, more effort to accurately measure sorptivity is needed to reduce uncertainty of the predicted infiltration.
c) The estimates of input parameters using different estimation methods (Table C2) can be used to provide reasonable prediction on infiltration. Using the mean values of the estimates would be appropriate for uncertainty analysis since these estimates obtained from different parameterization methods follow normal distributions (Figures C8a, and C8b).

10. Summary

The procedures of conducting sensitivity analysis are illustrated using two sets of reported experimental data for Philip's two-term model. Sensitivity results are used to quantify uncertainty of model prediction due to uncertainty of input parameters. The results indicate that sorptivity is the most sensitive and important input parameter to predicted infiltration and infiltration rate; and uncertainty of sorptivity contributes significantly to uncertainty of predicted infiltration at the early stage of infiltration.

References

Anderson, M.P., and W.W. Woessner. 1992. Applied groundwater modeling -- Simulation of flow and advective transport. Academic Press Inc., New York.

Barry, D.A., J.-Y. Parlange, R. Haverkamp, and P.J. Ross. 1995. Infiltration under ponded conditions: 4. An explicit predictive infiltration formula. Soil Sci. 160:8-17.

Dettinger, M.D., and J.L. Wilson. 1981. First order analysis of uncertainty in numerical models of groundwater. Part 1. Mathematical development. Water Resour. Res. 17:149-161.

Hamby, D.M. 1994. A review of techniques for parameter sensitivity analysis of environmental models. Environmental Monitoring and Assessment. 31:135-154.

Hamby, D.M. 1995. A numerical comparison of sensitivity analysis techniques. Health Phys. 68:195-204.

Lien, B.K. 1989. Field measurement of soil sorptivity and hydraulic conductivity, M.S. thesis, Univ. of Ariz., Tucson.

Nofziger, D.L., J.-S. Chen, and C.T. Haan. 1993. Evaluation of unsaturated/vadose zone models for superfund sites. EPA/600/R-93/184. Robert S. Kerr Environmental Research Laboratory, Ada, OK.

Philip, J.R. 1974. Recent progress in the solution of nonlinear diffusion equations. Soil. Sci. 116:257-264.

Philip, J.R. 1969. Theory of infiltration. Adv. Hydrosci. 5:215-290.

Skaggs, T.H., and D.A. Barry. 1996. Sensitivity methods for time-continuous, spatially discrete groundwater contaminant transport models. Water Resourc. Res. 32:2409-2420.

Zheng, C., and G.D. Bennett. 1995. Applied contaminant transport modeling: theory and practice. Van Nostrand Reinhold, New York.

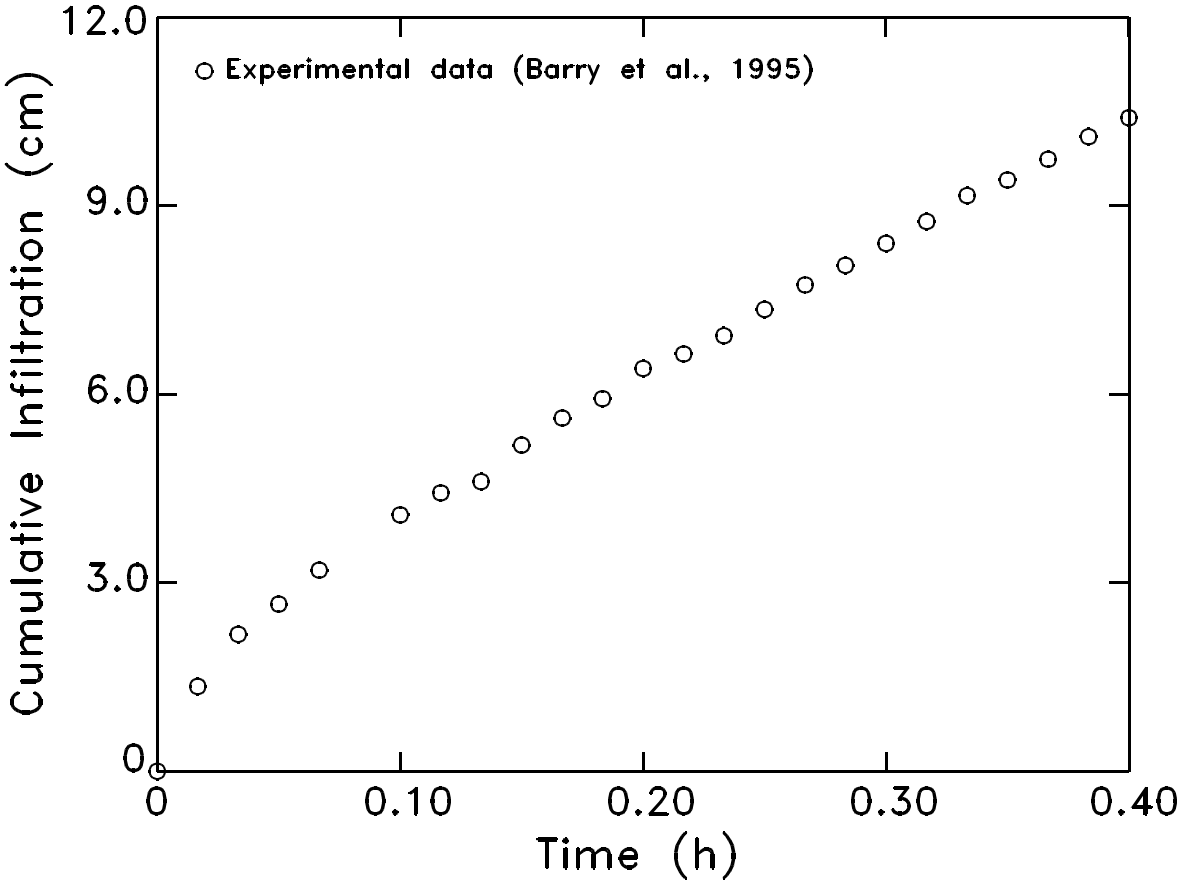

Figure C1a. Experimental infiltration data for Grenoble sand (Barry *et al.*, 1995)

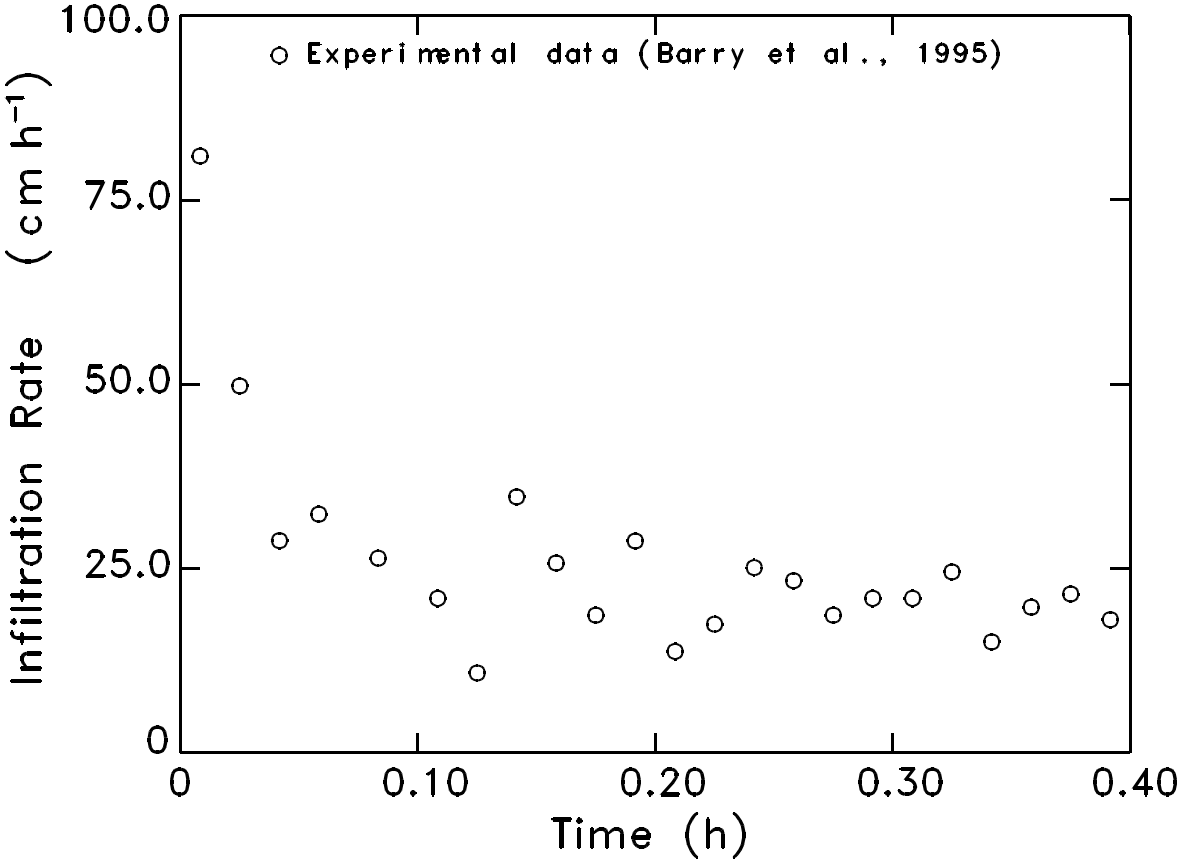

Figure C1b. Calculated infiltration rates from the experimental infiltration data for Grenoble sand (Barry *et al.*, 1995).

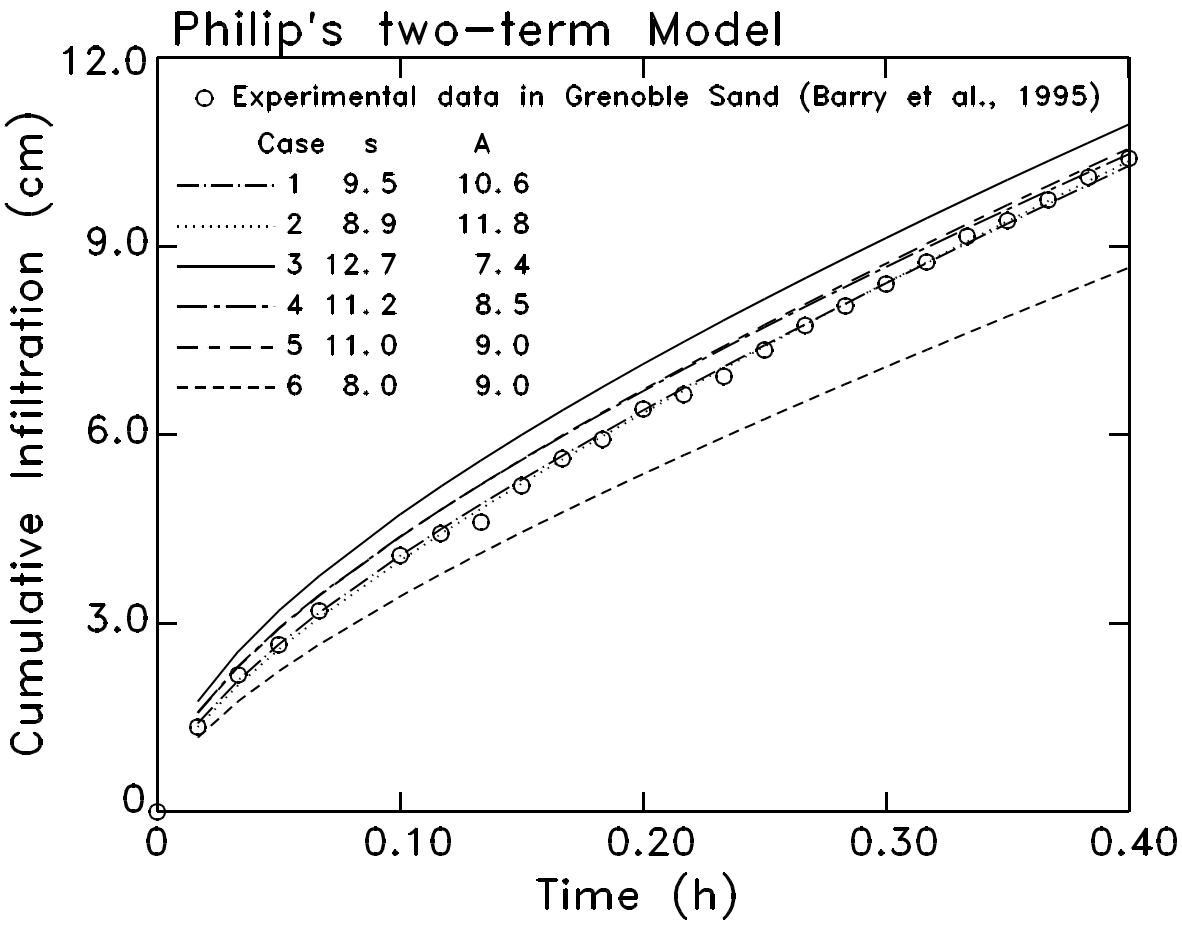

Figure C2a. Prediction of infiltration in Grenoble sand using the calibrated input parameters in Philip's two-term model.

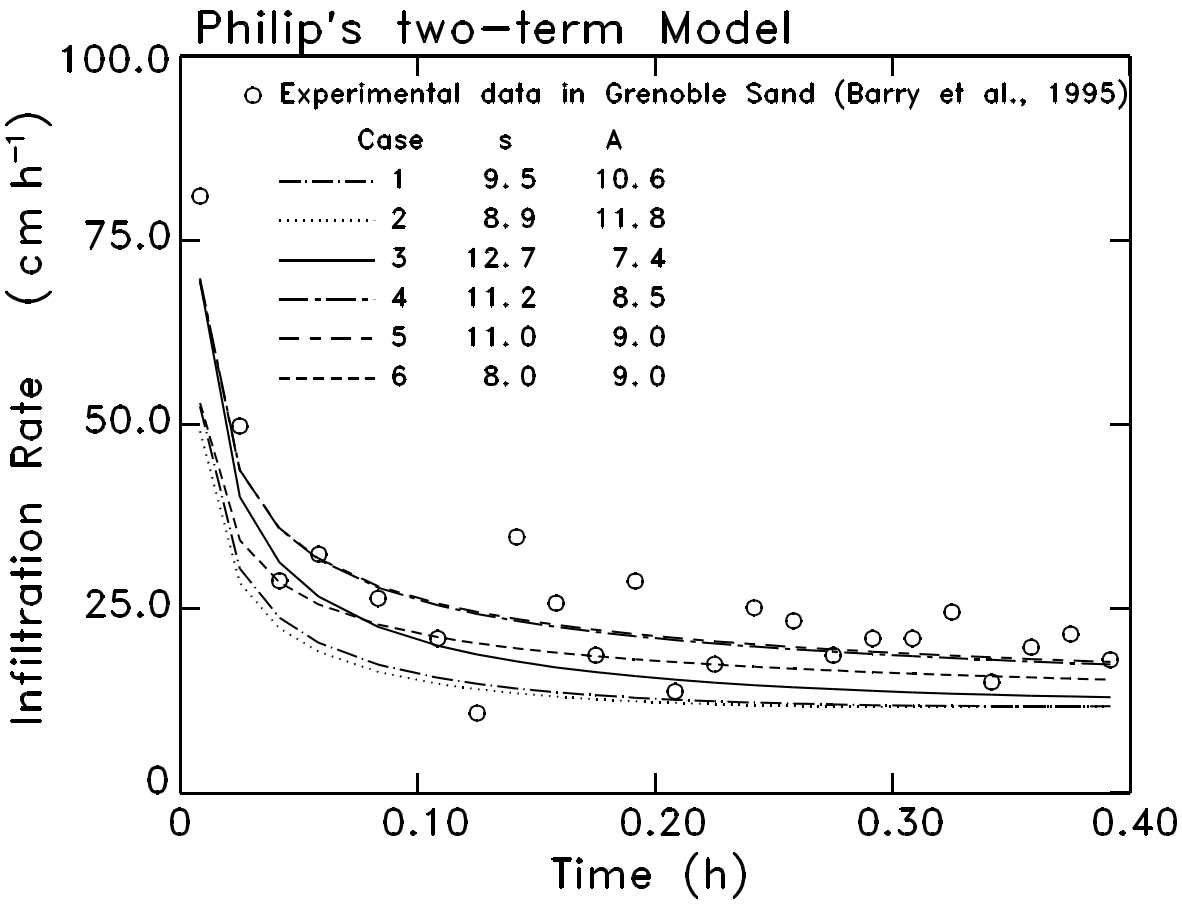

Figure C2b. Prediction of infiltration rates in Grenoble sand using the calibrated input parameters in Philip's two-term model.

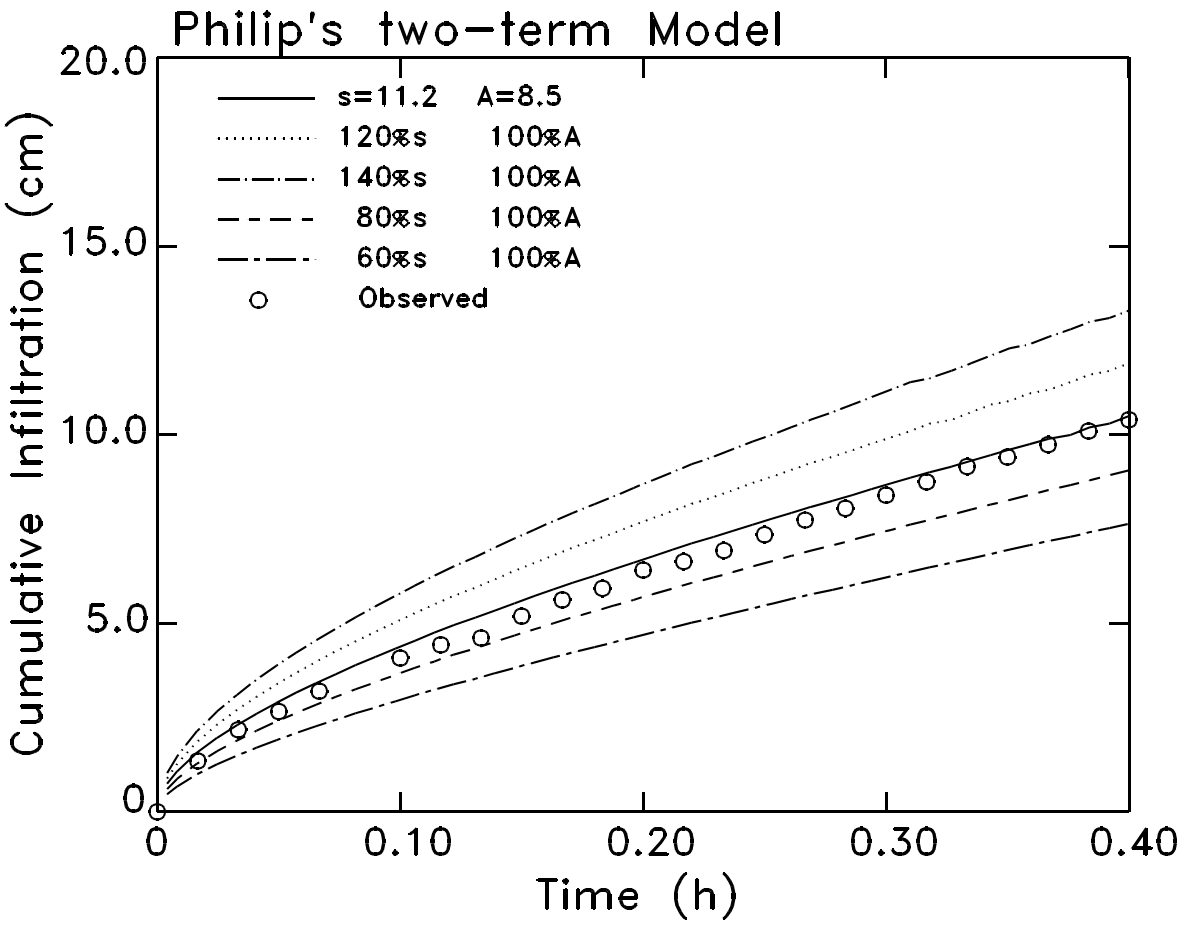

Figure C3a. Sensitivity of infiltration with respect to sorptivity (s) in Grenoble sand for Philip's two-term model.

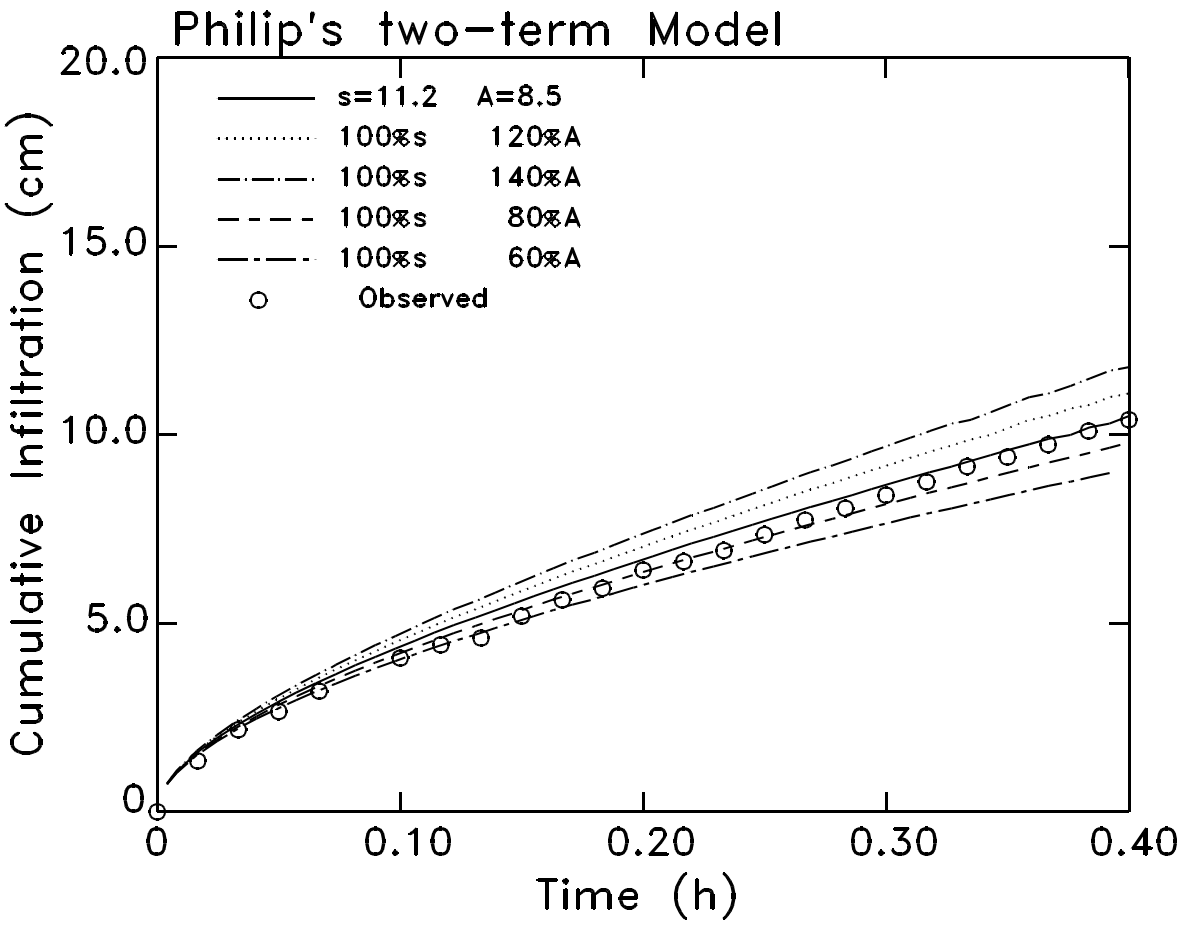

Figure C3b. Sensitivity of infiltration with respect to the constant A in Grenoble sand for Philip's two-term model.

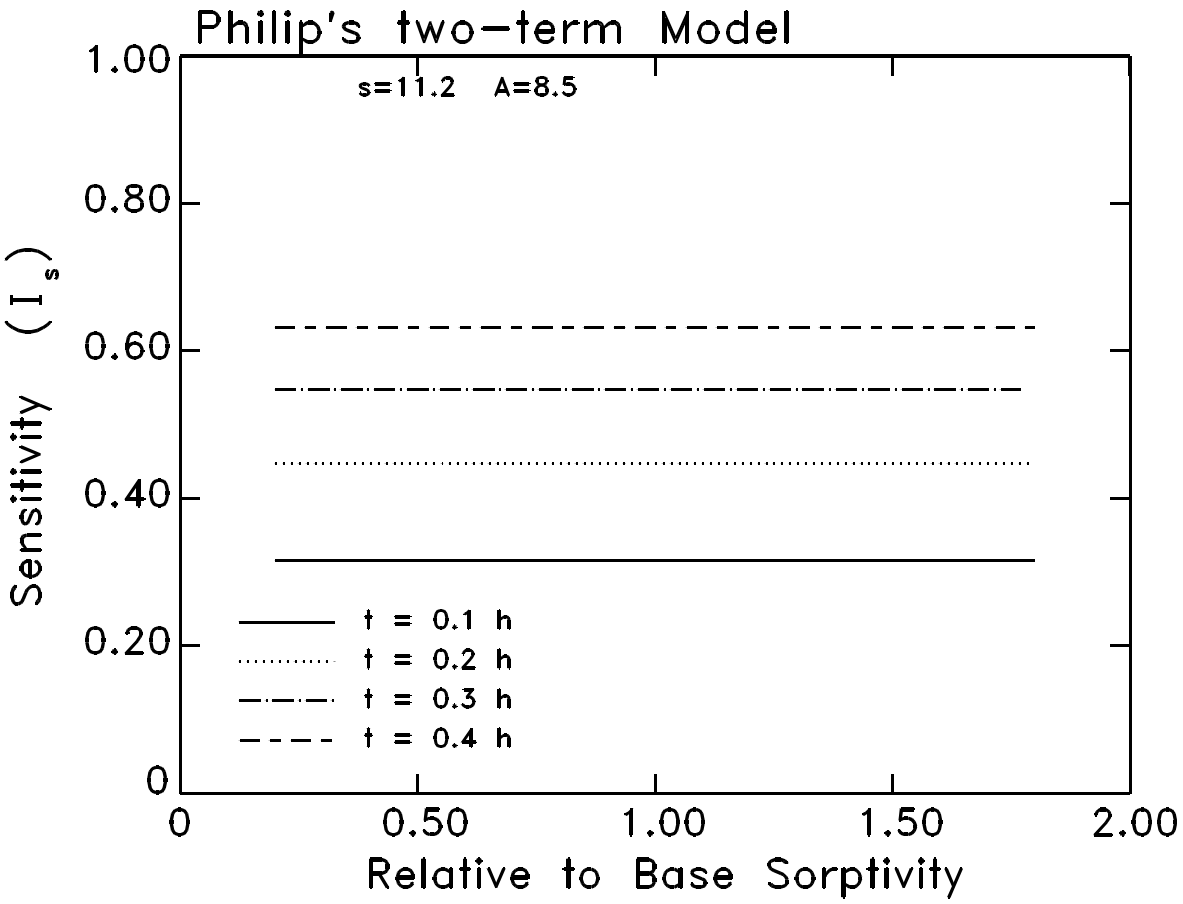

Figure C4a. Sensitivity of infiltration with respect to sorptivity (s) in Grenoble sand at different time periods for Philip's two-term model.

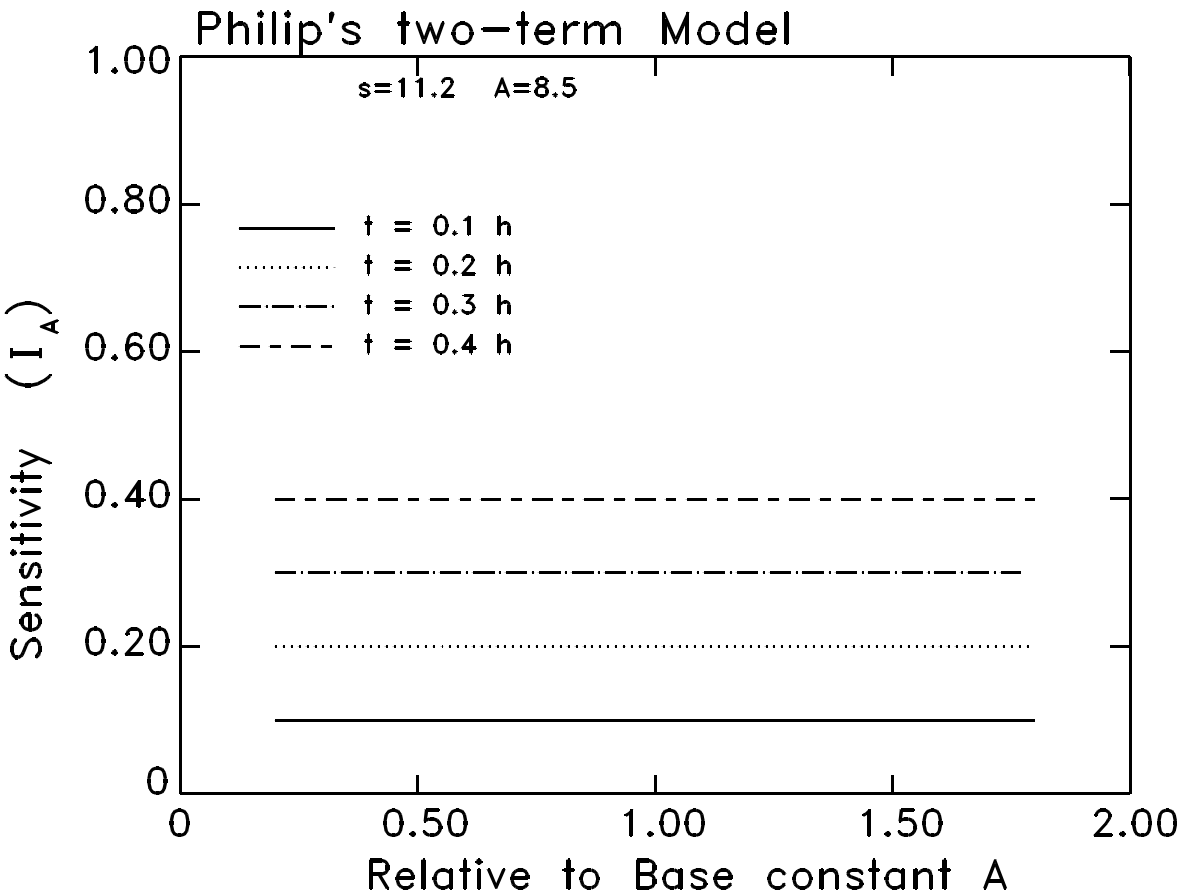

Figure C4b. Sensitivity of infiltration with respect to constant A in Grenoble sand at different time periods for Philip's two-term model.

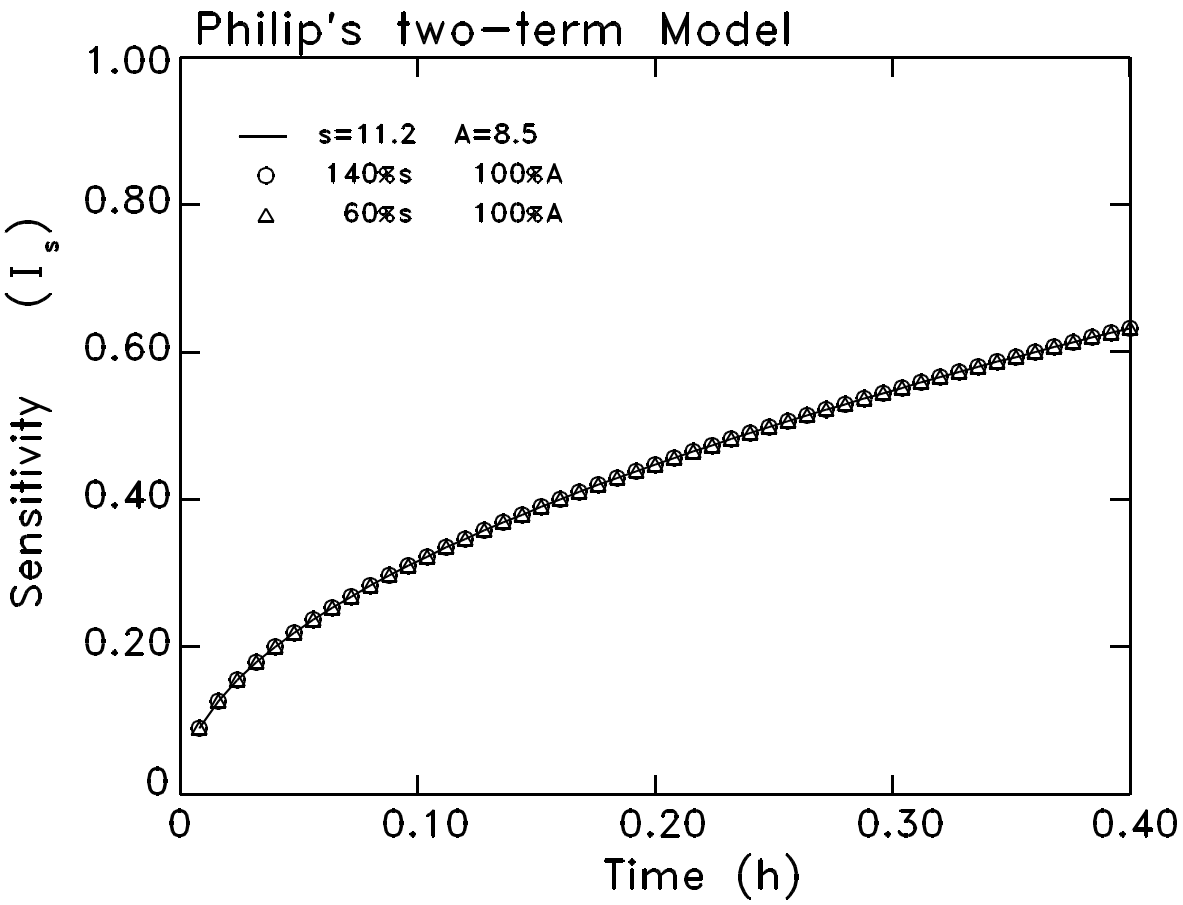

Figure C4c. Sensitivities of infiltration with respect to sorptivity (s) vary with time for 60%, 100%, and 140% of base values of s in Grenoble sand. Note that time curves (solid and dash lines) are coincident each other.

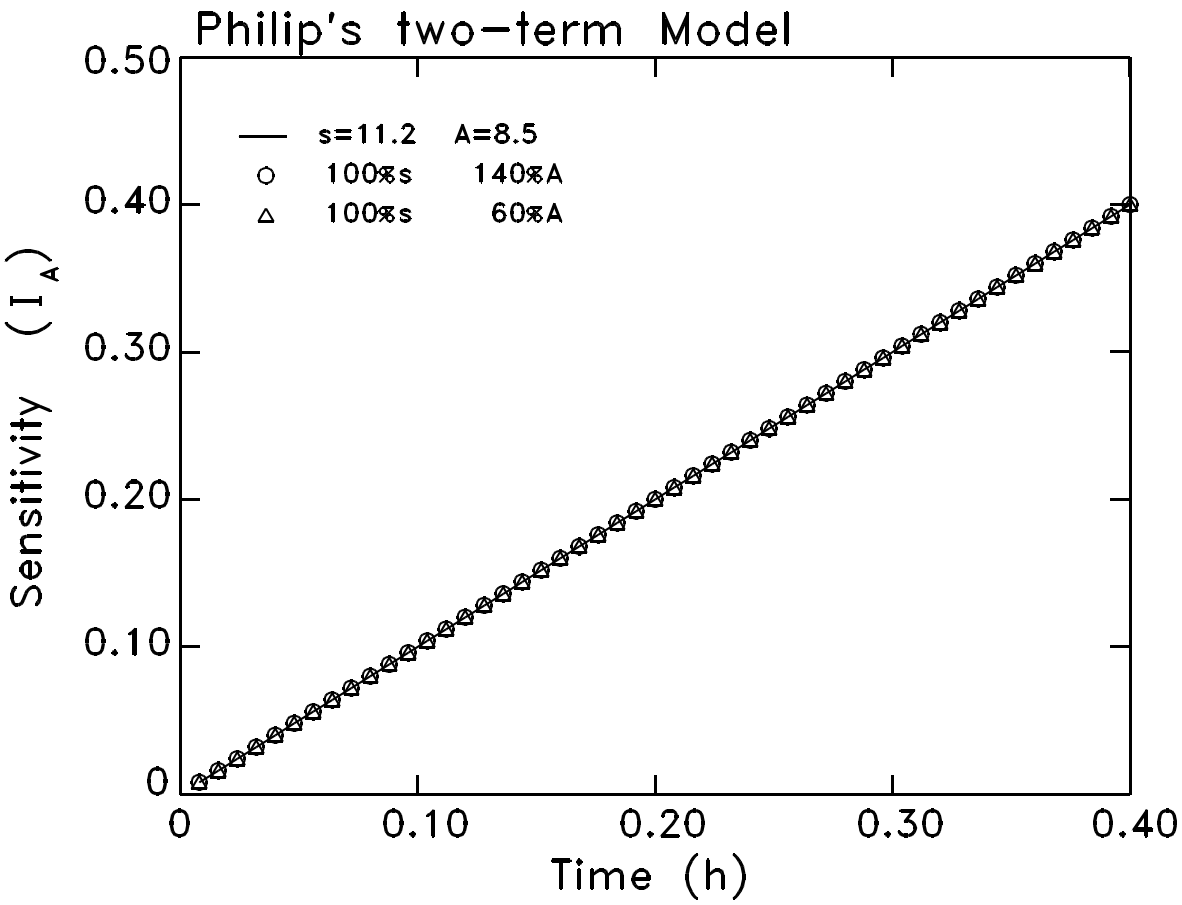

Figure C4d. Sensitivity of infiltration with respect to constant A vary with time for 60%, 100%, and 140% of base values of A in Grenoble sand. Note that time curves (solid and dash lines) are coincident each other.

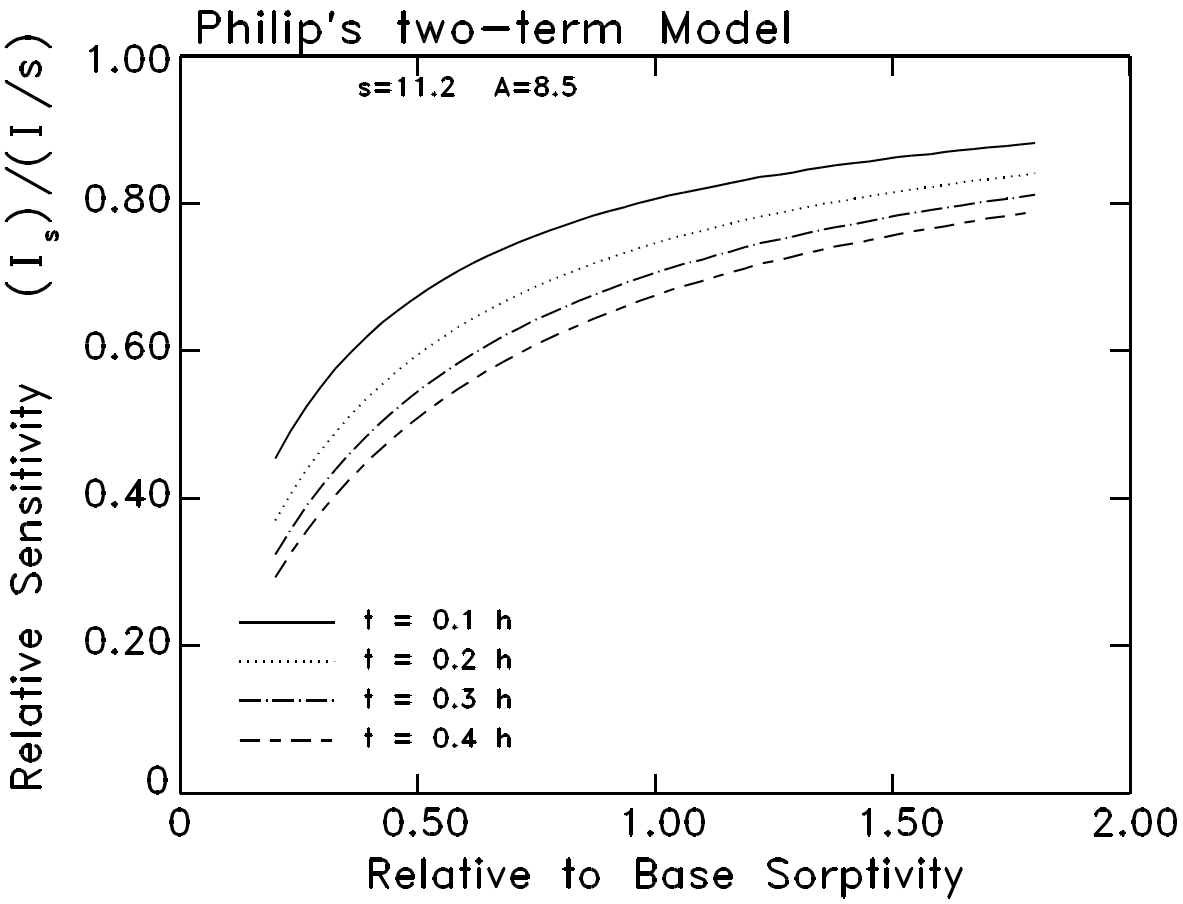

Figure C5a. Relative sensitivity of infiltration with respect to sorptivity (s) in Grenoble sand at different time periods for Philip's two-term model.

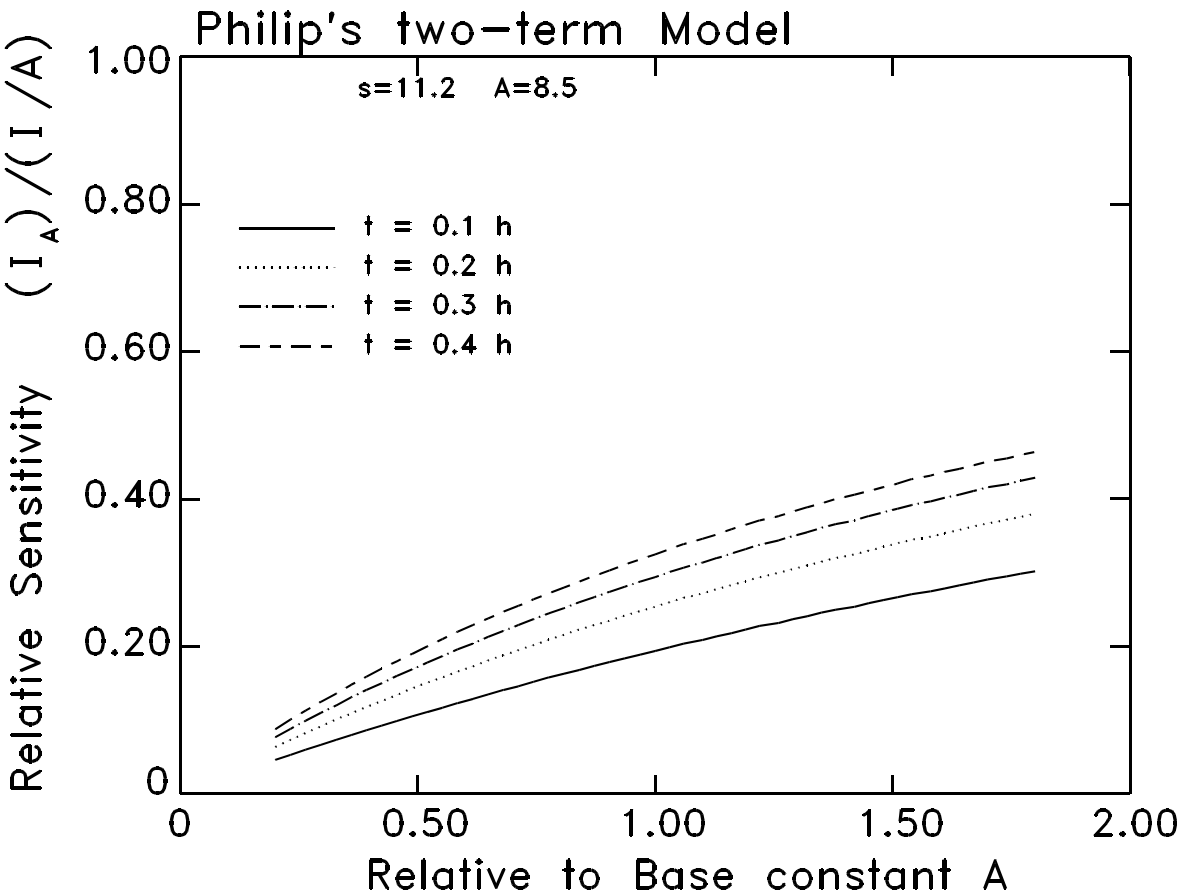

Figure C5b. Relative sensitivity of infiltration with respect to constant A in Grenoble sand at different time periods for Philip's two-term model.

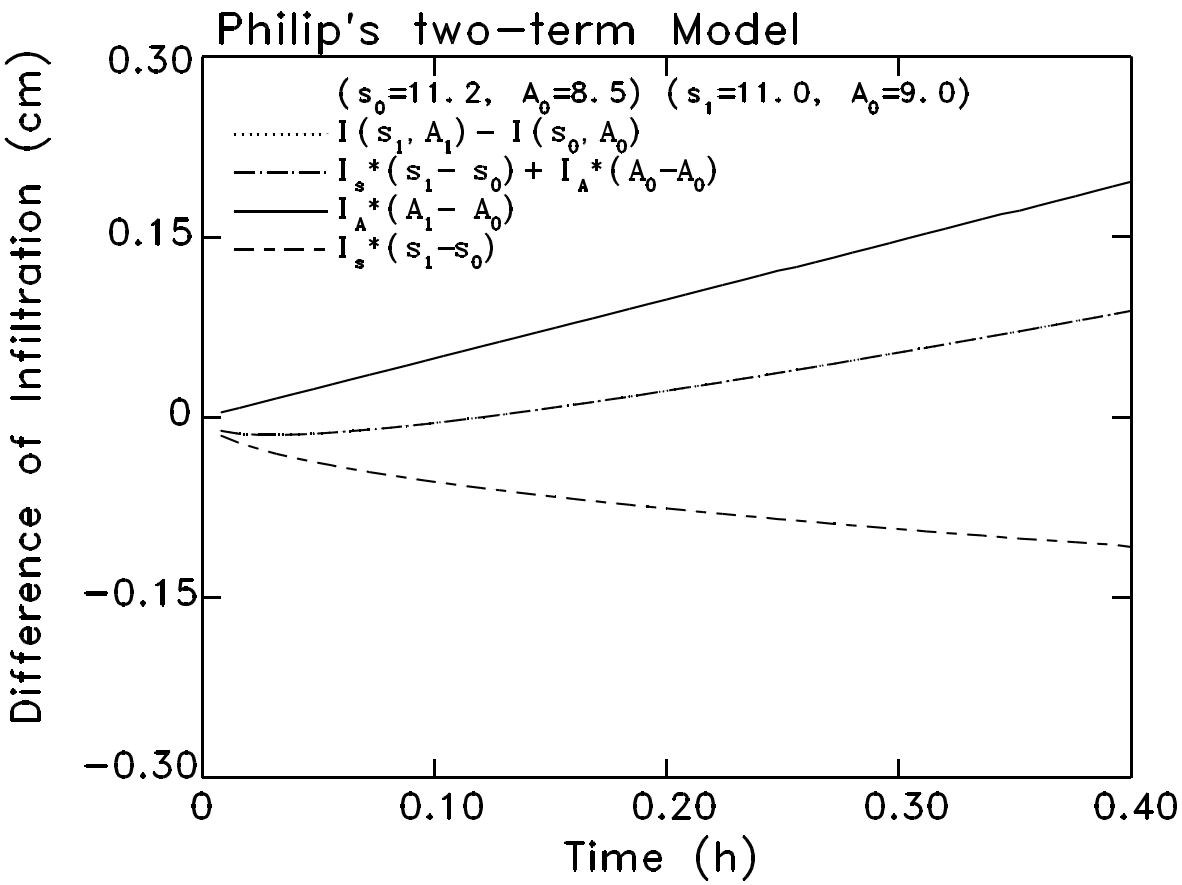

Figure C6. Deviation (difference) of predicted infiltration as the results of contribution from deviation of the values of input parameters from base values.

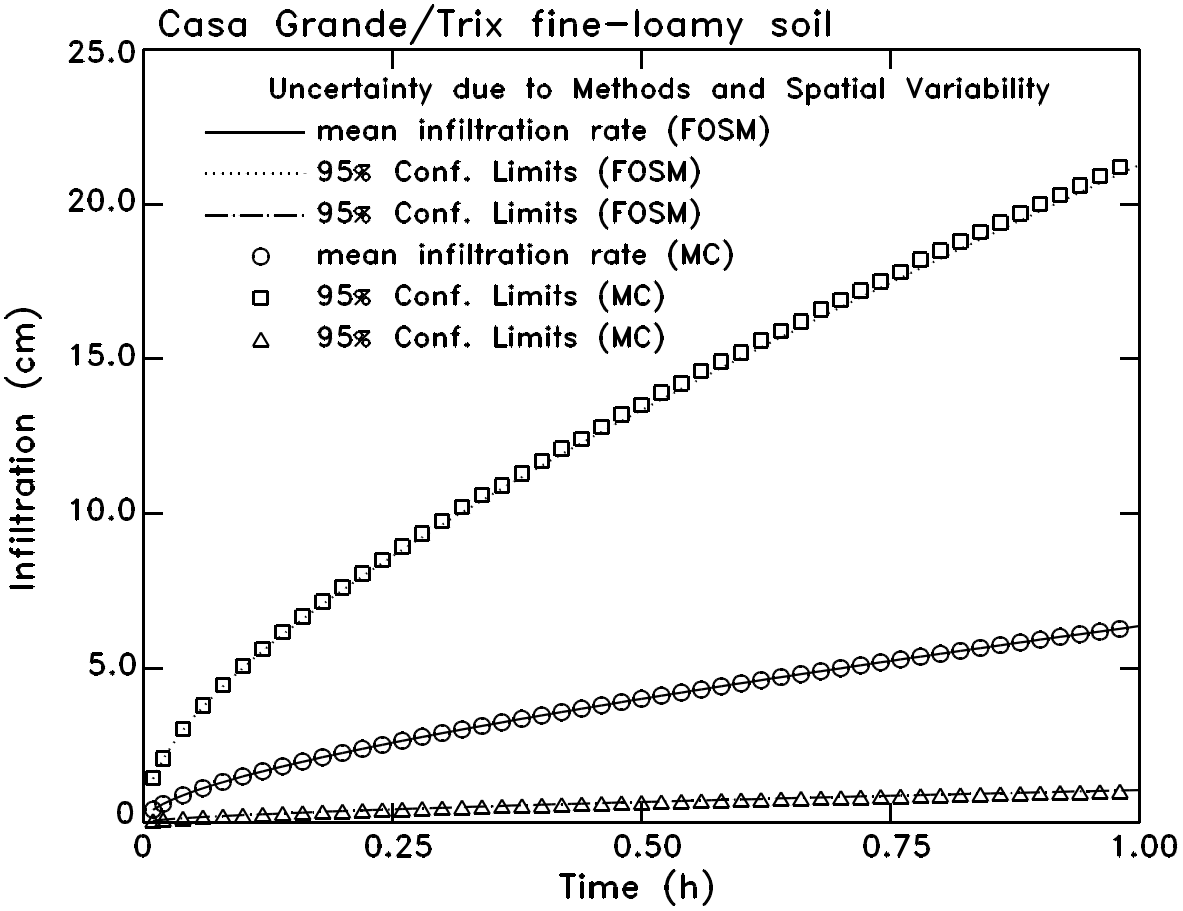

Figure C7a. Uncertainty of infiltration due to uncertainty of input parameters in Casa Grande-Trix fine-loamy soils. The mean predicted infiltration (solid line) as well as 95% confidence limits are shown.

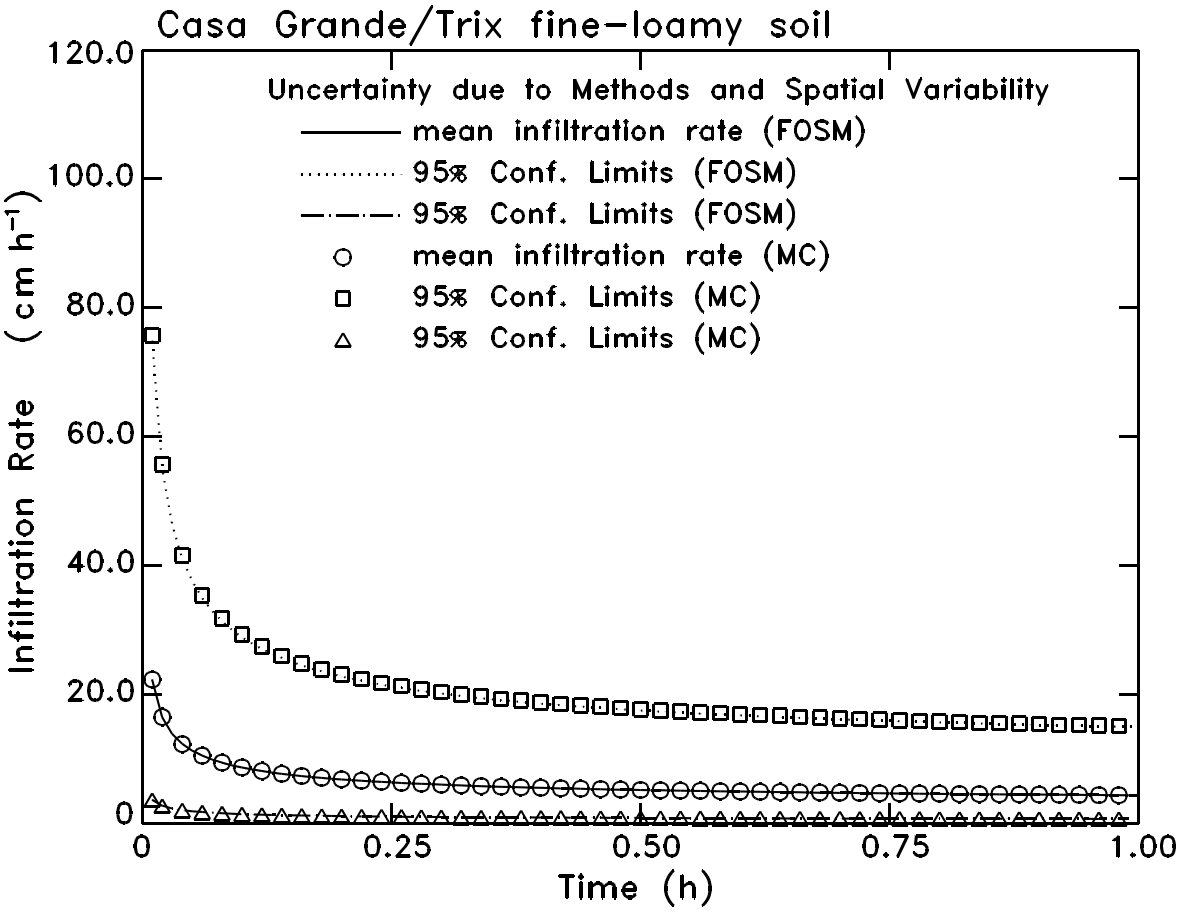

Figure C7b. Uncertainty of infiltration rate due to uncertainty of input parameters in Casa Grande-Trix fine-loamy soils. The mean predicted infiltration rate (solid line) as well as 95% confidence limits are shown.

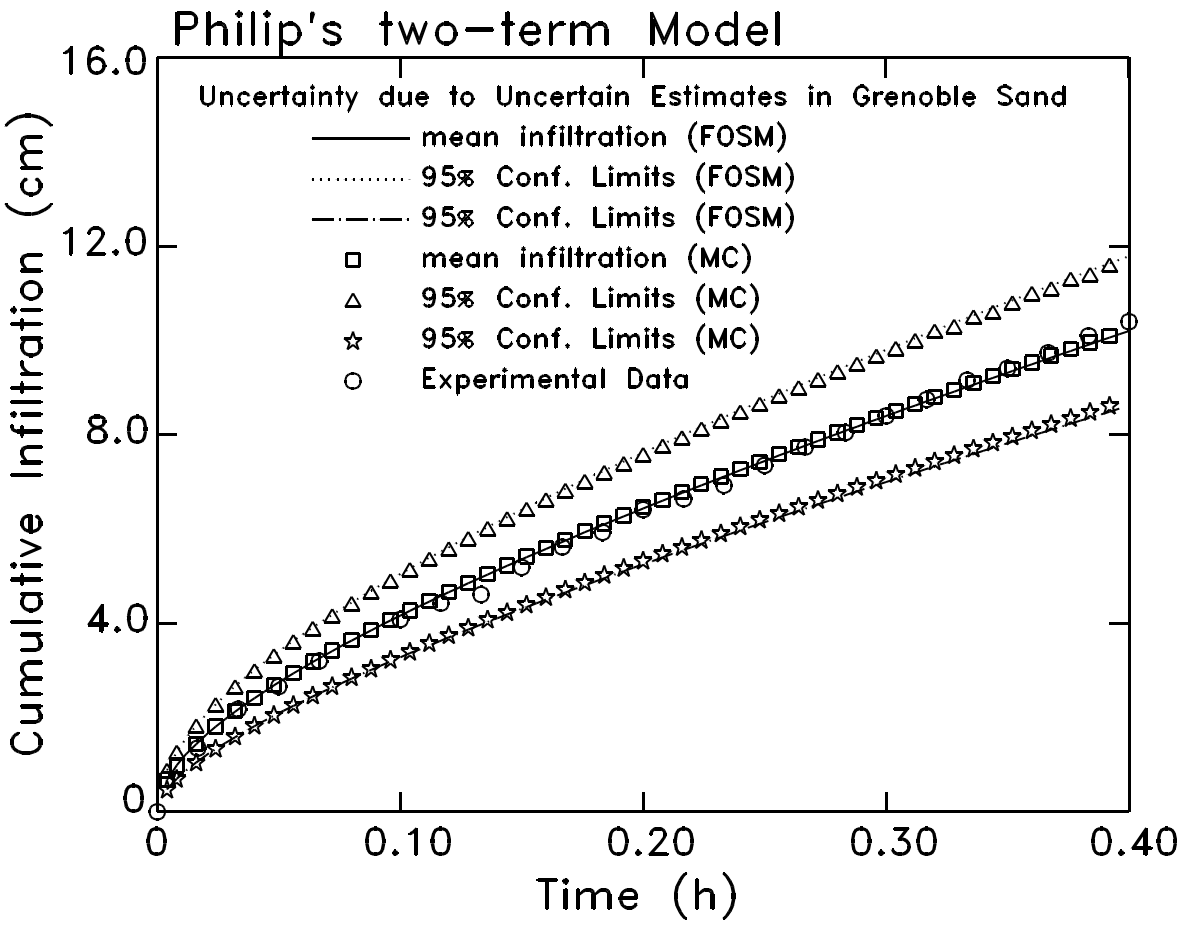

Figure C8a. Uncertainty of infiltration due to uncertainty of input parameters in Grenoble sand. The mean predicted infiltration (solid line) as well as 95% confidence limits are shown.

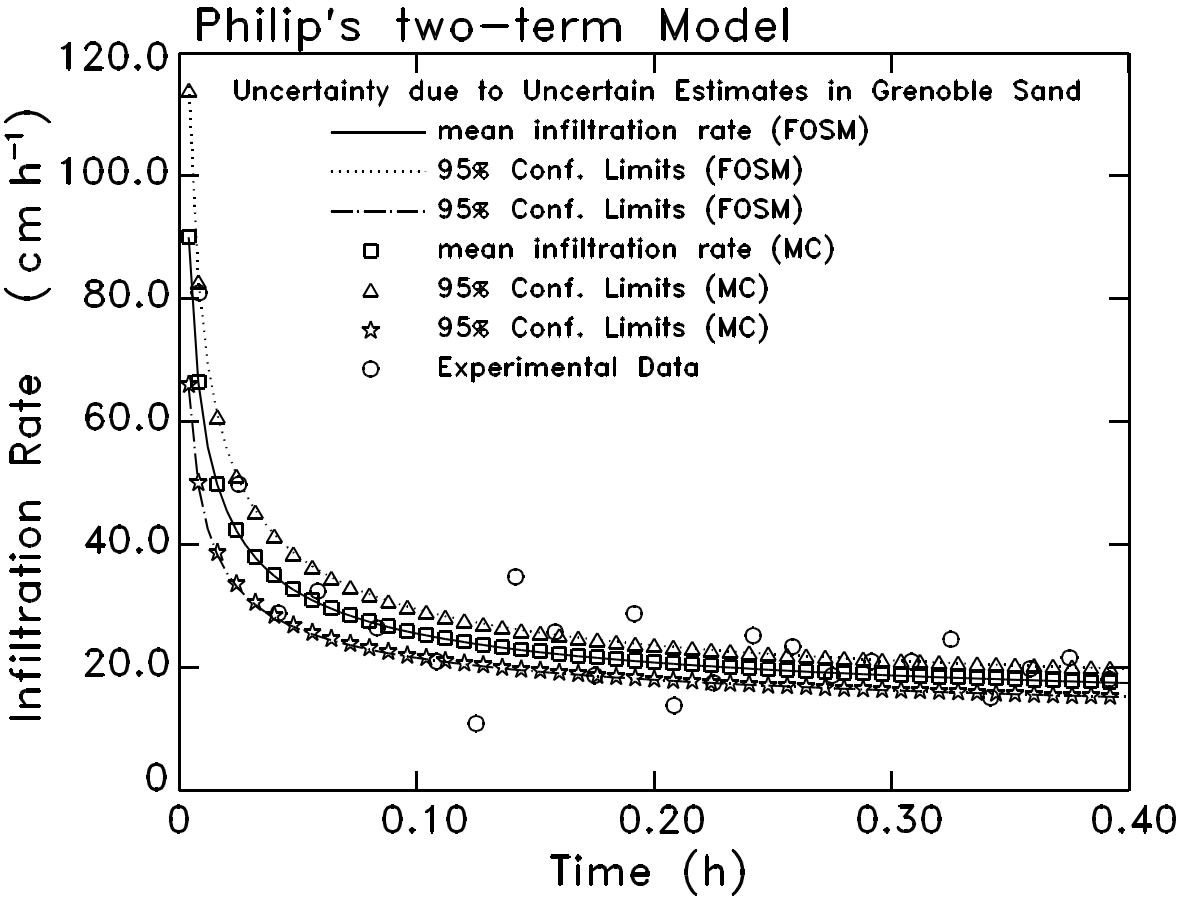

Figure C8b. Uncertainty of infiltration rate due to uncertainty of input parameters in Grenoble sand. The mean predicted infiltration rate (solid line) as well as 95% of confidence limits are shown.

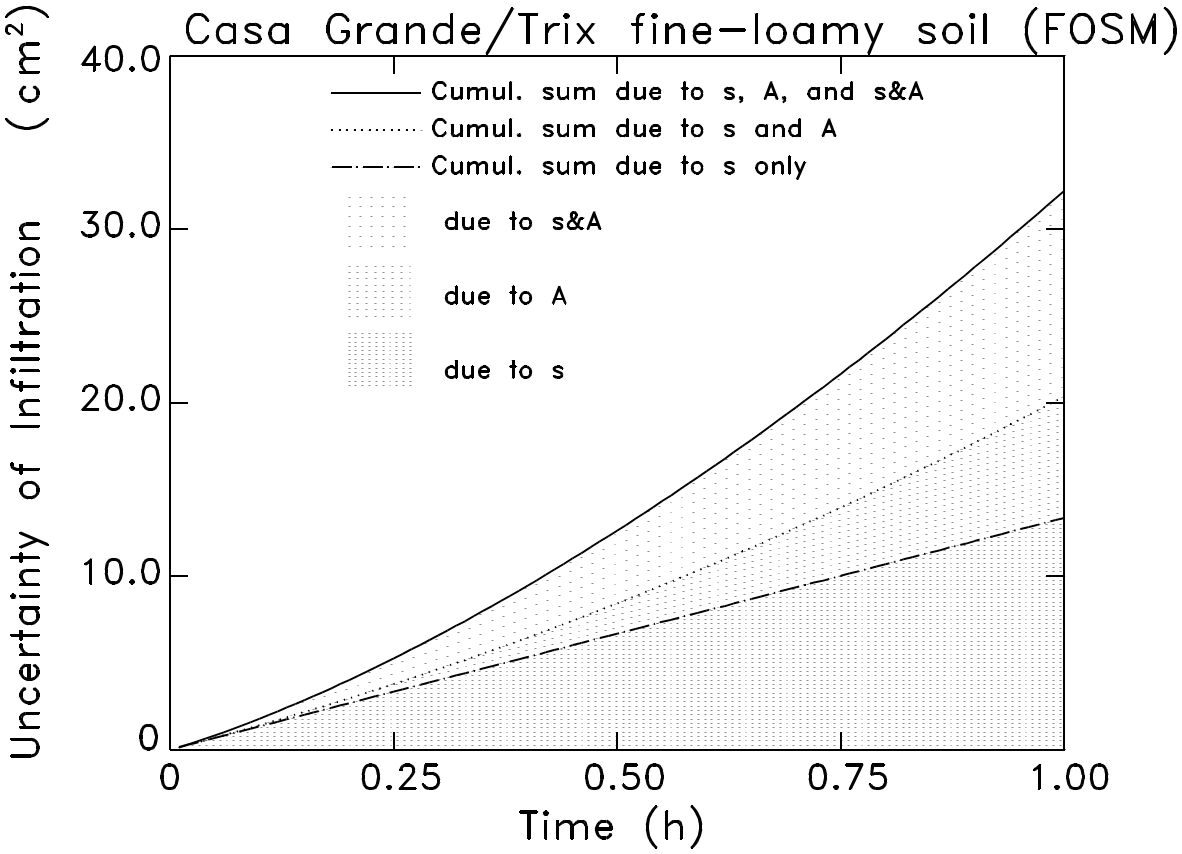

Figure C9a. Uncertainty of predicted infiltration as the results of contribution from input parameters in Casa Grande-Trix fine-loamy soils.

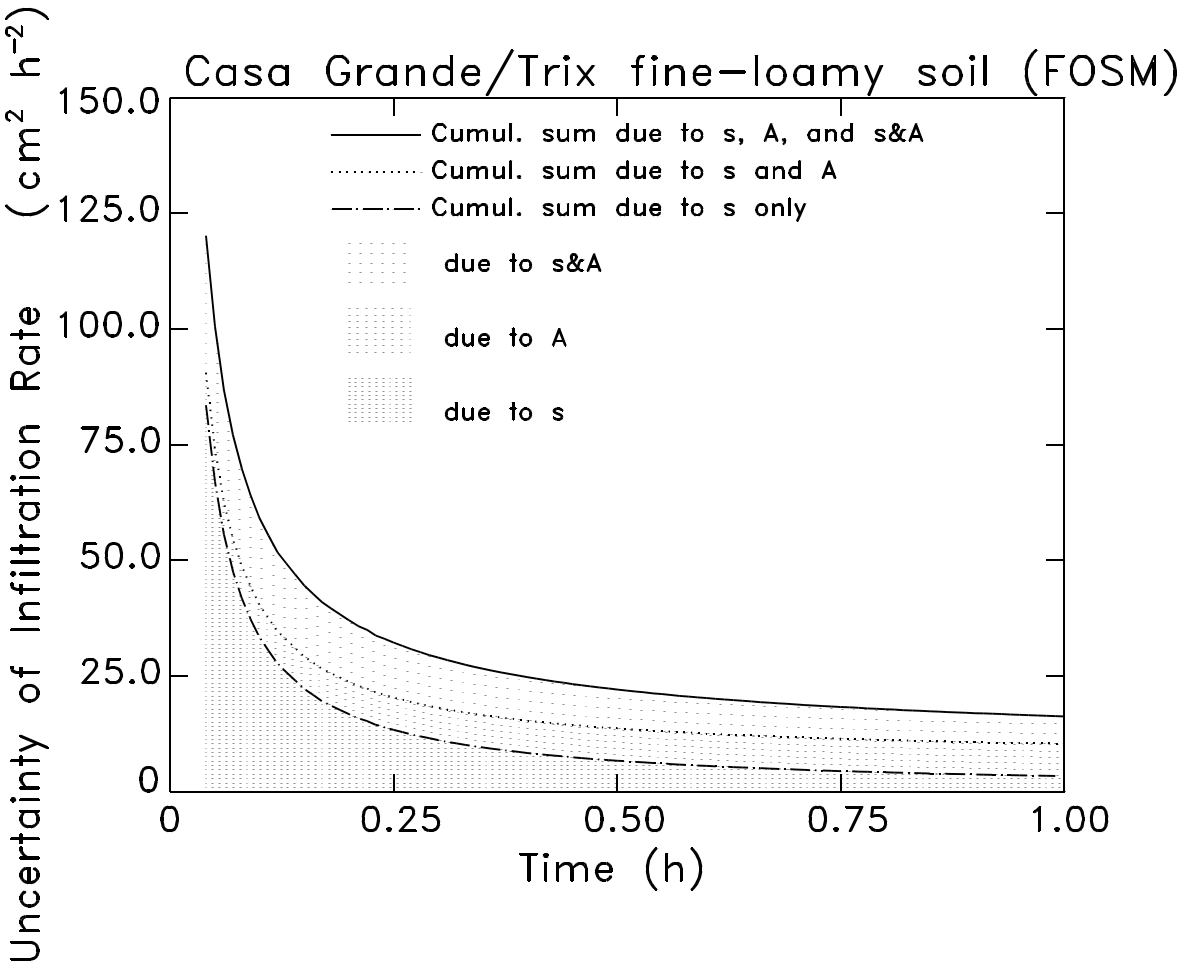

Figure C9b. Uncertainty of predicted infiltration rate as the results of contribution from input parameters in Casa Grande-Trix fine-loamy soils.